

STUDIES ON DESTRUCTION OF HYDROGEN  
SULFIDE MIXED WITH CARBON DIOXIDE  
IN AN ALTERNATING CURRENT  
PLASMA ARC REACTOR

By

SREENIVASULA REDDY MAGUNTA

Bachelor of Engineering

Shivaji University

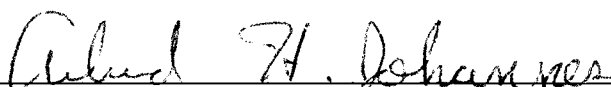
Kolhapur, Maharashtra, India

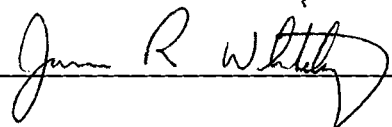
1991

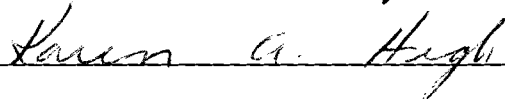
Submitted to the Faculty of the  
Graduate College of the  
Oklahoma State University  
in partial fulfillment of  
the requirements for  
the Degree of  
MASTER OF SCIENCE  
May, 1995.

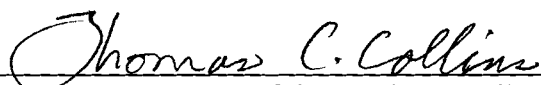
STUDIES ON DESTRUCTION OF HYDROGEN  
SULFIDE MIXED WITH CARBON DIOXIDE  
IN AN ALTERNATING CURRENT  
PLASMA ARC REACTOR

Thesis Approved:

  
\_\_\_\_\_  
Thesis Advisor

  
\_\_\_\_\_

  
\_\_\_\_\_

  
\_\_\_\_\_  
Dean of the Graduate College

## ACKNOWLEDGMENTS

I am grateful for this opportunity to express my appreciation to those who have contributed to this thesis in particular:

To Dr. Arland H. Johannes for his concern, guidance and encouragement throughout my graduate program and for his helpful discussion in the preparation of this thesis.

To Dr. Karen High and Dr. Robert Whiteley for serving on my graduate committee and for their helpful assistance during the course of this work.

To the Chemical Engineering Department for providing me with financial support, other faculty in the department and Mr. Charles Baker for their support during my graduate work.

To the various members of the plasma group who have provided a congenial atmosphere in which to work.

Finally to my parents who has been always supporting and encouraging throughout my life.

## TABLE OF CONTENTS

Chapter	Page
I. INTRODUCTION . . . . .	1
II. LITERATURE SURVEY . . . . .	6
BackGround . . . . .	6
Plasma Origin . . . . .	6
General Plasma Mechanisms . . . . .	7
Plasma Decomposition . . . . .	8
Thermal Decomposition . . . . .	10
Catalytic Decomposiiton . . . . .	11
Radiolytic Decomposition . . . . .	11
Photochemical Decomposition . . . . .	12
Other Decomposition Methods . . . . .	12
Literature Survey Summary . . . . .	13
III. EXPERIMENTAL APPARATUS AND SAFETY . . . . .	14
Experimental Apparatus Description . . . . .	14
Gas handling system . . . . .	14
Reactor system . . . . .	16
Power system . . . . .	18
Safety . . . . .	20
IV. NON-DESTRUCTIVE TESTS . . . . .	21
Procedure . . . . .	22
General Start Up Procedure . . . . .	22
Frequency Variation . . . . .	22
Relative Humidity Variation . . . . .	23
Flow Rate Variation . . . . .	23
Results and discussions . . . . .	23
Secondary Voltage Dependence on Frequency and primary voltage . . . . .	24
Effect of Humidity on Plasma Behavior . . . . .	30
Effect of changing Electrode Material and Reactor Size . . . . .	30

Chapter	Page
Effect of Flow rate on Secondary Voltage . . . . .	36
Power Dependence on Frequency and Primary Voltage . . . . .	36
Effect of Transformer on Plasma Behavior . . . . .	41
Error Analysis . . . . .	44
V. DESTRUCTIVE TESTS . . . . .	45
Procedure . . . . .	45
Dependence of Hydrogen sulfide conversion on frequency . . . . .	47
Dependence of Hydrogen sulfide conversion on primary voltage . . . . .	47
Effect of increasing humidity on H <sub>2</sub> S conversion . . . . .	60
Dependence of H <sub>2</sub> S conversion on Residence time . . . . .	60
Dependence of H <sub>2</sub> S conversion on duration of experiment . . . . .	63
Dependence of H <sub>2</sub> S conversion on the presence of carbon dioxide . . . . .	63
Reproducibility . . . . .	63
VI. THERMODYNAMIC CONSIDERATIONS . . . . .	67
Introduction . . . . .	67
Inference . . . . .	68
VII. CONCLUSIONS AND RECOMMENDATIONS . . . . .	75
Conclusions . . . . .	75
Recommendations . . . . .	77
BIBLIOGRAPHY . . . . .	79
APPENDIX A - SAMPLE CALCULATIONS . . . . .	82
APPENDIX B - NON DESTRUCTIVE TEST DATA . . . . .	84
APPENDIX C - DESTRUCTIVE DATA . . . . .	101

## LIST OF TABLES

Table	Page
3.1. Specifications of different reactors used . . . . .	18
5.1. Reproducibility data . . . . .	66
B1. Non-Destructive Data Corresponding to Figure 4.1 . . . . .	85
B2. Non-Destructive Data Corresponding to Figure 4.2 . . . . .	86
B3. Non-Destructive Data Corresponding to Figure 4.3 . . . . .	87
B4. Non-Destructive Data Corresponding to Figure 4.4 . . . . .	88
B5. Non-Destructive Data Corresponding to Figure 4.5 . . . . .	89
B6. Non-Destructive Data Corresponding to Figure 4.6 . . . . .	90
B7. Non-Destructive Data Corresponding to Figure 4.7 . . . . .	91
B8. Non-Destructive Data Corresponding to Figure 4.8 . . . . .	92
B9. Non-Destructive Data Corresponding to Figure 4.9 . . . . .	93
B10. Non-Destructive Data Corresponding to Figure 4.10 . . . . .	94
B11. Non-Destructive Data Corresponding to Figure 4.11 . . . . .	95
B12. Non-Destructive Data Corresponding to Figure 4.12 . . . . .	96
B13. Non-Destructive Data Corresponding to Figure 4.13 . . . . .	97
B14. Non-Destructive Data Corresponding to Figure 4.14 . . . . .	98
B15. Non-Destructive Data Corresponding to Figure 4.15 . . . . .	99
B16. Non-Destructive Data Corresponding to Figure 4.16 . . . . .	100

Table	Page
C1. Destructive Data Corresponding to Figure 5.1 . . . .	102
C2. Destructive Data Corresponding to Figure 5.2 . . . .	103
C3. Destructive Data Corresponding to Figure 5.3 . . . .	104
C4. Destructive Data Corresponding to Figure 5.4 . . . .	105
C5. Destructive Data Corresponding to Figure 5.5 . . . .	106
C6. Destructive Data Corresponding to Figure 5.6 . . . .	107
C7. Destructive Data Corresponding to Figure 5.7 . . . .	108
C8. Destructive Data Corresponding to Figure 5.8 . . . .	109
C9. Destructive Data Corresponding to Figure 5.9 . . . .	110
C10. Destructive Data Corresponding to Figure 5.10 . . . .	111
C11. Destructive Data Corresponding to Figure 5.11 . . . .	112
C12. Destructive Data Corresponding to Figure 5.12 . . . .	113
C13. Destructive Data Corresponding to Figure 5.13 . . . .	114
C14. Destructive Data Corresponding to Figure 5.14 . . . .	115
C15. Destructive Data Corresponding to Figure 5.15 . . . .	116
C16. Destructive Data Corresponding to Figure 5.16 . . . .	117

## LIST OF FIGURES

Figure	Page
3.1. Schematic of experimental apparatus . . . . .	15
3.2. Alternating current plasma arc reactor . . . . .	17
4.1. Dependence of secondary voltage on frequency for air at fixed primary voltages for reactor A . . . . .	25
4.2. Dependence of secondary voltage on frequency for air at fixed primary voltages for reactor B . . . . .	26
4.3. Dependence of secondary voltage on frequency for air at fixed primary voltages for reactor C . . . . .	27
4.4. Dependence of secondary voltage on frequency for Carbon dioxide at fixed primary voltages for reactor B and a flow rate of 79 cc/min . . . . .	28
4.5. Dependence of secondary voltage on frequency for H <sub>2</sub> S at fixed primary voltages for reactor B and a flow rate of 27 cc/min . . . . .	29
4.6. Dependence of secondary voltage on frequency for carbon dioxide with increased humidity (32.8% RH) at fixed primary voltages for reactor B and a flow rate of 79 cc/min . . . . .	31
4.7. Dependence of secondary voltage on frequency for hydrogen sulfide with increased humidity (34.2% RH) at fixed primary voltages for reactor B and a flow rate of 27 cc/min . . . . .	32
4.8. Effect of humidity on plasma behavior for carbon dioxide at a primary voltage of 70 V and a flow rate of 79 cc/min using reactor B . . . . .	33
4.9. Effect of humidity on plasma behavior for hydrogen sulfide at a primary voltage of 70 V and a flow rate of 27 cc/min using reactor B . . . . .	34
4.10. Effect of electrode configuration on plasma behavior for air . . . . .	35
4.11. Dependence of secondary voltage on frequency for carbon dioxide	



Figure	Page
at fixed flow rates for reactor B and a primary voltage of 60 V . . . . .	37
4.12. Dependence of secondary voltage on frequency for hydrogen sulfide at fixed flow rates for reactor B and a primary voltage of 60 V . . . . .	38
4.13. Dependence of power on frequency for carbon dioxide at fixed primary voltages for reactor B and a flow rate of 79 cc/min . . . . .	39
4.14. Dependence of power on frequency for hydrogen sulfide at fixed primary voltages for reactor B and a flow rate of 27 cc/min . . . . .	40
4.15. Effect of transformer on secondary voltage for air at a primary voltage of 40 V and for reactor C . . . . .	42
4.16. Effect of transformer on power for air at a primary voltage of 40 V and for reactor C . . . . .	43
5.1. Dependence of pure H <sub>2</sub> S conversion on frequency at a primary voltage of 80 V and a flow rate of 50.7 cc/min using reactor B . . . . .	48
5.2. Dependence of pure H <sub>2</sub> S conversion on frequency at a primary voltage of 70 V and a flow rate of 50.7 cc/min using reactor B . . . . .	49
5.3. Dependence of H <sub>2</sub> S conversion on frequency at a primary voltage of 80 V in the presence of CO <sub>2</sub> at a H <sub>2</sub> S/CO <sub>2</sub> molar ratio of 10/90 using reactor configuration B . . . . .	50
5.4. Dependence of H <sub>2</sub> S conversion on frequency at a primary voltage of 70 V in the presence of CO <sub>2</sub> at a H <sub>2</sub> S/CO <sub>2</sub> molar ratio of 10/90 using reactor configuration B . . . . .	51
5.5. Dependence of H <sub>2</sub> S conversion on frequency at a primary voltage of 80 V in the presence of CO <sub>2</sub> at a H <sub>2</sub> S/CO <sub>2</sub> molar ratio of 50/50 using reactor configuration B . . . . .	52
5.6. Dependence of H <sub>2</sub> S conversion on frequency at a primary voltage of 70 V in the presence of CO <sub>2</sub> at a H <sub>2</sub> S/CO <sub>2</sub> molar ratio of 50/50 using reactor configuration B . . . . .	53
5.7. Dependence of H <sub>2</sub> S conversion on frequency at a primary voltage of 80 V in the presence of CO <sub>2</sub> at a H <sub>2</sub> S/CO <sub>2</sub> molar ratio of 90/10 using reactor configuration B . . . . .	54

Figure	Page
5.8. Dependence of H <sub>2</sub> S conversion on frequency at a primary voltage of 70 V in the presence of CO <sub>2</sub> at a H <sub>2</sub> S/CO <sub>2</sub> molar ratio of 90/10 using reactor configuration B . . . . .	55
5.9. Effect of primary voltage on H <sub>2</sub> S conversion at a flow rate of 50.7 cc/min and a frequency of 600 Hz using reactor configuration B . . . . .	56
5.10. Effect of primary voltage on H <sub>2</sub> S conversion at a frequency of 600 Hz in the presence of CO <sub>2</sub> at a H <sub>2</sub> S/CO <sub>2</sub> molar ratio of 10/90 using reactor configuration B . . . . .	57
5.11. Effect of primary voltage on H <sub>2</sub> S conversion at a frequency of 600 Hz in the presence of CO <sub>2</sub> at a H <sub>2</sub> S/CO <sub>2</sub> molar ratio of 50/50 using reactor configuration B . . . . .	58
5.12. Effect of primary voltage on H <sub>2</sub> S conversion at a frequency of 600 Hz in the presence of CO <sub>2</sub> at a H <sub>2</sub> S/CO <sub>2</sub> molar ratio of 90/10 using reactor configuration B . . . . .	59
5.13. Effect of increasing humidity (36.5% RH) on H <sub>2</sub> S conversion at a primary voltage of 80 V and a flow rate of 48 cc/min using reactor configuration B . . . . .	61
5.14. Effect of residence time on H <sub>2</sub> S conversion at a primary voltage of 80 V and at a frequency of 600 Hz using reactor configuration B . . . . .	62
5.15. Dependence of H <sub>2</sub> S conversion on duration of equipment at a primary voltage of 80 V and a flow rate of 50.7 cc/min using reactor configuration B . . . . .	64
5.16. Effect of carbon dioxide composition on % H <sub>2</sub> S conversion at a primary voltage of 80 V, at a frequency of 600 Hz and at a flow rate of 70 cc/min using reactor B configuration . . . . .	65
6.1. Product distribution for H <sub>2</sub> S decomposition process at atmospheric pressure and various temperatures. . . . .	69
6.2. Product distribution for H <sub>2</sub> S decomposition process at atmospheric pressure and various temperatures including sulfur polymers. . . . .	70
6.3. Product distribution for H <sub>2</sub> S decomposition process at atmospheric pressure and various temperatures in presence of carbon dioxide at a H <sub>2</sub> S/CO <sub>2</sub> molar ratio of 10/90 . . . . .	71

Figure	Page
6.4. Product distribution for H <sub>2</sub> S decomposition process at atmospheric pressure and various temperatures in presence of carbon dioxide at a H <sub>2</sub> S/CO <sub>2</sub> molar ratio of 50/50 . . . . .	72
6.5. Product distribution for H <sub>2</sub> S decomposition process at atmospheric pressure and various temperatures in presence of carbon dioxide at a H <sub>2</sub> S/CO <sub>2</sub> molar ratio of 90/10 . . . . .	73

## **CHAPTER I**

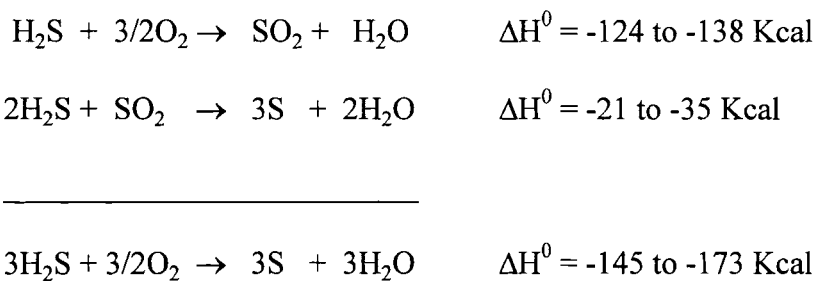
### **INTRODUCTION**

Although hydrogen sulfide is a well-known naturally occurring substance, the technological potential of its decomposition has not been fully investigated. This thesis is an attempt to investigate a new technology, frequency tuned capacitive reactors, to dissociate hydrogen sulfide to hydrogen and sulfur. This frequency tuned capacitive plasma technology appears to be more economical over the current technology.

Hydrogen sulfide is recovered in large quantities in the sweetening of natural gas and in the removal of organically bound sulfur from coal and petroleum light and heavy fractions by the hydrodesulphurization process. Some natural gas wells are so rich in hydrogen sulfide that they are simply capped because H<sub>2</sub>S is difficult and costly to dispose of in an environmentally acceptable way.

The depletion of pure sulfur deposits capable of being mined by Frasch process, the accelerated use of sour gases and high sulfur bearing petroleum crudes and strict environmental restrictions on sulfur emissions have focused attention on sulfur recovery from the waste hydrogen sulfide and promoted the development of the Claus process.

The Claus process represents the only commercially successful technique for processing hydrogen sulfide, and more than 90% of the elemental sulfur recovered from the gas streams is produced by this method. The Claus process involves burning part of the waste stream combined with a stoichiometric quantity of air to produce sulfur dioxide and water. A shift reaction then occurs between the sulfur dioxide and the remaining hydrogen sulfide as summarized in the following reactions.



Though this process has been successfully used for several years there are still several disadvantages. The hydrogen component of H<sub>2</sub>S is oxidized to water and is unrecoverable. With increasing interest being focused on the concept of a hydrogen economy the possibility of recovering the hydrogen and sulfur as usable products is intriguing. At the current rate of H<sub>2</sub>S generation, 6.4x10<sup>6</sup>tons/yr, this amounts to losing almost 150x10<sup>9</sup> standard cubic foot of hydrogen per year, for a lost energy investment of more than 60x10<sup>12</sup>Btu/yr with an annual value of over \$450 million [8]. This hydrogen if recovered could be recycled to the hydrodesulphurization units to achieve further sulfur removal from feed stocks, thereby conserving those hydrocarbon reserves that are otherwise used to obtain hydrogen.

The total conversion of the Claus process is not sufficiently high (90-98%). The emissions contain unreacted H<sub>2</sub>S and other sulfur compounds such as carbonyl sulfide and carbon disulfide. The Federal regulations limit H<sub>2</sub>S emissions to 50 ppm and forbids any gas containing more than 160 ppm H<sub>2</sub>S to be combusted directly in to the atmosphere [17]. Therefore to achieve higher efficiencies, a tail gas treatment such as the SCOT process is necessary. As the refinery acid gas generated from the hydrodesulphurization process is a mixture of hydrocarbons, hydrogen, carbon dioxide and hydrogen sulfide, separation of mixed gas is required prior to the Claus process.

The petrochemical industry has looked at several alternatives to the Claus process in order to recover hydrogen, such as thermal decomposition, chemically promoted thermal decomposition, electrolysis and liquid metal conversions. These were abandoned because of poor yield, high energy cost or some process complications [8]. The decomposition of hydrogen sulfide has been achieved in thermal plasmas but their high energy input and process complications limit their use.

Recently, a much simpler process for the direct decomposition of hydrogen sulfide was described in the Soviet literature [1]. A microwave discharge was used to create a cold, nonequilibrium plasma that dissociated H<sub>2</sub>S into hydrogen and sulfur. Currently a 500 kW demonstrative microwave hydrogen sulfide treatment plant operating at near atmospheric pressure is being tested at the natural gas fields in Orenberg, USSR [10]. This thesis is an attempt to achieve nonoxidative decomposition of H<sub>2</sub>S to hydrogen and sulfur under reasonable process conditions.

Research on alternating current silent glow discharge reactors (SGDR) began at Oklahoma State University (OSU) in 1987 as a cooperative effort with the Naval Research Center. Earlier work [21,33] at Oklahoma State University has shown that a SGDR can be fine tuned by varying the frequency applied to the reactor. Desai [7] demonstrated the potential of breaking pure hydrogen sulfide to hydrogen and sulfur at ambient conditions. Most of the plasma chemical reactions under consideration are carried out far from the optimum conditions because their mechanisms are often not known. Not knowing the existence of an optimum frequency was one major reason why past investigators did not fully exploit and develop plasma reactors using alternating current [13].

The following are advantages of destructing H<sub>2</sub>S in a SGDR.

- The reaction can be carried out at or near atmospheric pressure and at low temperatures.
- An extra salable product, namely hydrogen, is obtained.
- The products coming out of reactor are easy to separate.
- No catalyst is required to carry out the reaction within the reactor.
- Reduced energy requirements.

The objectives of this research are as follows.

- To build a safe and operable plasma reactor.
- To determine the degree of H<sub>2</sub>S conversion.
- To experimentally study the effect of carbon dioxide and water on the degree of H<sub>2</sub>S conversion.

- To experimentally determine the key operational and design parameters for the reactor.
- To assess future possibilities of this new technology.

Chapter II details a review of literature on destruction of hydrogen sulfide and carbon dioxide. The experimental setup and safety considerations are outlined in chapter III. Chapter IV details the procedures and observations of the electrical characteristics of various reactors and electrode configurations used under non-destructive testing. Chapter V details the procedures and the results of the destructive tests. Chapter VI gives a brief description on thermodynamic considerations and finally chapter VII gives a general discussion of the relevant data obtained and possible implications for further studies. The sample calculations are given in appendix A and the non-destructive test data and the destructive data are given in appendix B and appendix C, respectively. Results are presented in the form of graphs wherever necessary.



## **CHAPTER II**

### **LITERATURE SURVEY**

#### **Background**

The dissociation of molecules into atoms or smaller molecular species can be achieved in a number of different ways. Essentially all the processes are the same in each case, namely that sufficient energy to rupture a chemical bond is supplied to a molecule in a form that can be absorbed under a given set of conditions. However the energy requirement may vary depending up on the conditions and the type of technique used to supply that energy. In alternating current plasma reactors electrical energy is used to elevate the effective electron temperature thereby causing decomposition. This chapter is divided into different sections each dealing with a different technique for supplying the required energy. A brief introduction to plasmas and their reaction mechanisms is given below.

#### **Plasma Origin [7]**

Plasma, the most abundant form of matter in existence, dates back to the beginning of time. Plasma can be defined as a partially ionized gas consisting of molecules, atoms, ions, electrons and free radicals each moving with a certain velocity

[30]. Broadly speaking, plasma can be described as a system with electrical neutrality composed of positive and negative charge carriers.

Plasma, described in 1879 by Crookes as “a world where matter may exist in a fourth state” has attained an important and more recently a crucial place in research and industry. In 1928 Langmuir renamed Crookes “fourth state of matter”, plasma [11].

Plasmas are subdivided into two categories, one being thermally induced and the other electrically induced. There exists a major difference between these two types of plasmas. The thermally induced plasmas are in thermal equilibrium, and the temperature of the neutral and charged species are in equilibrium. However in electrically induced plasmas, the temperature of the charged and the neutral species can be quite different.

Thomas et al., [28] suggested that in thermally induced plasmas, energy would be concentrated in a given bond and causes a chemical reaction whereas in electrically induced plasmas, the collision with an electron produces activation directly without adding to the translational or rotational energy of the molecules.

### General Plasma Mechanisms

The alternating current plasma reactor utilizes electrical energy to create a relatively low temperature plasma in a reactor cavity. When organic or inorganic materials flow in the plasma, their chemical bonds are broken by absorbing the electrical energy of the plasma.

Because of the complexity of plasma systems, mechanisms for many reaction paths are not yet known. The variety of species, positive and negative ions, atoms and molecules at various states of excitement, free radicals and neutral molecules offers a range of different interactions under glow discharge conditions.

In most of the reactions, molecules are first excited through direct collisions via negative ions or by recombination of positive ions with electrons. The excited molecules

can fragment or they can isomerise to form either stable compounds or reactive intermediates. Given the variety of the species and the shift in reactivities with changes in variables such as concentration, flow condition and species location in the plasma zone, as well as equipment condition it is very complicated to estimate the importance of the diverse elementary processes in such an environment. In most plasma experiments, only the starting components and final products are known. Intermediates are rarely identified as to duration of existence and concentration. Therefore, many questions regarding the mechanisms remain unanswered.

### Plasma Decomposition

Schwarz and Kunzer [25] were the first to study the influence of electrical discharge on hydrogen sulfide in 1929. They found that the dissociation of hydrogen sulfide took place to a certain extent and then was overcome by recombination caused by activation of the sulfur by the discharge.

Soviet scientists [1] in 1985 used a microwave discharge that was used to create a cold non-equilibrium plasma that dissociates hydrogen sulfide to hydrogen and sulfur. They reported conversions ranging from 45 to 80% of the H<sub>2</sub>S fed to the reactor, with a power consumption of 0.7 to 1.9 eV per H<sub>2</sub>S molecule converted.

Gorski et al., [8] at Argonne national laboratory reported that conversions in excess of 99% were obtained by recycling back unconverted H<sub>2</sub>S to the reactor. They also reported that the specific energy of hydrogen sulfide is low enough that a waste treatment process with a microwave induced plasma is economically feasible.

The effect of spatial non-equilibrium in the dissociation of hydrogen sulfide in plasma was studied by Rusanov et al. [24]. They have shown that the spatial distribution of clusters by size differs considerably from an equilibrium distribution and this effect

can be used to stabilize the products of many plasma chemical processes and to reduce a considerable amount of energy spent on them.

Vastola and Stacy [32] studied the induced reaction of hydrogen sulfide with hydrocarbons and reported that as the amount of hydrocarbon is increased the production of elemental sulfur decreases.

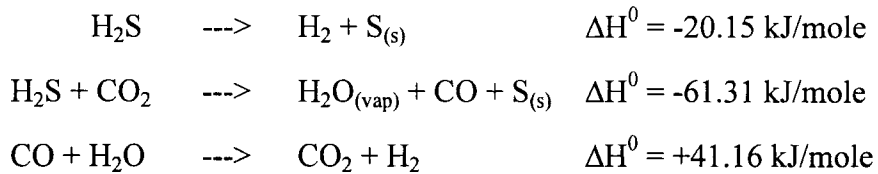
Potapkin et al., [22] has numerically investigated the dissociation of hydrogen sulfide in thermal plasma. They also found out that energy costs of obtaining the products is significantly reduced by the presence of oxygen in the initial mixture.

Reaction mechanisms in thermal plasmas have been investigated by several authors. Desai [7] has discussed the various mechanisms and found that inconsistencies exist and suggested the need for further investigation.

Blanchet et al., [3] investigated the decomposition of CO<sub>2</sub> in an argon plasma jet reactor with a 10% volumetric rate of CO<sub>2</sub> to argon flow rate and found the yield of oxygen was from 1 to 3%. However higher yields were obtained at higher power input to the torch and a total conversion of CO<sub>2</sub> as high as 60% was attained.

Gorski et al., [8] at Argonne National Laboratories Studied the destruction of hydrogen sulfide in presence of carbon dioxide in a MicroWave plasma reactor at pressures of 10 to 30 Torr and flow rates of 1.0 to 6.1 SLM. They concluded that the presence of carbon dioxide has shown a very weak increase in hydrogen sulfide conversion. Major by products were carbon monoxide and sulfur dioxide with minor amounts of CS<sub>2</sub> (<0.6%) and COS (<0.03%)

Czernichowski et al., [5] has studied the dissociation of a mixture of hydrogen sulfide and carbon dioxide in a high intensity electric arc or gliding high tension electric discharges under atmospheric pressure. The following gives the complete reaction mechanism proposed by Czernichowski et al.

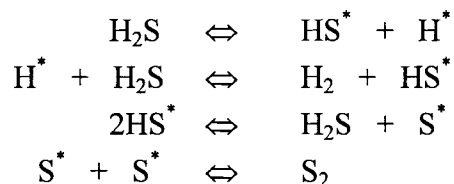


Their experimental results show that a maximum decomposition of hydrogen sulfide was obtained at a CO<sub>2</sub>/H<sub>2</sub>S ratio of 1.75 and was found to be 99.1% at a flow rate of 13.8 liter/min and the conversion was observed to increase with increasing CO<sub>2</sub>/H<sub>2</sub>S ratio.

### Thermal Decomposition

Raymont [23] in his authoritative work on the thermal decomposition of H<sub>2</sub>S suggested the use of either upset equilibrium conditions or loop systems to increase reactions yields under fixed process conditions.

Kaloidas et al., [14] studied the kinetics of the thermal, non-catalytic decomposition of H<sub>2</sub>S in a non-isothermal flow reactor at pressures of 1.3-3.0 atm, temperatures of 600-860°C, and flow rates of 3.4 x 10<sup>-4</sup> - 3.6 x 10<sup>-3</sup> mol/cm<sup>2</sup>-s. The proposed mechanism includes as the initial and rate limiting step the splitting of H<sub>2</sub>S into intermediate free radicals. The non-catalytic decomposition of H<sub>2</sub>S can be explained by the following free radical mechanism.



Kappauf et al., [15] has studied the thermolysis of H<sub>2</sub>S using solar energy as the source of heat in a solar furnace. They observed at low feed rates and a reactor temperature of 1800 K conversions that were virtually 100% of the maximum expected

value. At lower temperatures the conversions were slightly reduced because recombination occurred during the quench. They also found that although high feed rates may reduce conversion, the overall effect of higher feed rates was increased production rates.

### Catalytic Decomposition

Hydrogen sulfide reacts with a variety of inorganic substances to give hydrogen or water and a sulfide. These reactions have been extensively investigated not only because they provide data on thermodynamic properties and chemisorptive processes, but also because of their application to metallurgical and corrosion problems.

Ni [2], Al<sub>2</sub>O<sub>3</sub> [26], NiO [29], are some of the surfaces which have been used to investigate the chemisorption of hydrogen sulfide. In most cases, the hydrogen sulfide is dissociatively chemisorbed resulting in the formation of a sulfide layer. As the fraction of surface coverage increases, the rate of chemisorption decreases. The use of carbon [16] and germanium [4] for interaction with hydrogen sulfide has also been studied. It again results in dissociative absorption on the bulk solid resulting in the formation of chemisorbed sulfur or a sulfide and a hydrogen.

### Radiolytic Decomposition

Wourtzel [34] first studied the effect of alpha particles on hydrogen sulfide and found that H<sub>2</sub>S was decomposed to its elemental components, but the rate decreased with an increase in temperature. The radiolysis of hydrogen sulfide and a mechanism involving high energy hydrogen atoms and SH radicals has been investigated by Torrey [31]. Huyton and Woodward [12] found that neither SF<sub>6</sub> nor N<sub>2</sub>O had any effects on the yield of hydrogen and sulfur.

## Photochemical Decomposition

The effect of light of various wave lengths on hydrogen sulfide decomposition has been studied by several authors. Smits and Aten [27] using ultra violet radiation as the energy source showed that detectable quantities of hydrogen were produced even at room temperatures. Darwent and Roberts [6] studied extensively the photochemical decomposition of hydrogen sulfide at various temperatures and pressures using the narrow cadmium line and the broad mercury line as the energy source. They deduced a free radical mechanism and an expression for the quantum yield of hydrogen. Their yields calculated from the experiments agree with their observation that the yield was independent of hydrogen sulfide pressure above 200 Torr, and the temperature difference appeared to vary with the wave length used.

Gratzel [9] recently has shown that hydrogen sulfide can be split catalytically into its components by visible light using an aqueous transparent suspension of colloidal cadmium sulfide particles loaded with ruthenium dioxide.

## Other Decomposition Methods [7]

There are several other methods for the decomposition of hydrogen sulfide, but these are basically abandoned because of their poor yields, high energy costs or other process complications. Some of the methods include

- Ultrasonic irradiation
- Electrochemical oxidation
- Chemically promoted thermal decomposition
- Combination of electrolysis and chemical decomposition
- Liquid metal conversion
- Biological treatment, etc.

## Literature Survey Summary

The literature cited in the previous paragraphs gives us basic background information on different reaction mechanisms and methods involved in the decomposition of hydrogen sulfide. In conclusion, it appears that the direct decomposition of hydrogen sulfide can only be brought under relatively severe conditions and even then, the yields are poor as dictated by the thermodynamics. The experimental findings of this work and their implications as discussed in the remaining chapters may help in exploring the commercial possibilities of this new technology (plasma technology).



## CHAPTER III

### EXPERIMENTAL APPARATUS AND SAFETY

This chapter describes the experimental setup and the safety measures taken during experimentation. This chapter is divided into four sections. Section one explains the gas handling system, section two gives a description of the reactor system, section three describes the power system and finally section four describes the safety measures taken during this work. A schematic of the experimental apparatus is shown in Figure 3.1.

#### Experimental Apparatus Description

##### GAS HANDLING SYSTEM

Since hydrogen sulfide is a hazardous chemical all the experiments were conducted in the OSU Hazardous Reaction Laboratory. The gases were stored in high pressure containers connected with pressure regulators to regulate the inline pressure of the feed gas and the purge gas. The flow of gases was controlled by means of Linde FM4575 Mass Flow Meter/Flow Controller. The mass flow meter/flow controller provided control of multiple flow rates by the use of separate control modules. Modules are calibrated using helium. Actual individual flow rate is a correction factor times the reading shown on the mass flow meter/flow controller. The correction factor varies for different gases. The correction factor, provided by the manufacturer of the flow

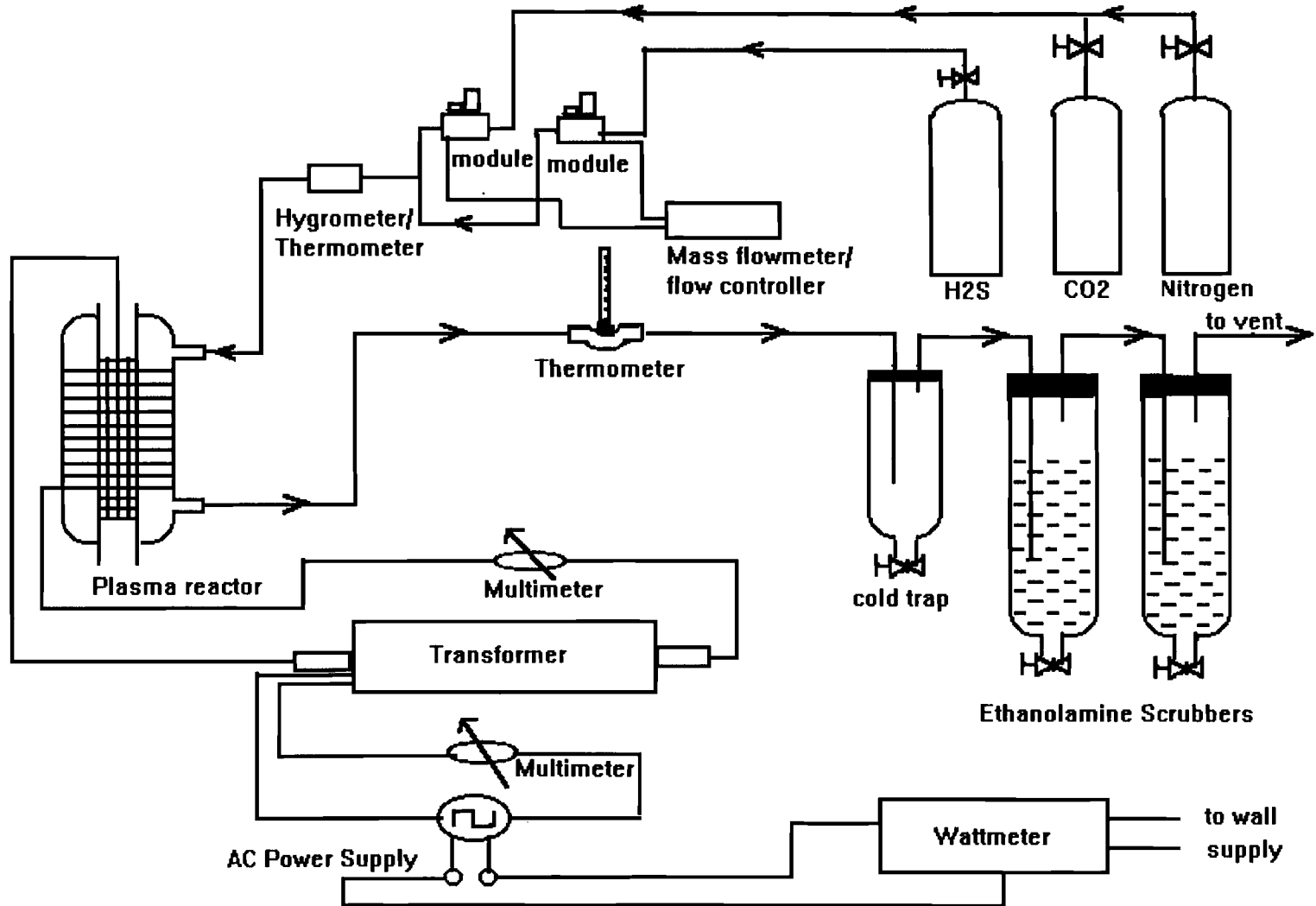


Figure 3.1. Schematic of experimental apparatus

meter/flow controller, was 0.85 for hydrogen sulfide and 0.78 for carbon dioxide. H<sub>2</sub>S was passed through channel one (Linde Mass Flow Control Module 9C-202-4124). A provision was made to use either nitrogen or CO<sub>2</sub> through the second channel (Linde Mass Flow Control Module 10C-202-4124). Gases are then either passed through two 500 ml. Erlenmeyer flasks filled with water to increase the humidity or directly passed to the reactor. The humidity and temperature of the gas were measured using a Davis Instruments Model digital Hygrometer/Thermometer. The gases coming out of the reactor were then passed through a cold trap and finally through ethanolamine solution scrubbers before being vented.

#### Materials:

##### a) Gases:

H<sub>2</sub>S - AGA Gas Inc. - Specialty Gas, 99.5% pure H<sub>2</sub>S.

CO<sub>2</sub> - Linde Specialty Gases, Bone dry grade.

N<sub>2</sub> - Linde Specialty Gases, Dry grade.

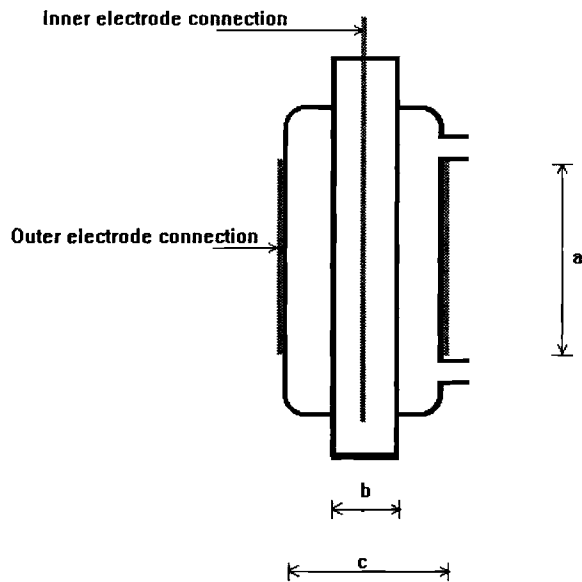
##### b) Solvents:

Ethanolamine - Fisher Scientific.

CS<sub>2</sub> - Aldrich Chemicals.

### REACTOR SYSTEM

The alternating current plasma arc reactor, basically a combination of capacitive and inductive devices, consists of two concentric glass tubes to form an annulus for gas flow. The reactors used were made of quartz. Electrodes were placed around the outer cylinder and inside the inner cylinder thereby forming plasma in the annulus. The plasma



Reactor A:

a: 25 cm                      b: 1.80 cm                      c: 3.40 cm  
 Inside Electrode: Copper mesh  
 Outside Electrode: Copper wire wrapped spirally

Reactor B:

a: 25.4 cm                      b: 1.80 cm                      c: 2.78 cm  
 Inside Electrode: Copper mesh  
 Outside Electrode: Copper mesh wrapped

Reactor C:

a: 122 cm                      b: 2.80 cm                      c: 4.80 cm  
 Inside Electrode: Copper mesh  
 Outside Electrode: Copper mesh wrapped

Figure 3.2. Alternating Current Plasma Reactor

is formed due to the diffusion of current into the annulus when a potential is applied because of the dielectric effects of glass. The electrodes are arranged such that there can be no corrosion or electrode fouling due to gaseous interaction with the electrode. Three different reactors were used in this study. The major difference between the reactors is the annulus gap, the effective length of the reactor and the electrode configuration. Reactor A uses copper wire tightly wrapped, 8 times as an outer electrode and 40 mesh copper sheet as an inner electrode. Reactor B and C use 40 mesh copper sheet for both inside and outside electrodes. Table 3.1 lists the reactor specifications.

TABLE 3.1  
REACTOR SPECIFICATIONS

Reactor	Inside dia. of outer tube, cm	Outside dia. of inner tube, cm	Annulus gap cm	Length cm
A	3.40	1.80	0.80	25
B	2.78	1.80	0.49	25.4
C	4.80	2.80	1.00	122

### POWER SYSTEM

The major components of this system are an AC power supply, an oscillator for frequency tuning, a transformer to increase the voltage, two multimeters to measure the current and secondary voltage and a wattmeter to measure the total power consumption. The voltage to the system is regulated from the 110 volt wall socket by a California instruments power source. The strong electrical potential required to generate a plasma,

up to 15,000 volts, was attained by using a transformer. The secondary voltage coming out of the transformer was tuned by varying the frequency of the primary voltage using the BK Precision Model 3011B wave generator. The primary current and the secondary voltage is measured using a digital multimeter (Fluke model 8050 A). A wave generator was used to generate different wave forms and study their effects. A wattmeter installed between the AC power supply equipment and the 110 V wall supply measures the total power consumed by the whole setup. The material and equipment specifications are given below.

#### Electrical Equipment:

1. AC power supply - California Instruments, Model 1001TC.
2. Oscillator - California Instruments, Model 850T.
3. Function Generator - BK Precision, Model 3011B.
4. Wattmeter - General Electric, Model No.3720341, Amp - 5/10, volts 100/200, Watts 500/1000/2000.
5. Multimeters - John Fluke Mfg. Co., Model No.8050A.
6. High voltage probe - John Fluke Mfg. Co. Model 80K6.
7. High voltage wiring - Taylor pro-wire, 8mm Silicone wire.
8. Transformers 1 & 2 - Jefferson Luminous Tube Transformer, Cat. No. 721-411, Primary 120V, 60 Hz, Secondary 15000V, 60 MA, Mid point grounded.
9. Hygrometer/Thermometer - Davis Instruments Model DTH-1.
10. Mass Flowmeter / Flow controller - Linde FM4575 Mass Flow Meter/Flow Controller.

## Safety

Since hydrogen sulfide is highly flammable, toxic and extremely poisonous even in small quantities, safety was given more attention while performing the experiments. Continuous exposure to low (15-50 ppm) concentrations will generally cause irritation to mucous membranes, conjunctivae of the eyes, headache and dizziness or nausea. Higher concentrations (200-300 ppm) can lead to coma or unconsciousness. Exposures for more than 30 minutes at concentrations of greater than 700 ppm have been fatal.

The reactor, gas cylinders and all the pipelines connecting hydrogen sulfide were placed in the explosion bay in the Hazardous Reaction Laboratory. The electrical equipment except the transformer was placed inside the main building and was connected to the reactor system by means of cables running through ports that connect the main building and the explosion bay. This arrangement helps the operator to avoid contact with hydrogen sulfide gas or the high voltage wires. All the connections were tested for leaks. The outlet gases were passed through two ethanolamine scrubbers connected in series to absorb any traces of unreacted hydrogen sulfide. A gas mask was used when disconnecting the H<sub>2</sub>S gas pipeline connections.

Carbon disulfide that was used to clean the reactor is also highly flammable and readily absorbs through the skin causing neurologic and reproductive hazards. The target organs being cardio vascular systems, eye, liver and kidneys. The CS<sub>2</sub> bottles were stored separately in a flammable liquid storage area. Hand gloves and protection glasses were used when using CS<sub>2</sub>.

## **CHAPTER IV**

### **NON-DESTRUCTIVE TESTS**

This chapter details the procedures carried out while performing experiments called non-destructive tests and discusses the findings of the physical and electrical characteristics of the silent glow discharge reactor (SGDR). Although tests from previous work, using SGDRs characterizing various reactors, gave some general trends of the reactors, they were limited. The previous work on SGDRs was expanded by studying the effect of transformers and the effect of various gases under study on the physical and electrical characteristics of the SGDR.

Since this chapter deals with the physical and electrical characteristics of the plasmas, the preliminary destructive tests of hydrogen sulfide and carbon dioxide are also presented in this chapter. Although these tests are a kind of destructive tests, the main aim in conducting these tests is to obtain the information on plasma optimum conditions for that gas.



## Procedure

A brief outline of the experimental procedure for non-destructive tests is given below.

### General Start Up Procedure

1. The reactor with the desired electrode configuration was placed in the experimental setup and all the electrical connections were made.
2. After the flow connections were tightened and checked for leakage, the inlet valve to the reactor was opened and the gas was allowed to flow through the reactor at a desired flow rate.
3. The power supply was turned on and the primary voltage was set at a desired value.

### Frequency Variation

1. After the general start up procedure, frequency was varied in steps of 10 Hz and the secondary voltage and power readings were noted down after sufficient time was allowed for the reading to stabilize.
2. Step 1 was repeated for the same reactor at different primary voltages.
3. The whole procedure was repeated for different reactors and different gases.

### Relative Humidity variation

1. Step 2 in the general start up procedure is slightly modified by bubbling the gas through water, to increase the relative humidity of the gas, before the gas was allowed to pass through the reactor.
2. The power supply was then turned on and the primary voltage was set at a desired value.
3. Frequency was varied and the secondary voltage and the input power were recorded.
4. Steps 1,2, and 3 were repeated for different gases and reactors at different primary voltages.

### Flow rate variation

1. The flow rate to the reactor is varied at a set primary voltage and the secondary voltage and the input power are noted.
2. Step 1 is repeated at different primary voltages for different gases.

All the non-destructive tests were carried out at night to observe visible operation of the plasma.

## Results and Discussion

The results are presented in a graphical form and discussed in the following sections. Experimental data with all fixed conditions are tabulated in Appendix B.

## Secondary Voltage Dependence on Frequency and Primary Voltage

Figures 4.1, 4.2 and 4.3 graphically represent the relationship between secondary voltage and frequency at different primary voltages for ambient air using reactor A, reactor B and reactor C configuration, respectively. Figures 4.4 and 4.5 graphically represent the relationship between secondary voltage and frequency at different primary voltages for carbon dioxide and hydrogen sulfide using reactor B configuration.

The secondary voltage initially decreases from a certain level at 60 Hz and then increases. The secondary voltage then goes through a peak for certain value of frequency for a particular primary voltage and then starts decreasing with increase in frequency. The reason for this condition is believed to be a result of resonance. The whole system can be considered as an parallel R-L-C network with a transformer as an inductive device, reactor as an capacitive device and a resistance. By tuning the frequency of this system we obtain a frequency where the inductive reactance is equal to the capacitive reactance, this condition is called resonance and the frequency at which this occurs is called resonant frequency. At this resonant frequency the total impedance of the system is maximum and drops off to the right and left of this frequency. Since the current from the source is constant, the voltage through the capacitor follows the same trend as the total impedance, because voltage through the capacitor is product of total impedance and the constant magnitude of the current source.

It is observed as primary voltage is increased , the magnitude of secondary voltage increased and the frequency at which the resonance occurred shifted towards the left. The

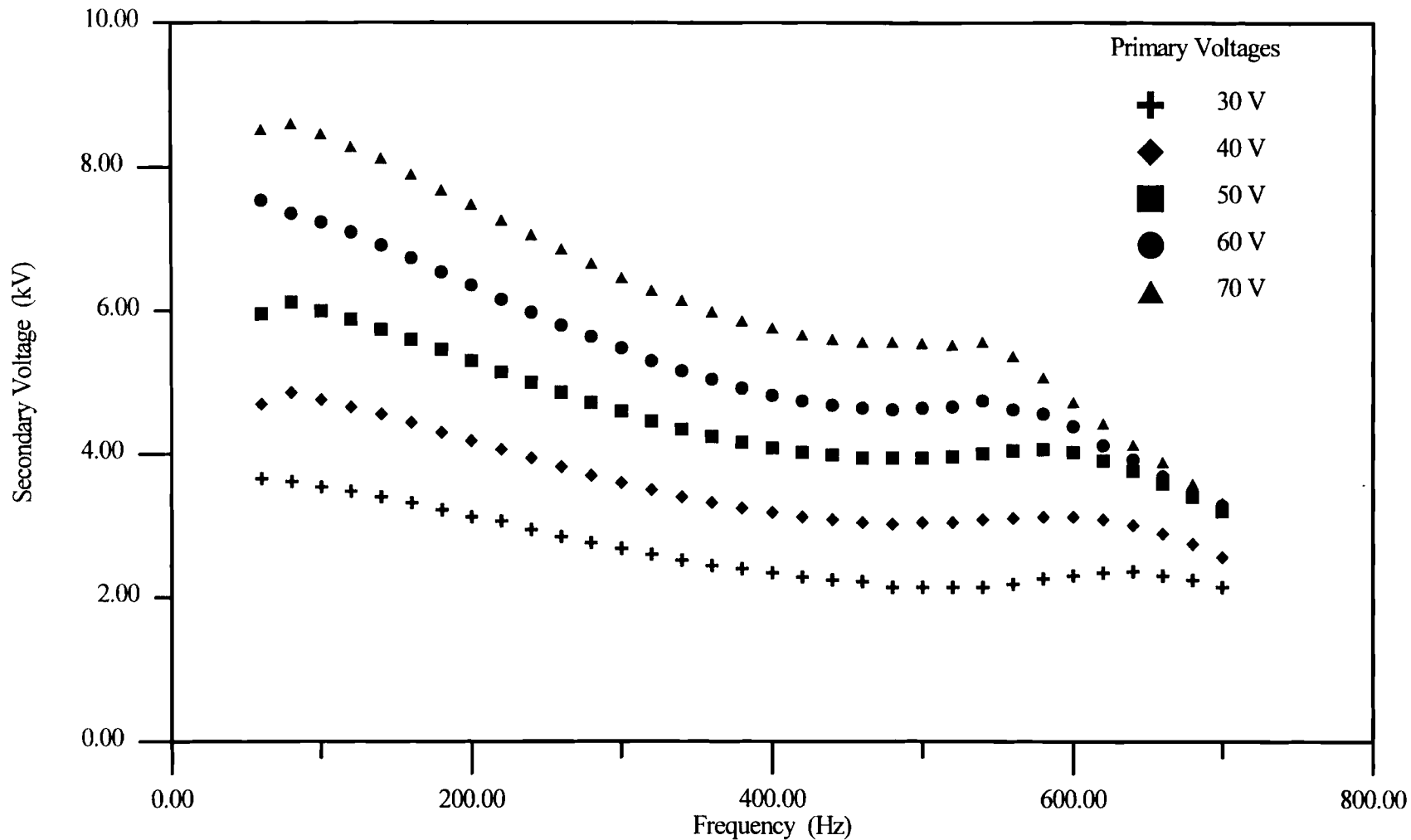


Figure 4.1. Dependence of secondary voltage on frequency for air at fixed primary voltages for reactor A.

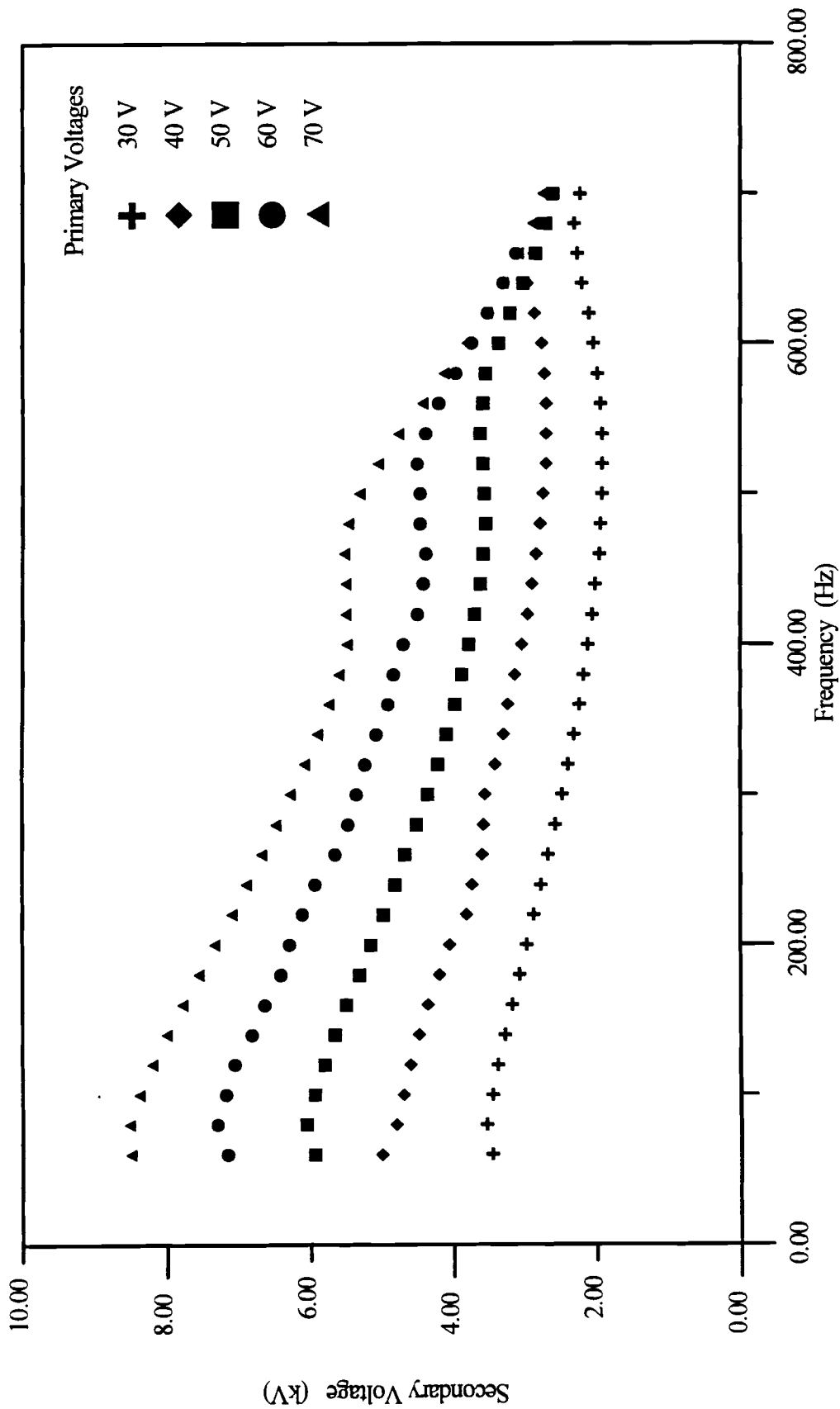


Figure 4.2. Dependence of secondary voltage on frequency for air at fixed primary voltages for reactor B.

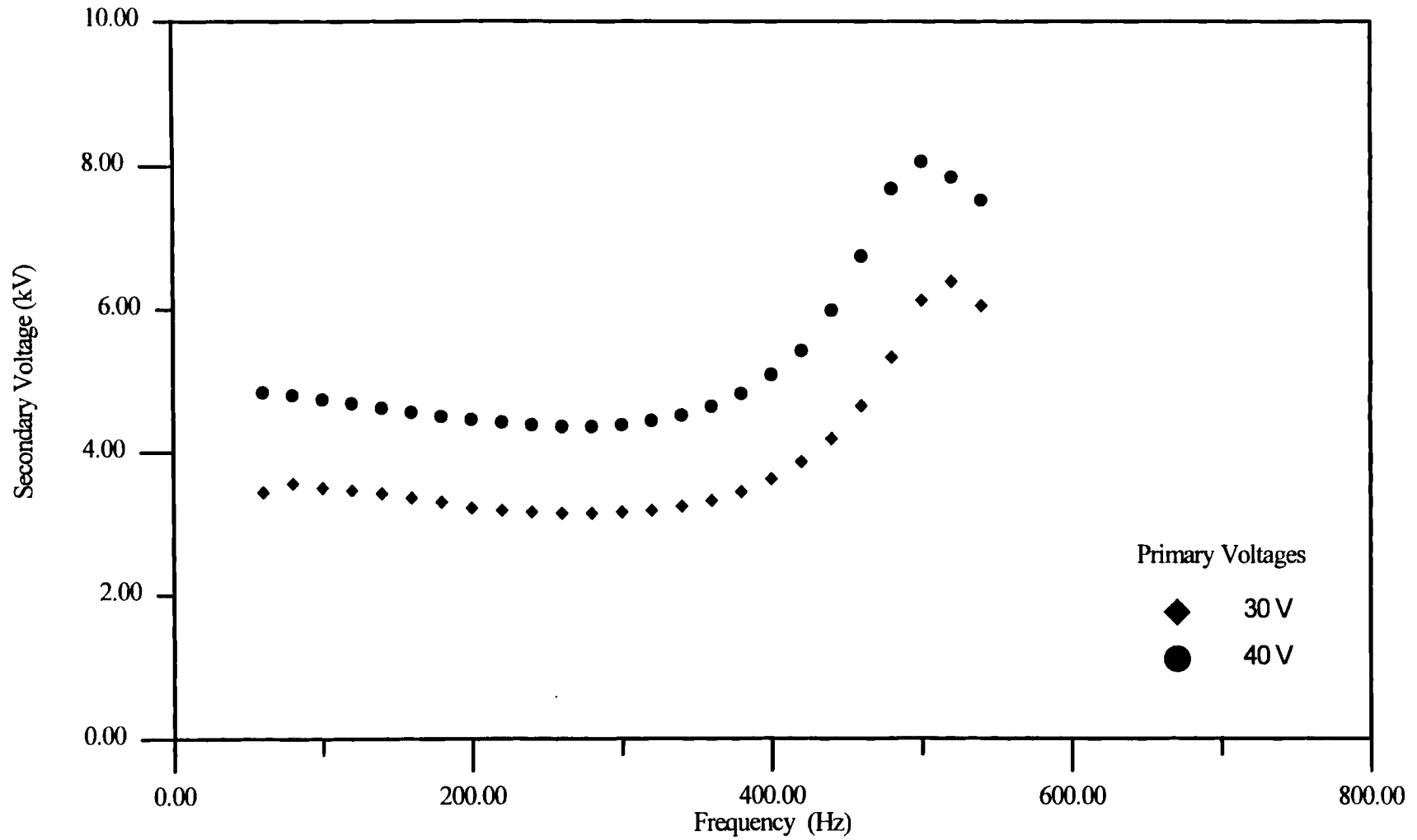


Figure 4.3. Dependence of secondary voltage on frequency for air at fixed primary voltages for reactor C.

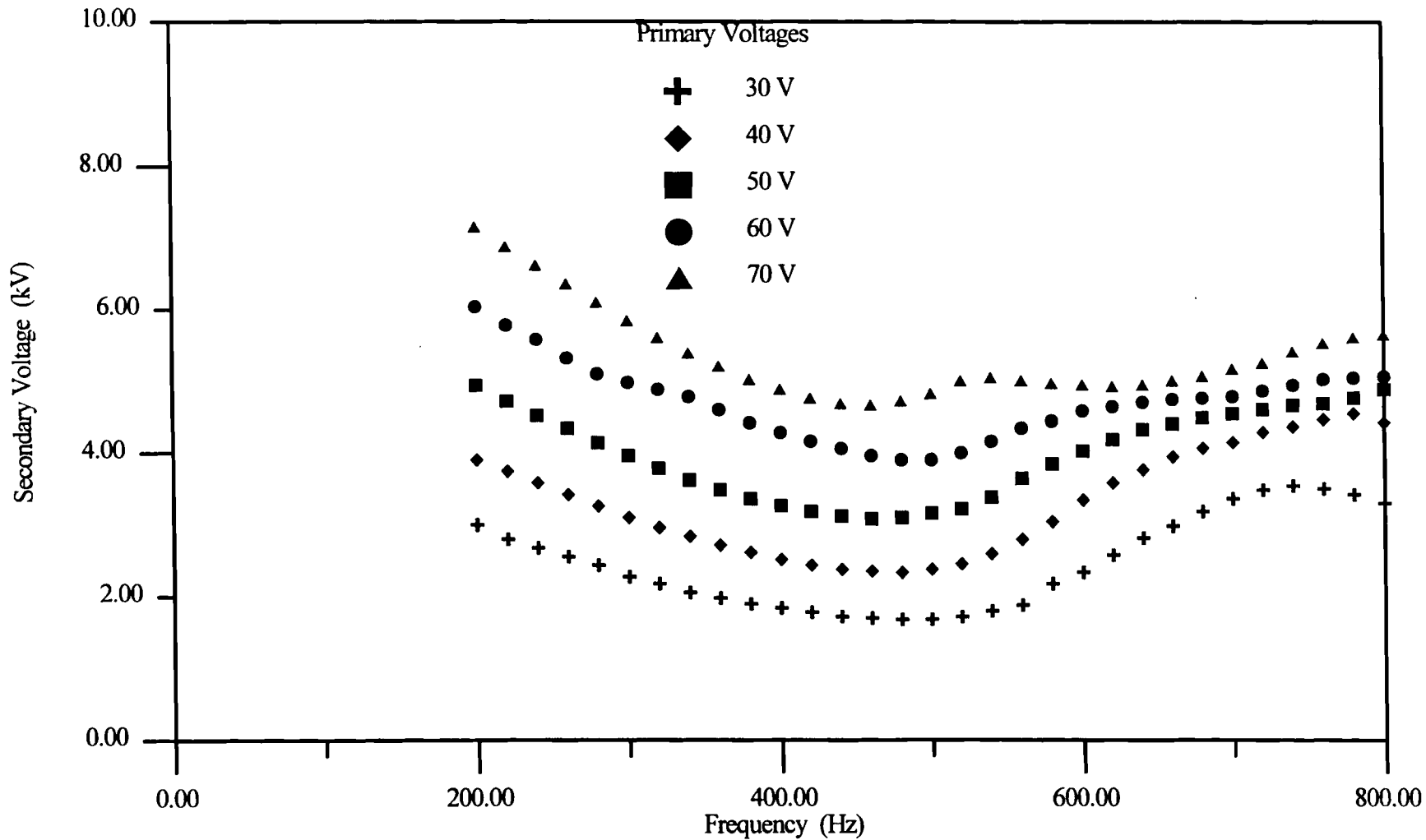


Figure 4.4. Dependence of secondary voltage on frequency for Carbon Dioxide at fixed primary voltages for reactor B and a flow rate of 79 cc/min.

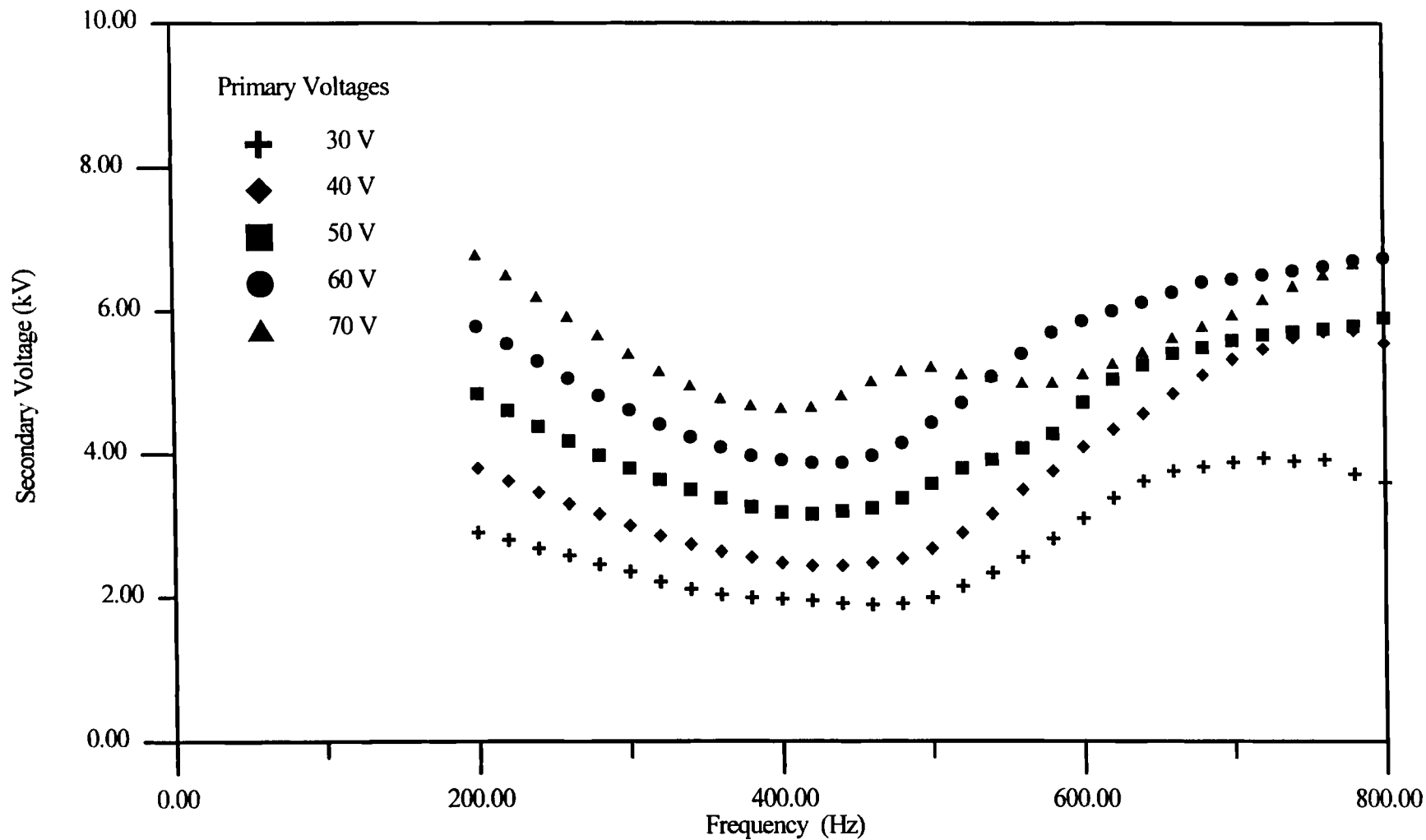


Figure 4.5. Dependence of secondary voltage on frequency for Hydrogen Sulfide at fixed primary voltages for reactor B and a flow rate of 27 cc/min.



trend remained basically same for all the reactors and different gases. The magnitude of secondary voltage changed with different gases, however this change was not of major significance.

### Effect of Humidity on Plasma Behavior

Figure 4.6, 4.7 illustrates the dependence of secondary voltage on frequency for carbon dioxide and hydrogen sulfide with increased humidity. The secondary voltage follows the same trends as observed for dry gas. Figure 4.8 and 4.9 show the effects of increasing humidity on secondary voltage for carbon dioxide and hydrogen sulfide. From the graphs we can see that by increasing the humidity the secondary voltages are little higher. The frequency at which the maximum occurred is shifted towards the left and also the rate at which secondary voltage drops is increased by increasing the humidity of the gas. This may be due to an increase in the capacitance in the circuit. By increasing the humidity in the gas the relative permittivity of the capacitor (Reactor) is increased, thereby increasing the capacitance.

### Effect of Changing Electrode Material and Reactor Size

Figure 4.10 shows how the secondary voltage is effected just by changing the electrode configuration at a fixed primary voltage for reactor A. It can be seen from the graph that the reactor with mesh outer and inner electrode configuration gives maximum

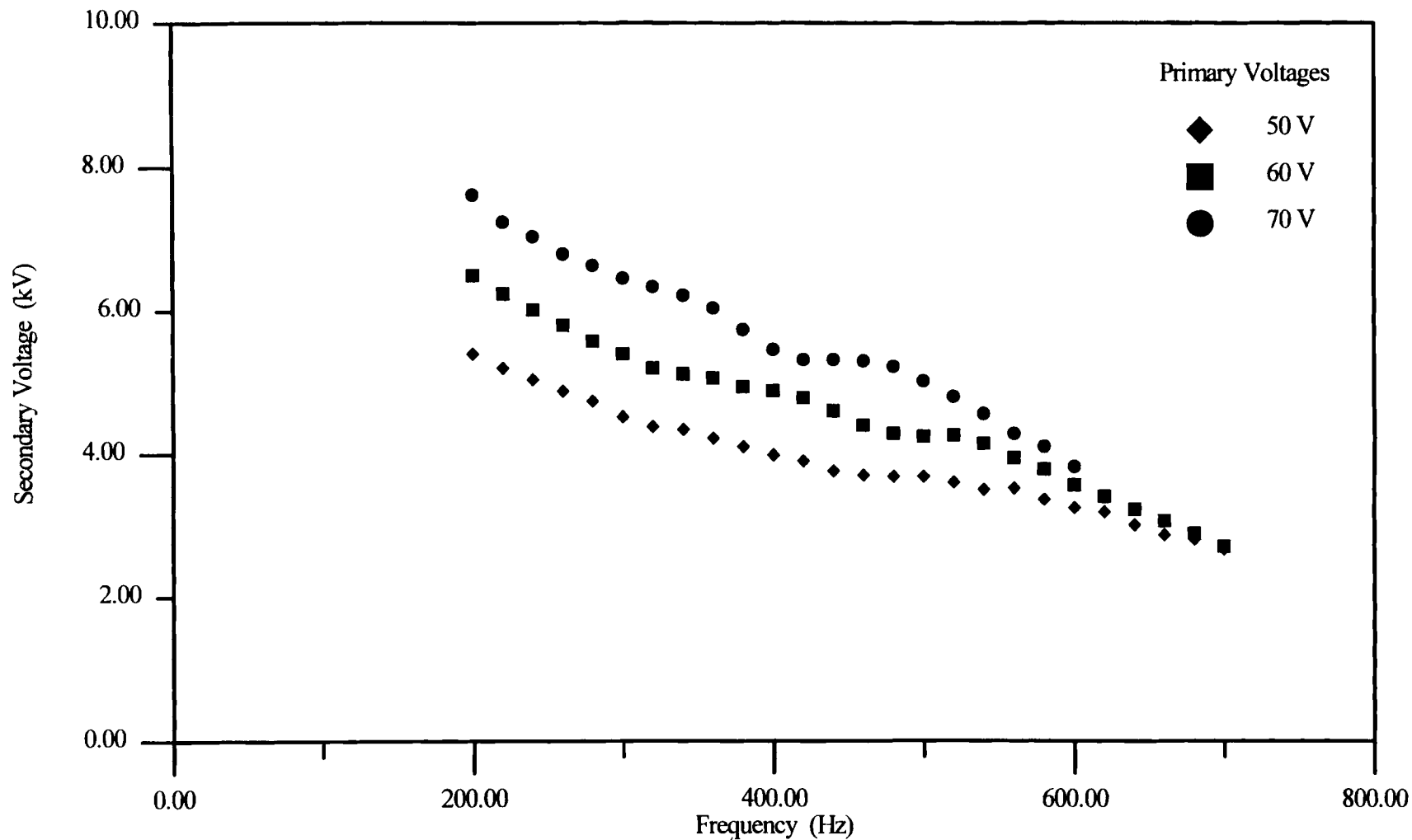


Figure 4.6. Dependence of secondary voltage on frequency for carbon dioxide with increased humidity (32.8%) at fixed primary voltages for reactor B and a flow rate of 79 cc/min.

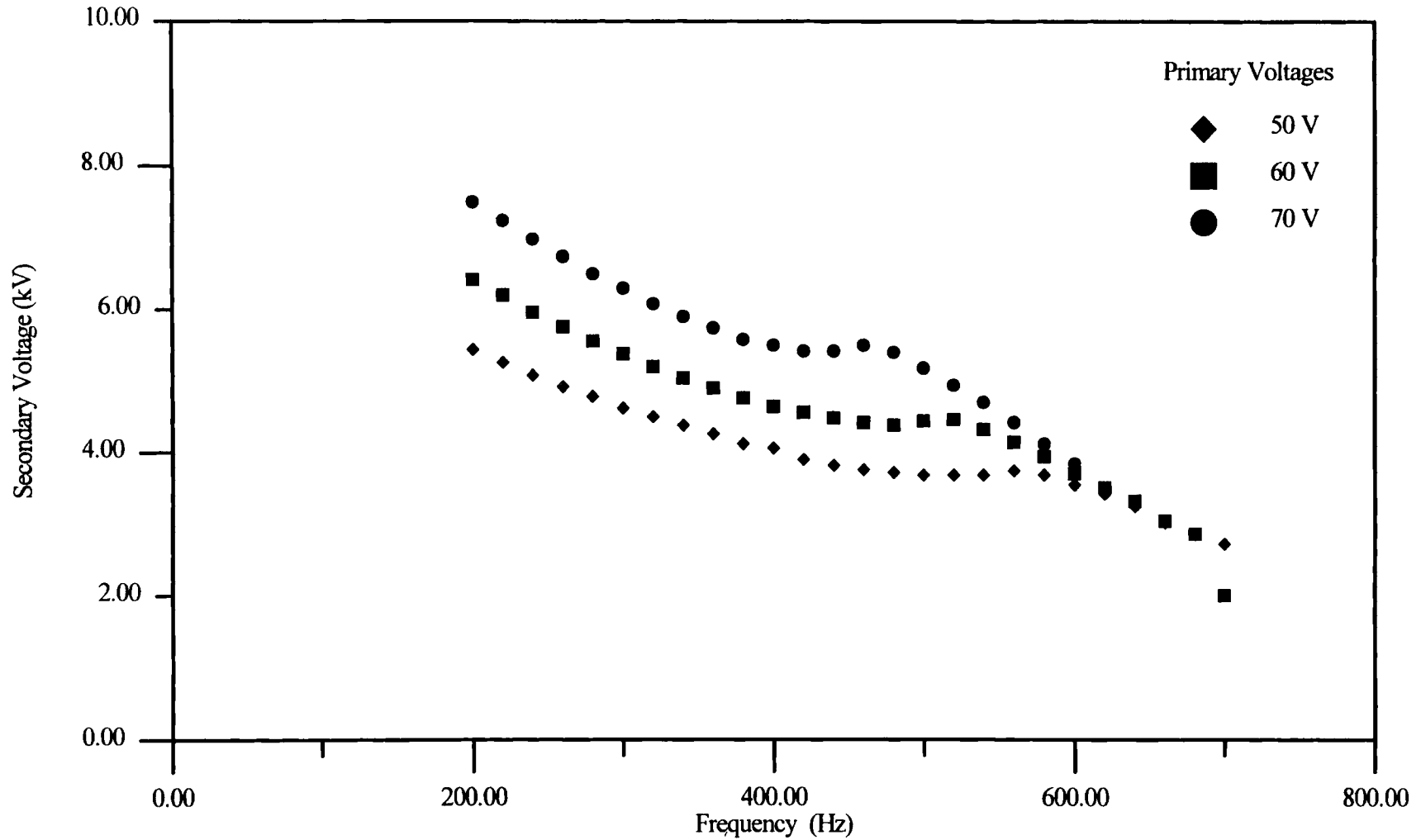


Figure 4.7. Dependence of secondary voltage on frequency for Hydrogen Sulfide with increased humidity (34.2%) at fixed primary voltages for reactor B and a flow rate of 27 cc/min.

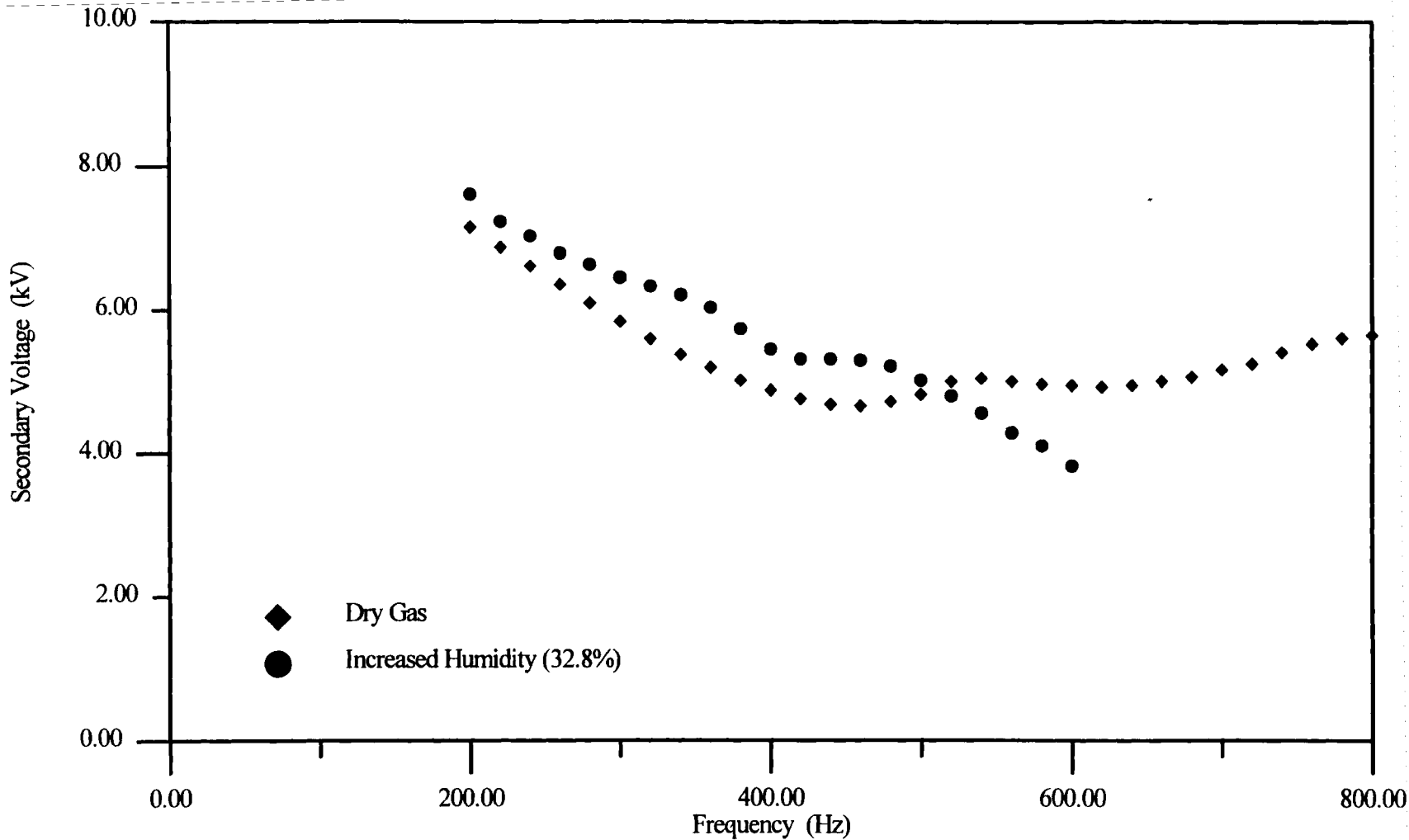


Figure 4.8. Effect of humidity on plasma behaviour for carbon dioxide at a primary voltage of 70 V and a flow rate of 79 cc/min using reactor B.

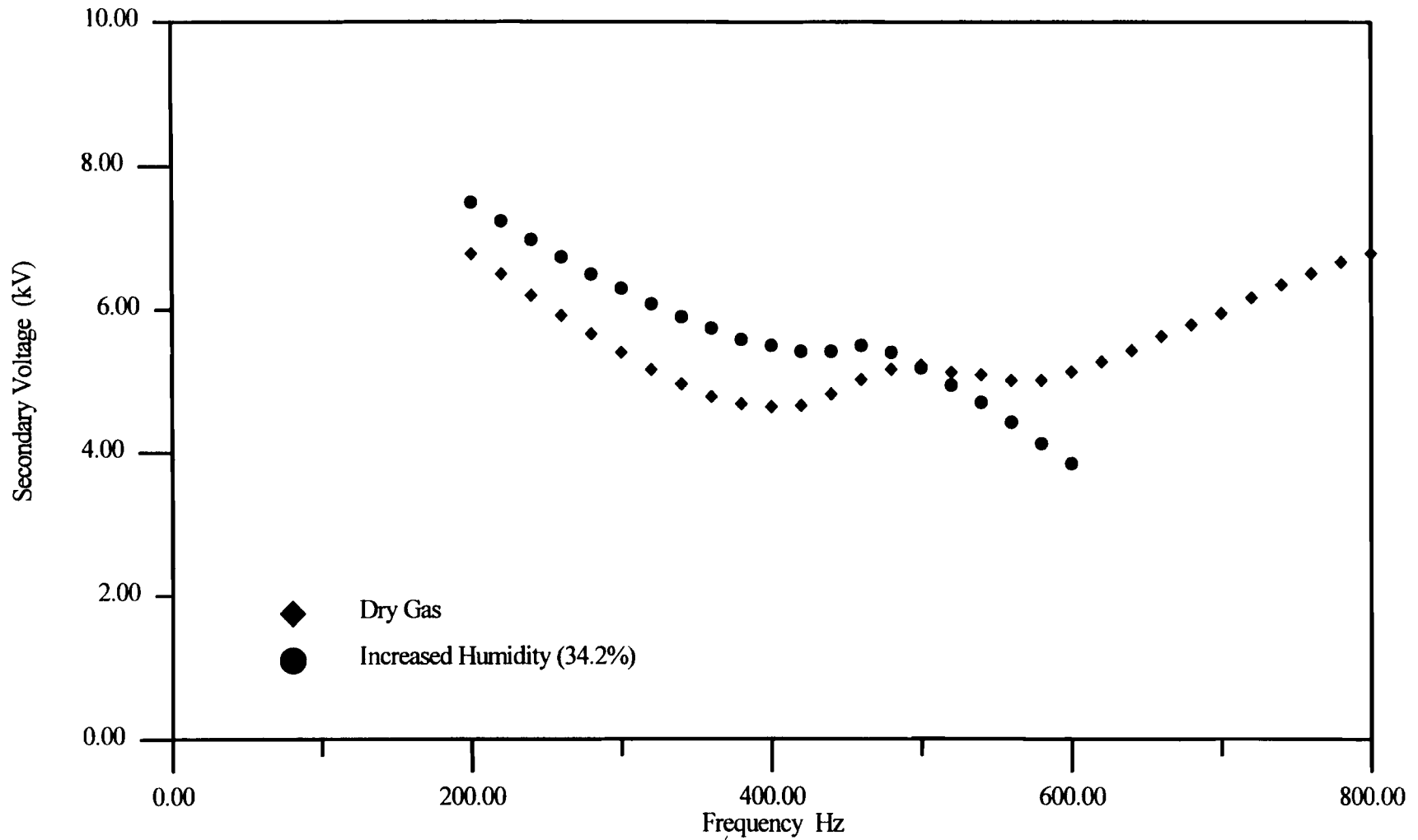


Figure 4.9. Effect of humidity on plasma behaviour for hydrogen sulfide at a primary voltage of 70 V and a flow rate of 27 cc/min using reactor B.

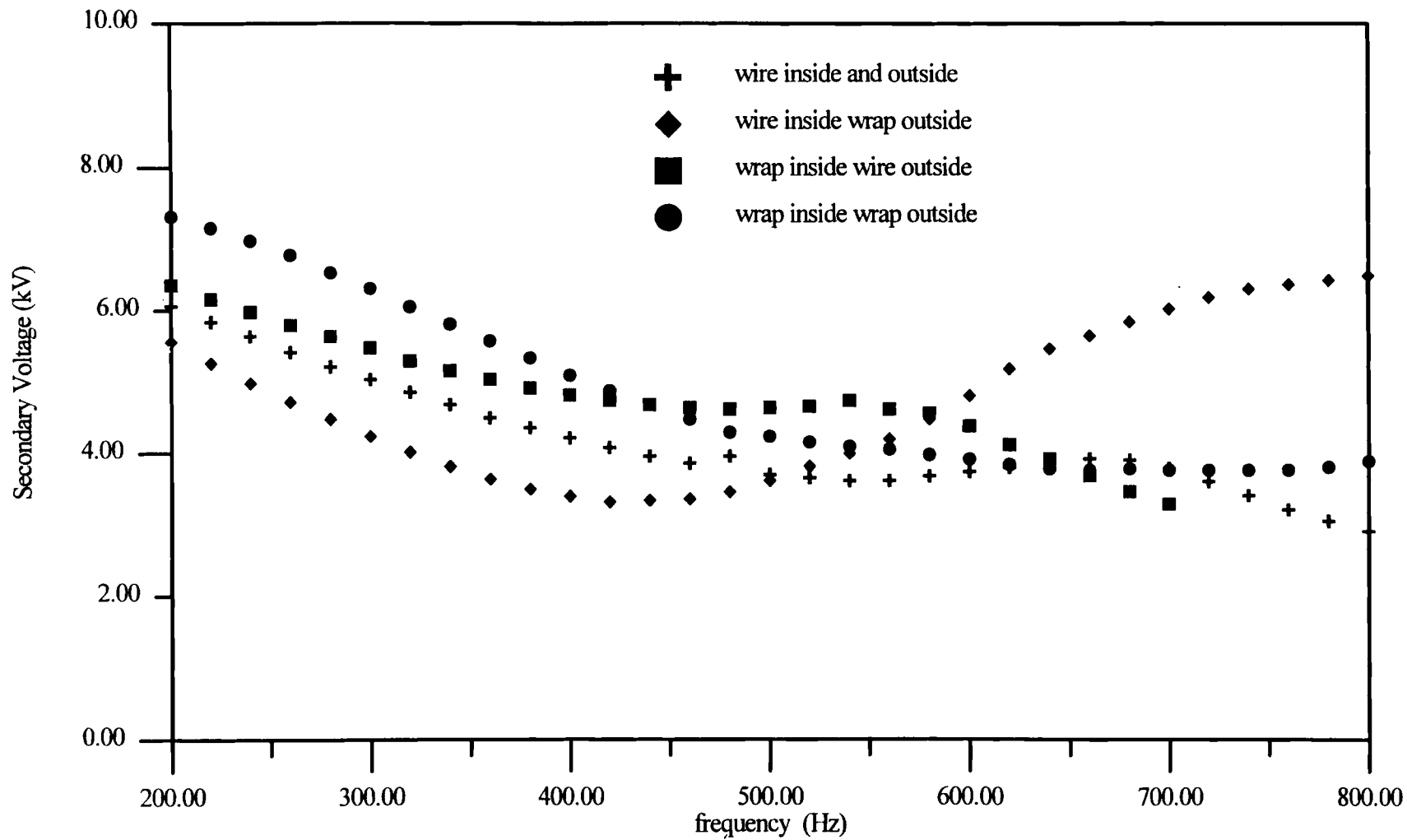


Figure 4.10. Effect of electrode configuration on plasma behaviour for air.

secondary voltage at a lower frequency. It was also observed that the reactor with wire spirally wrapped configuration the plasma is formed in spiral form, whereas for the reactor with mesh outer and inner electrode configuration the plasma was more uniform.

As the reactor size is increased the magnitude of the secondary voltage increased, the frequency at which the maximum occurred shifted towards the left and the power input increased. By increasing the size of the reactor the area of electrode increases thereby increasing the capacitance.

#### Effect of Flow rate on Secondary Voltage

Figure 4.11 and 4.12 shows the effect of changing the flow rate for carbon dioxide and hydrogen sulfide. It can be seen from the graph that the flow rate variation has a negligible effect on the secondary voltage.

#### Power Dependence on Frequency and Primary Voltage

Figures 4.13 and 4.14 shows the power dependence on frequency for carbon dioxide and hydrogen sulfide using reactor configuration B. It can be seen that the input power to the reactor increases with an increase in the primary voltage. As the primary voltage is increased, the frequency at which this maximum power level is obtained shift towards the left. The same trends were observed by Tsai[33], Piatt[21] and Desai[7]. However, previous work did not look at the power levels at lower frequencies.

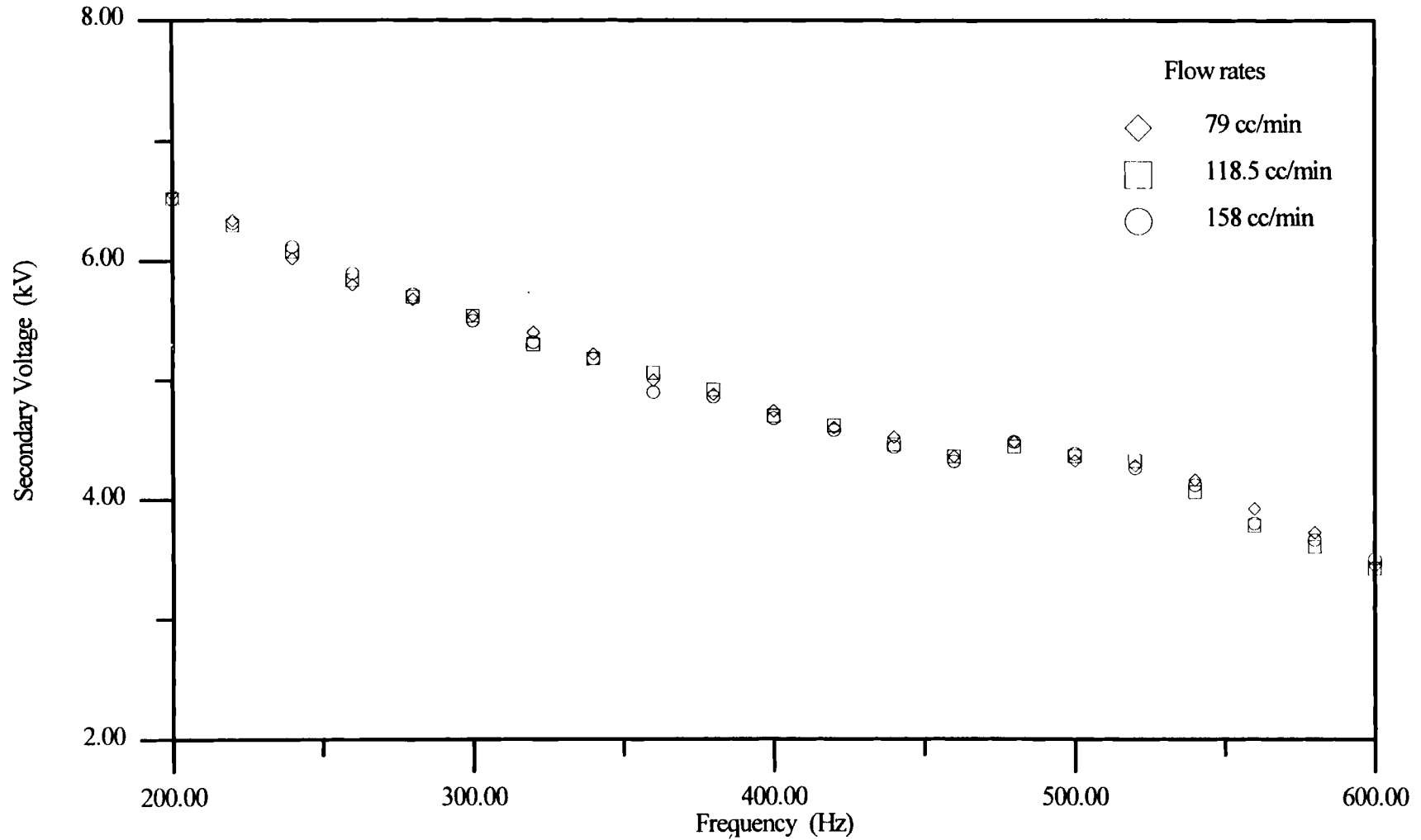


Figure 4.11. Dependence of secondary voltage on frequency for carbon dioxide at fixed flow rates for reactor B and a primary voltage of 60 v.



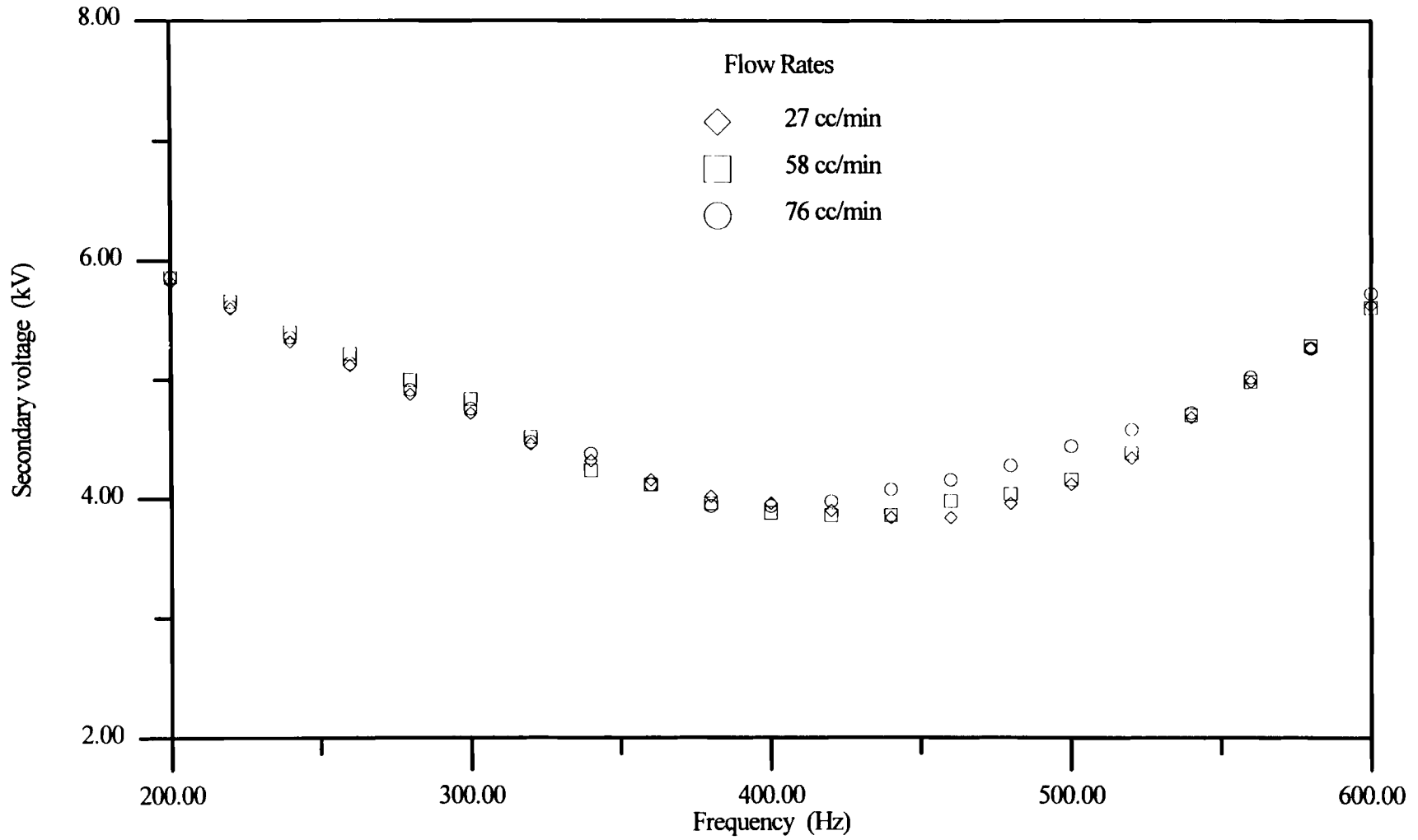


Figure 4.12. Dependence of secondary voltage on frequency for Hydrogen Sulfide at fixed flow rates for reactor B and a primary voltage of 60 v.

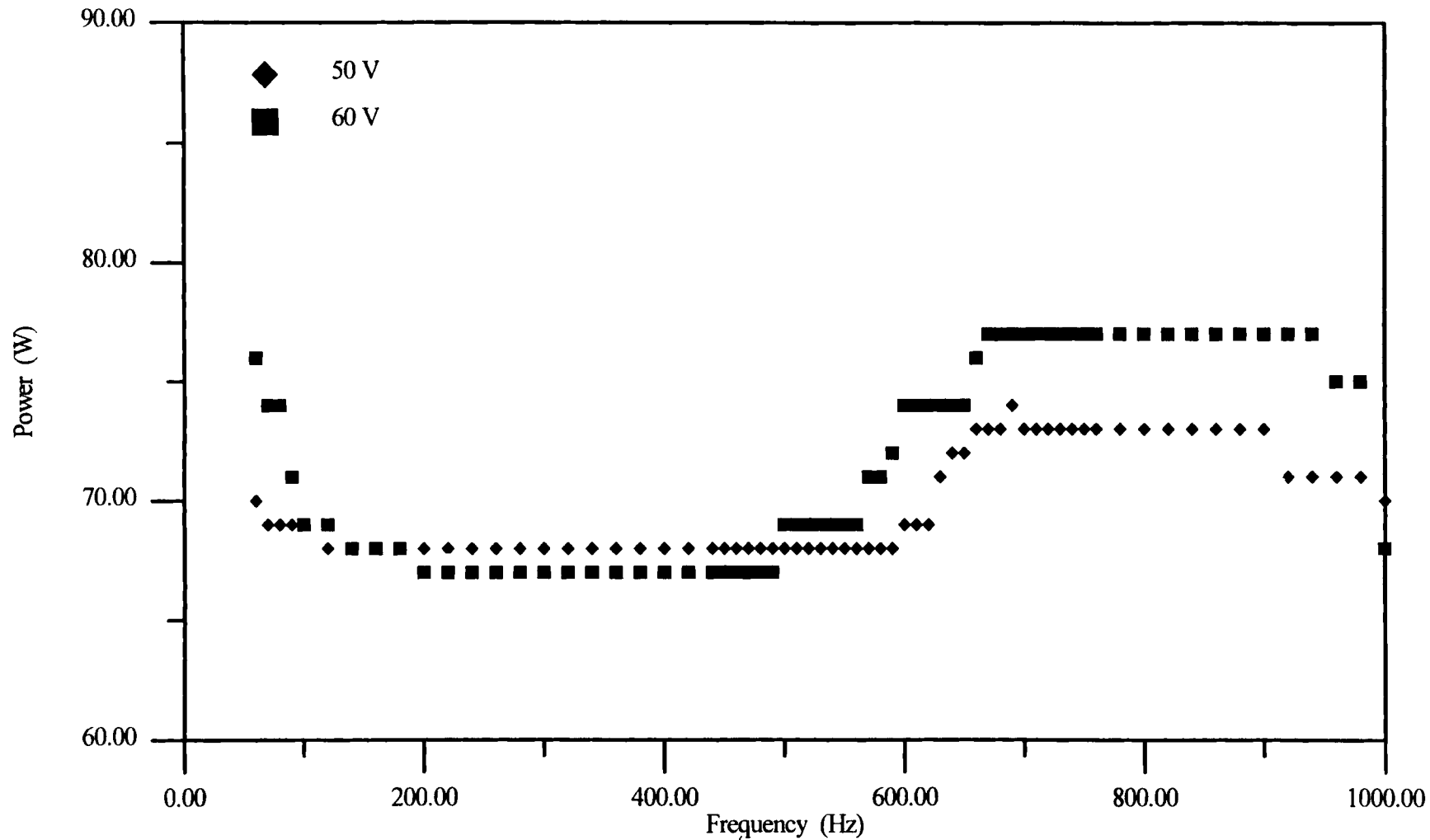


Figure 4.13. Dependence of power on frequency for Carbon dioxide at fixed primary voltages for reactor B and a flow rate of 79 cc/min.

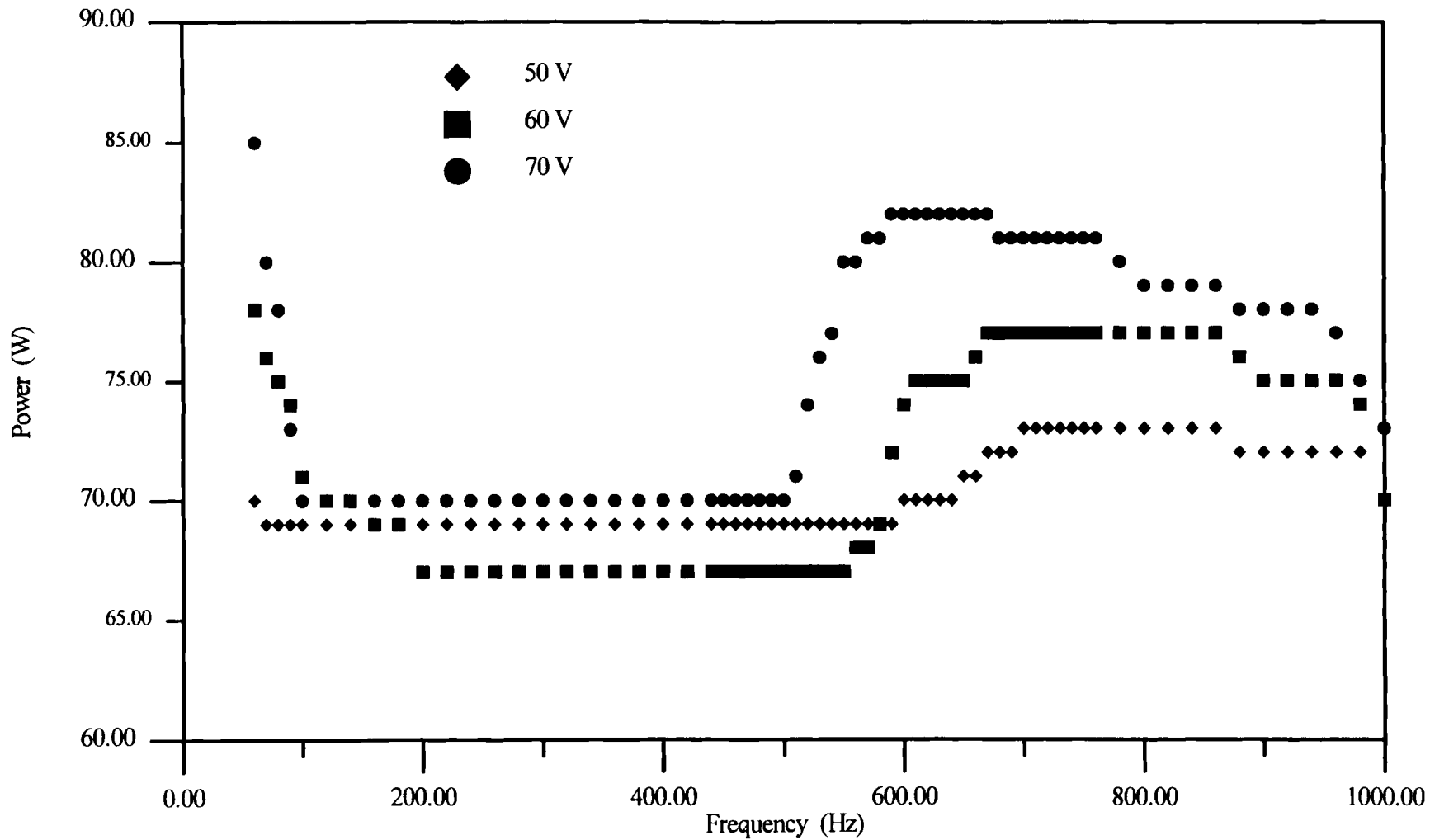


Figure 4.14. Dependence of power on frequency for Hydrogen Sulfide at fixed primary voltages for Reactor B and a flow rate of 27 cc/min.

At a fixed primary voltage the power consumption dropped initially from a maximum at 60 Hz, remained constant until the frequency at which the plasma started, then increases, stays constant and then decreases. This initial drop in the power level can be explained from the fact that the transformer used in this work is designed in such a way that the maximum power is at 60 Hz. The power consumption is maximum at optimum conditions also called as resonance. At resonance the impedance, voltage through the capacitor of the parallel circuit is maximum, hence the maximum power.

It was observed that wire wrapped outside in the form of coil gives maximum power levels at a point frequency whereas the mesh wrapped outer configuration gives maximum levels over a range of frequencies.

### Effect of Transformer on Plasma Behavior

The change of transformer effects the electrical behavior of the system. Figures 4.15 and 4.16 show the effect of the two different transformers used in this experiments. Although the general trends are the same, an optimum frequency exists at which the power and secondary voltage are maximum, but there is difference in the magnitude and the electrical behavior of the system. From graph 4.15 we can see that the secondary voltage increased slowly, initially and then sharply at the optimum condition and decreased for transformer1. The secondary voltage was almost constant for a while, then increases and then decreases after optimum condition is reached. The secondary

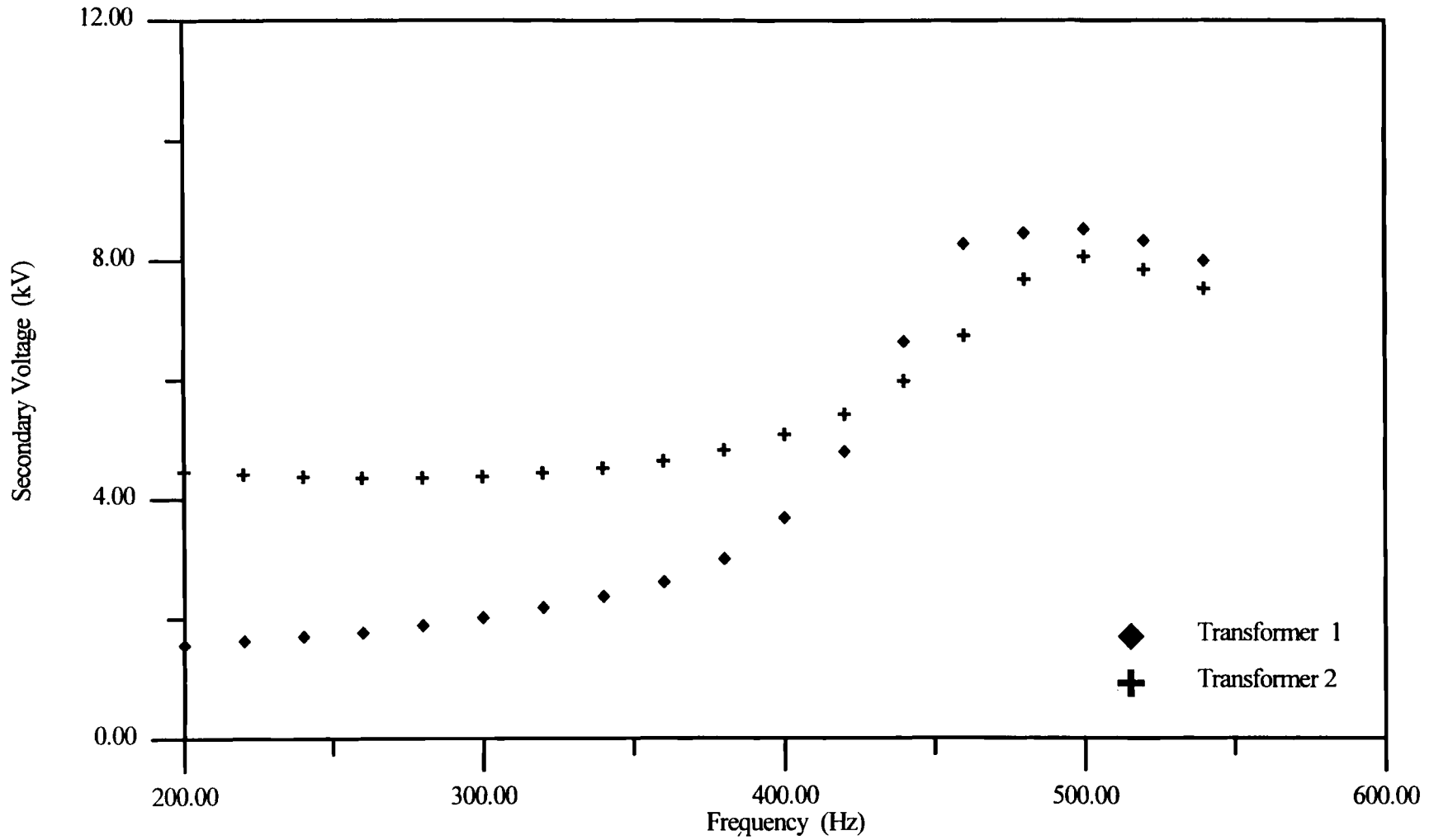


Figure 4.15. Effect of transformer on secondary voltage for air at a primary voltage of 40 V and for reactor C.

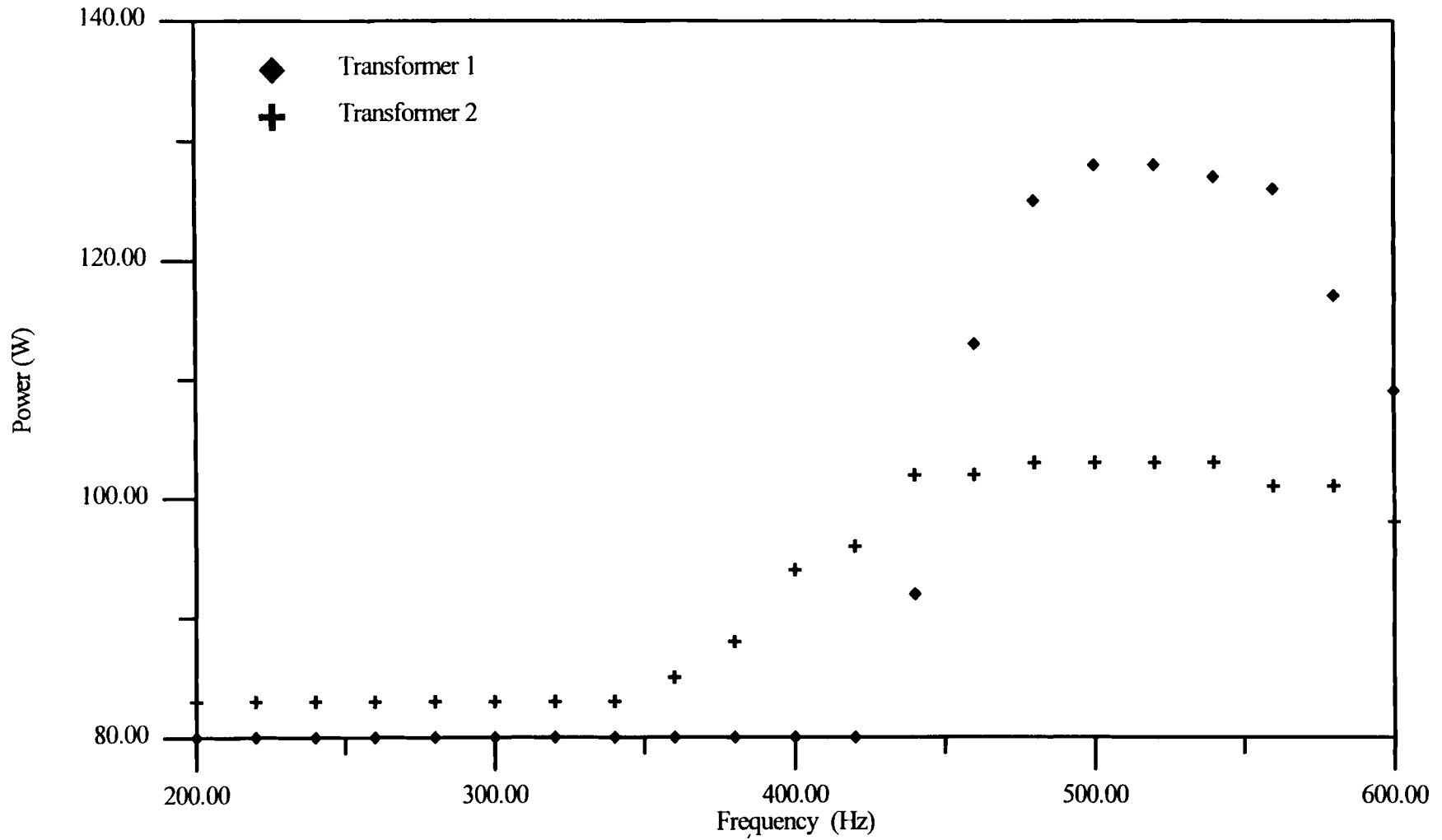


Figure 4.16. Effect of transformer on power for air at a fixed primary voltage of 40 V and for reactor C.

voltage was maximum for a range of frequencies for transformer1 and was maximum at a single frequency for transformer2 for the same configuration.

From graph 4.16 we can see that the maximum power level for transformer2 was constant for a larger range of frequencies at a lower magnitude compared to transformer1. This behavior in electrical characteristics can be due to the difference in the design of transformer such as the number of windings, etc.

### Error Analysis

The maximum deviation from the original reading was  $\pm 30$  volts in the secondary voltage,  $\pm 10$  Hz in optimum frequency and  $\pm 1$  W in power. The deviation in secondary voltage is higher at the optimum conditions and was found to be  $\pm 80$  volts.

## CHAPTER V

### DESTRUCTIVE TESTS

The primary objective of these experiments was to study whether or not hydrogen sulfide can be decomposed in the presence of carbon dioxide and how the conversion of hydrogen sulfide is affected by primary voltage, frequency, flow rate and humidity variations. The experimental procedure, which is divided into two parts, consists of runs with pure hydrogen sulfide and the second part includes runs with a mixture of carbon dioxide and hydrogen sulfide. The results of these experiments are presented in graphical manner and discussed in the sections below.

#### Procedure

The experimental procedure followed during the course of these experiments is given below.

1. The reactor with the desired electrode configuration was thoroughly cleaned with acetone and dried. It was placed in the experimental setup and all the electrical connections were made.



2. After the flow connections were made and checked for leakage , the inlet valve to the reactor was opened and nitrogen gas was allowed to pass through the reactor as a purge gas.
3. After nitrogen is allowed to pass through the reactor for sufficient time, the valve connecting the hydrogen sulfide tank is opened. When doing runs with a hydrogen sulfide and carbon dioxide mixture, both the valves were opened and the flow rates were adjusted in a pre-calculated way to achieve molar ratios of approximately 10/90, 50/50 and 90/10 (hydrogen sulfide/carbon dioxide).
4. Depending on the flow rate, sufficient time was allowed to lapse for the nitrogen to pass out of the reactor before starting a destructive run.
5. Secondary voltage, power input and atmospheric temperature were recorded at the end of a run and then the reactor was switched off and the time of the run was also recorded.
6. H<sub>2</sub>S was shut off and nitrogen was passed through the reactor in order to purge the system of H<sub>2</sub>S. When dealing with a mixture of gases both the valves were shut off and then nitrogen was passed through the system.
7. The reactor was then dismantled and the sulfur deposits are dissolved in carbon disulfide and carefully collected in previously weighed bottles.
8. The solution was then set in a hood for the solvent to evaporate, leaving sulfur behind.
9. The above procedure was repeated for different frequencies and at different primary voltages and flow rates.

Calculation of hydrogen sulfide conversion was based on ideal gas behavior. The details for the calculation are given in appendix A. The key factor in these calculations is the amount of sulfur recovered. Experimental data are tabulated in appendix C.

### Dependence of H<sub>2</sub>S Conversion on Frequency

Figure 5.1 and 5.2 and illustrates the dependence of H<sub>2</sub>S conversion on frequency at fixed primary voltages. It is seen that as the frequency is increased, the dissociation of hydrogen sulfide to hydrogen and sulfur does not start until it reaches a certain frequency. The conversion then increases with the frequency and remains constant over a range of frequencies, and then decreases. The same trend was observed by Desai[7]. Figures 5.3, 5.4, 5.5, 5.6, 5.7 and 5.8 illustrate the dependence of H<sub>2</sub>S conversion on frequency for a mixture of hydrogen sulfide and carbon dioxide at approximate molar ratio of 10/90, 50/50 and 90/10, respectively. The graphs followed the same trend as that of pure hydrogen sulfide.

### Dependence of H<sub>2</sub>S Conversion on Primary Voltage

Figures 5.9, 5.10, 5.11 and 5.12 shows dependence of H<sub>2</sub>S conversion on primary voltage for hydrogen sulfide and a mixture of hydrogen sulfide and carbon dioxide mixed at approximate molar ratio of 10/90,50/50 and 90/10, respectively. From these graphs it can be seen that the conversion increases with increase in primary voltage. Very high

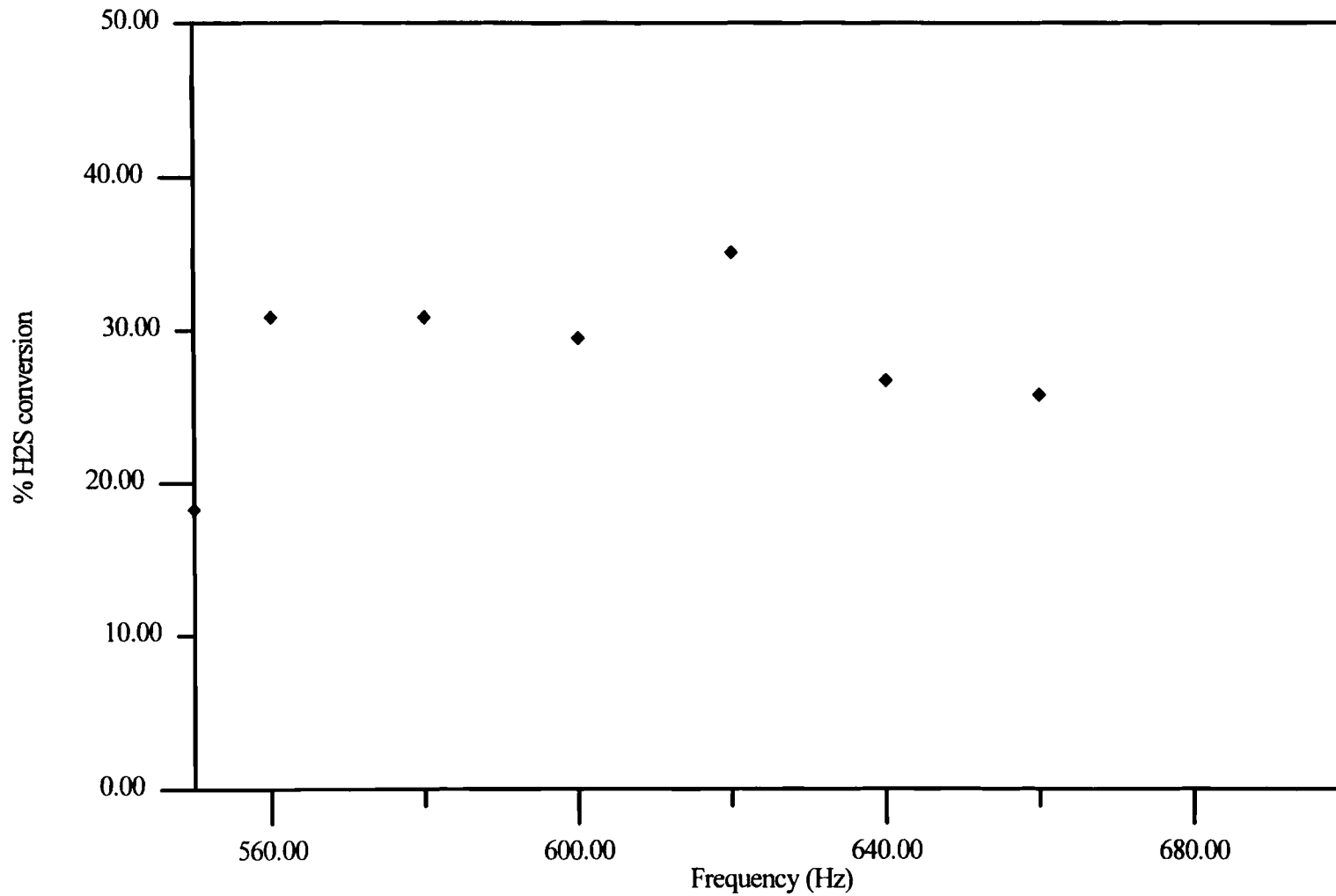


Figure 5.1. Dependence of pure H<sub>2</sub>S conversion on frequency at a primary voltage of 80 volts and a flow rate of 50.7 cc/min using reactor B.

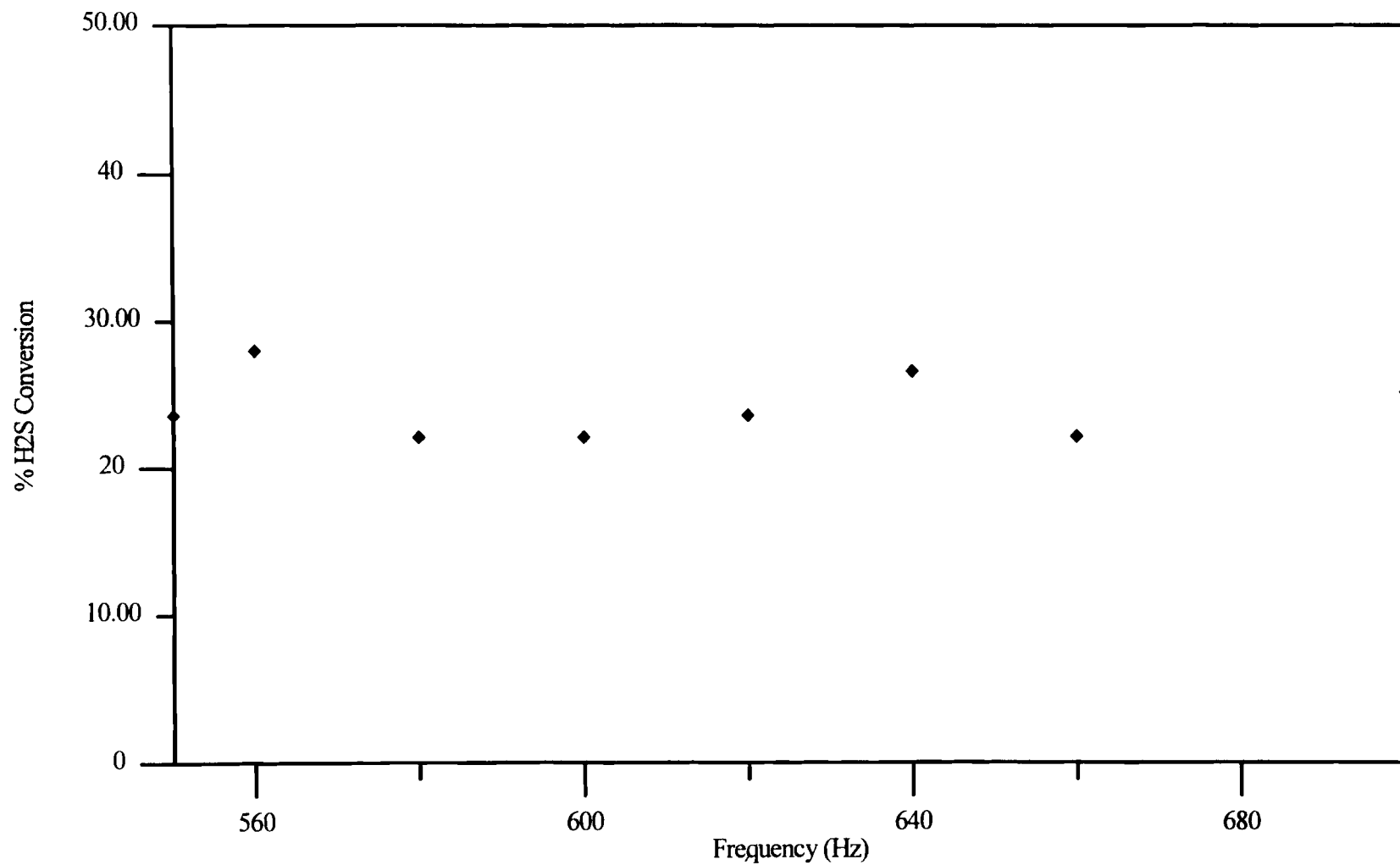


Figure 5.2. Dependence of H<sub>2</sub>S conversion on frequency at primary voltage of 70 V and a flow rate of 50.7 cc/min using reactor B.

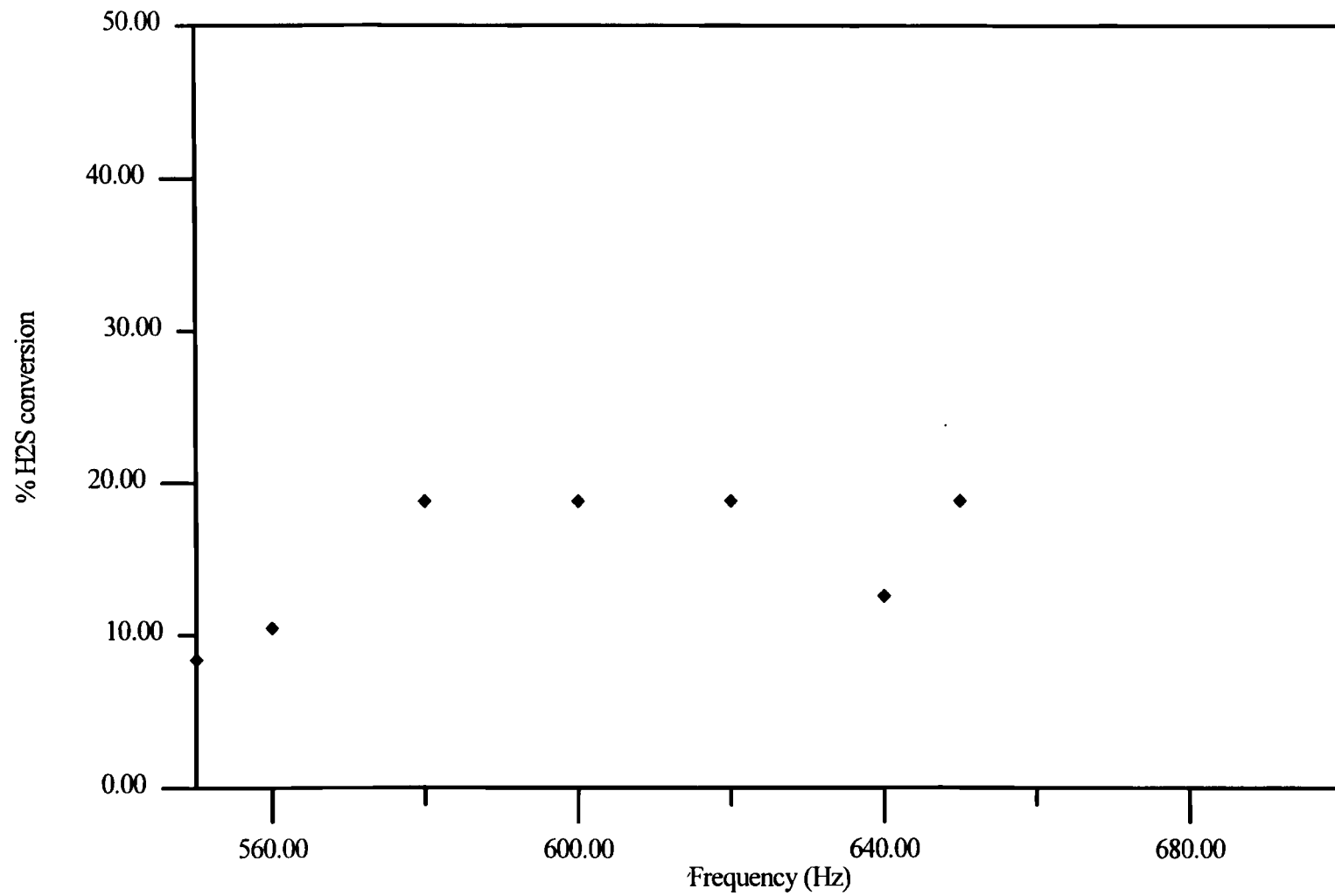


Figure 5.3. Dependence of H<sub>2</sub>S conversion on frequency at a primary voltage of 80 volts in the presence of CO<sub>2</sub> at a H<sub>2</sub>S/CO<sub>2</sub> molar ratio of 10/90 using reactor configuration B.

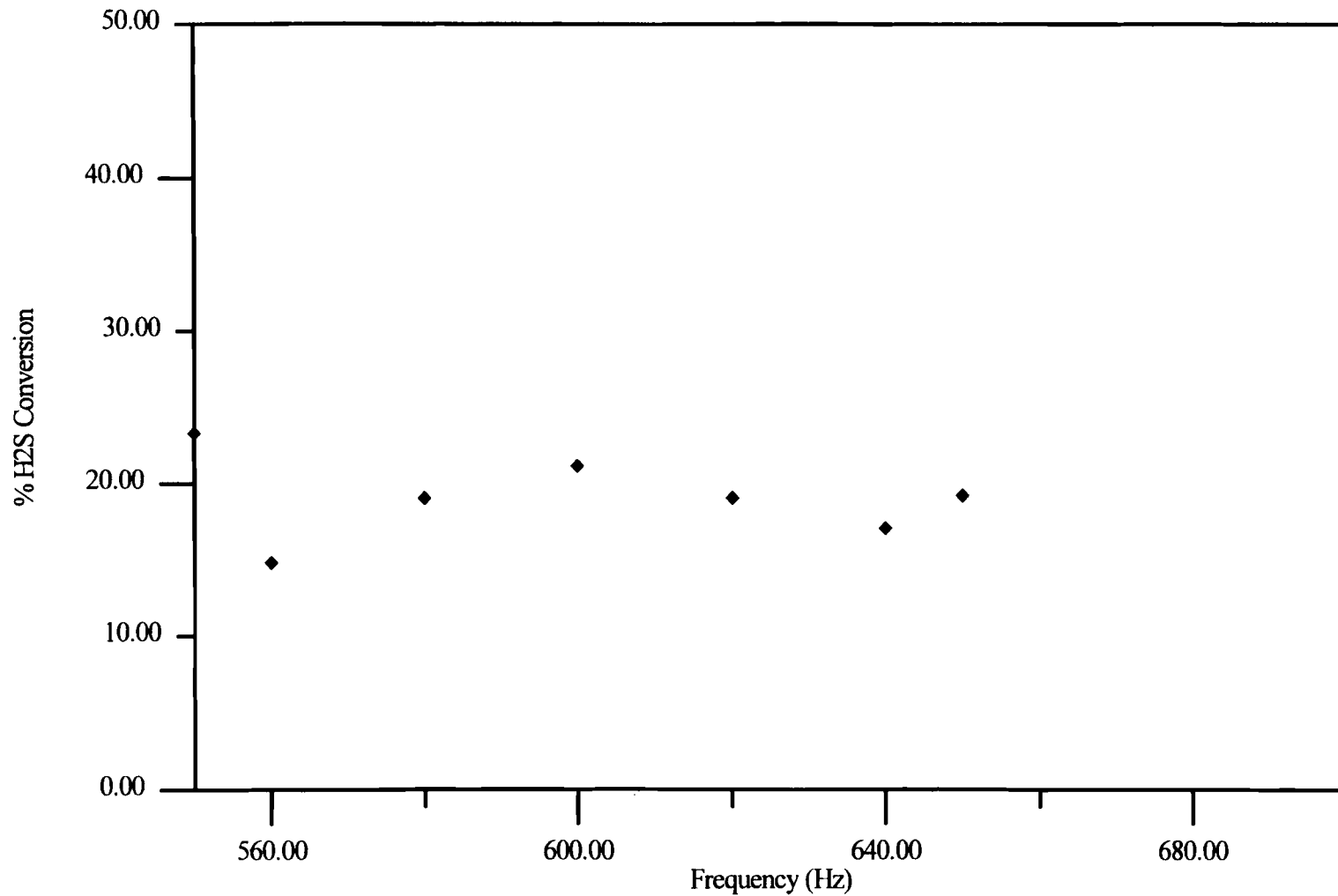


Figure 5.4. Dependence of H<sub>2</sub>S conversion on frequency at a primary voltage of 70 volts in the presence of CO<sub>2</sub> at a H<sub>2</sub>S/CO<sub>2</sub> molar ratio of 10/90 using reactor configuration B.

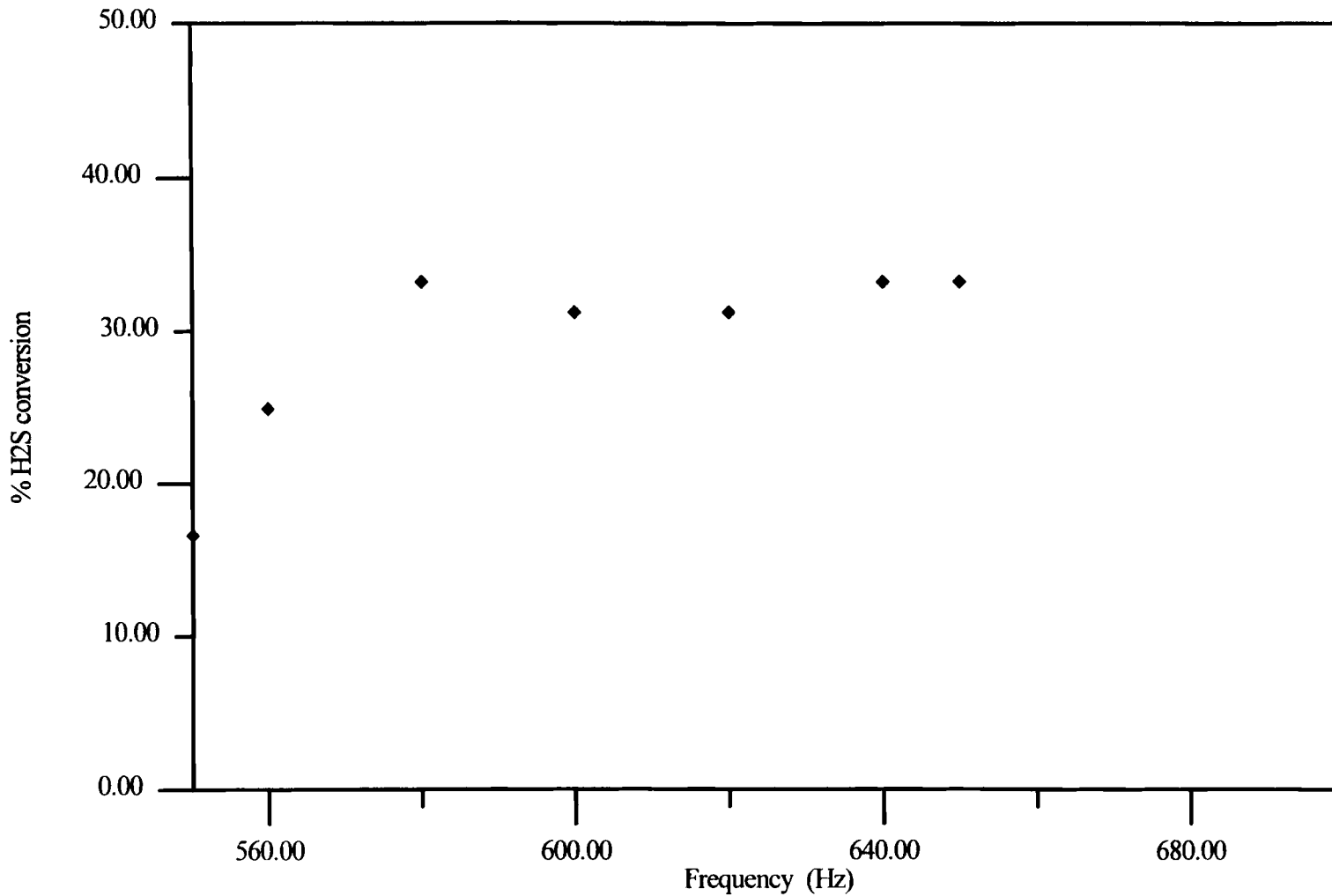


Figure 5.5. Dependence of H<sub>2</sub>S conversion on frequency at a primary voltage of 80 V in the presence of CO<sub>2</sub> at a H<sub>2</sub>S/CO<sub>2</sub> molar ratio of 50/50 using reactor configuration B.

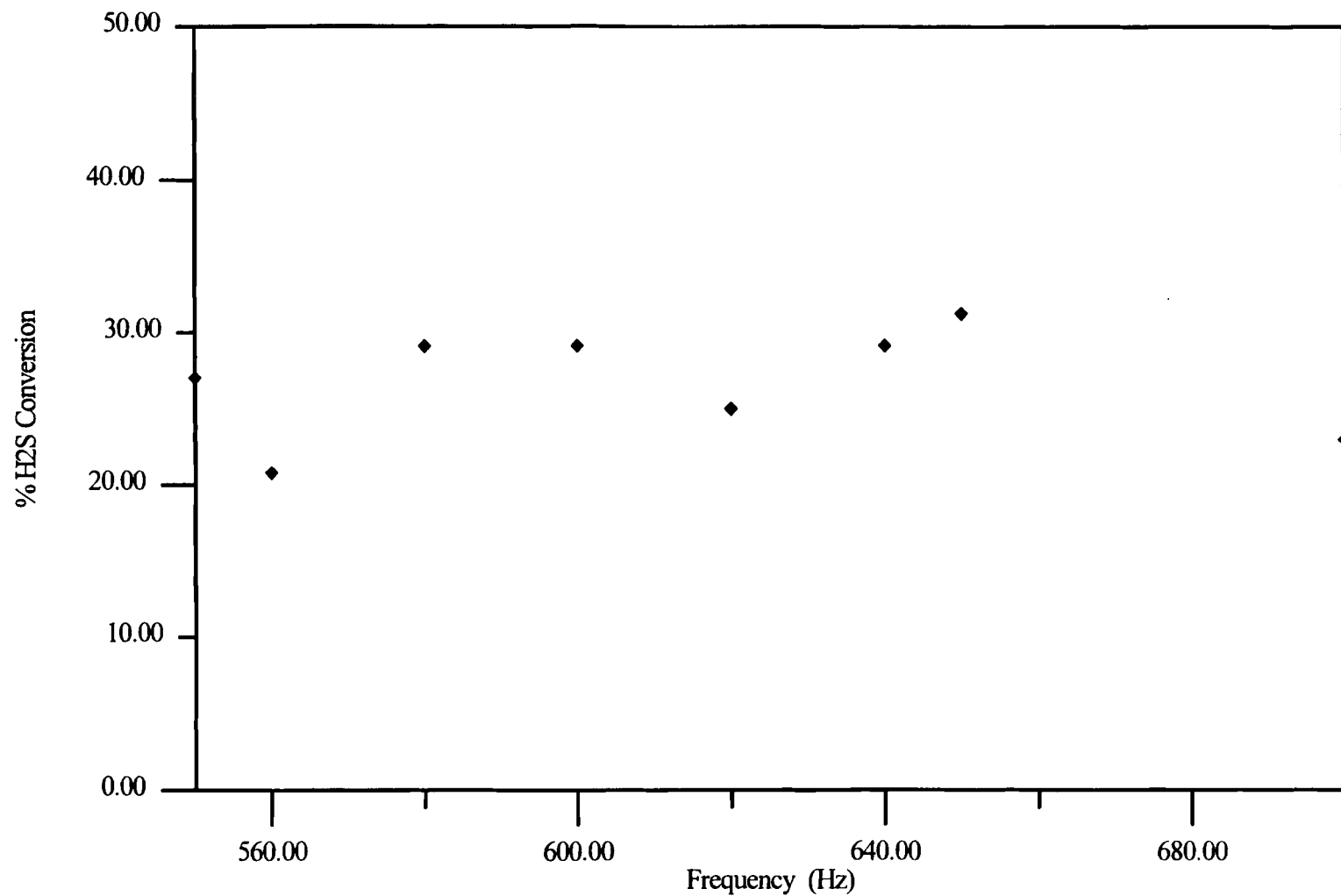


Figure 5.6. Dependence of H<sub>2</sub>S conversion on frequency at a primary voltage of 70 V in the presence of CO<sub>2</sub> at a H<sub>2</sub>S/CO<sub>2</sub> molar ratio of 50/50 using Reactor B.



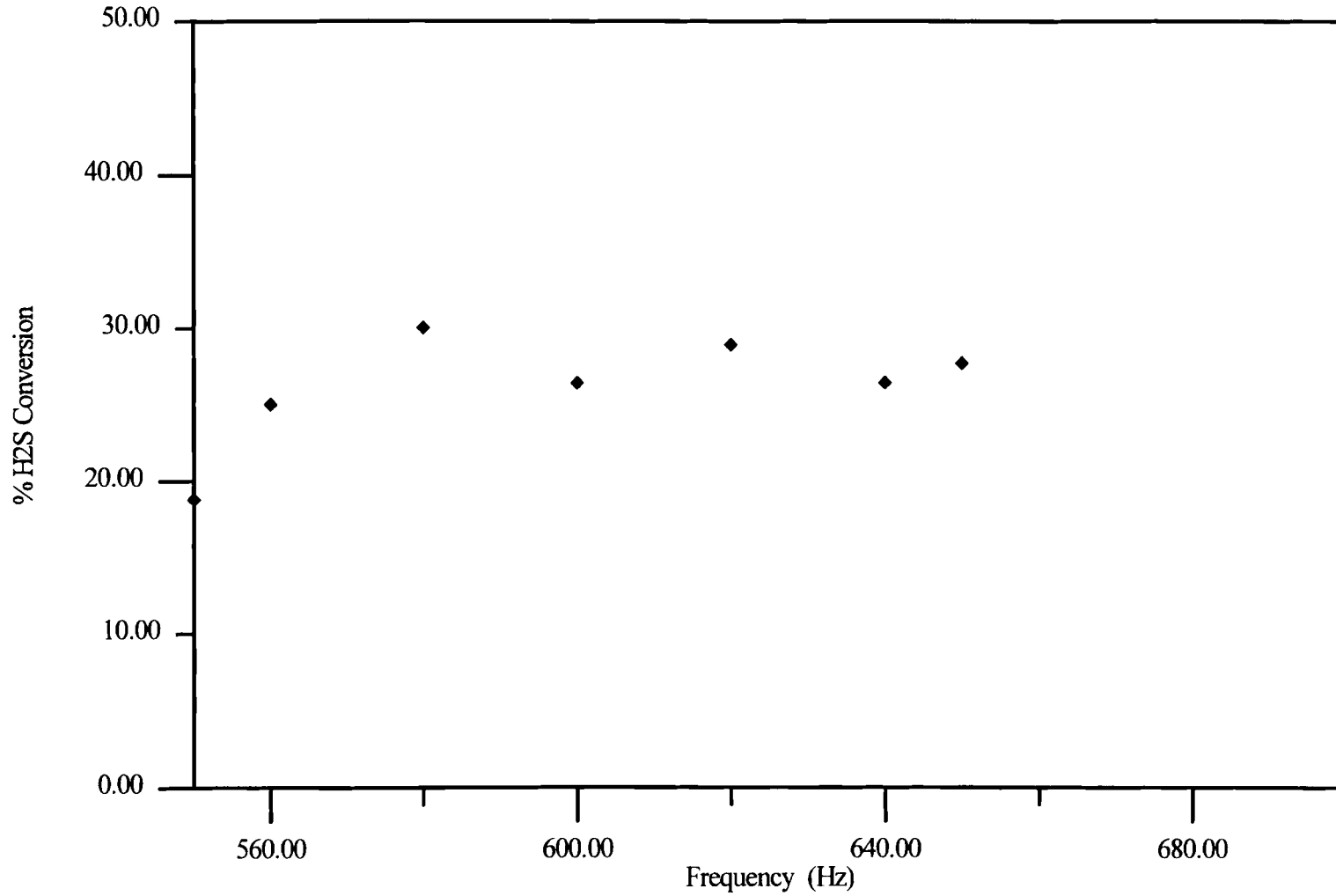


Figure 5.7. Dependence of H<sub>2</sub>S conversion on frequency at a primary voltage of 80 V in the presence of CO<sub>2</sub> at a H<sub>2</sub>S/CO<sub>2</sub> molar ratio of 90/10 using reactor configuration B.

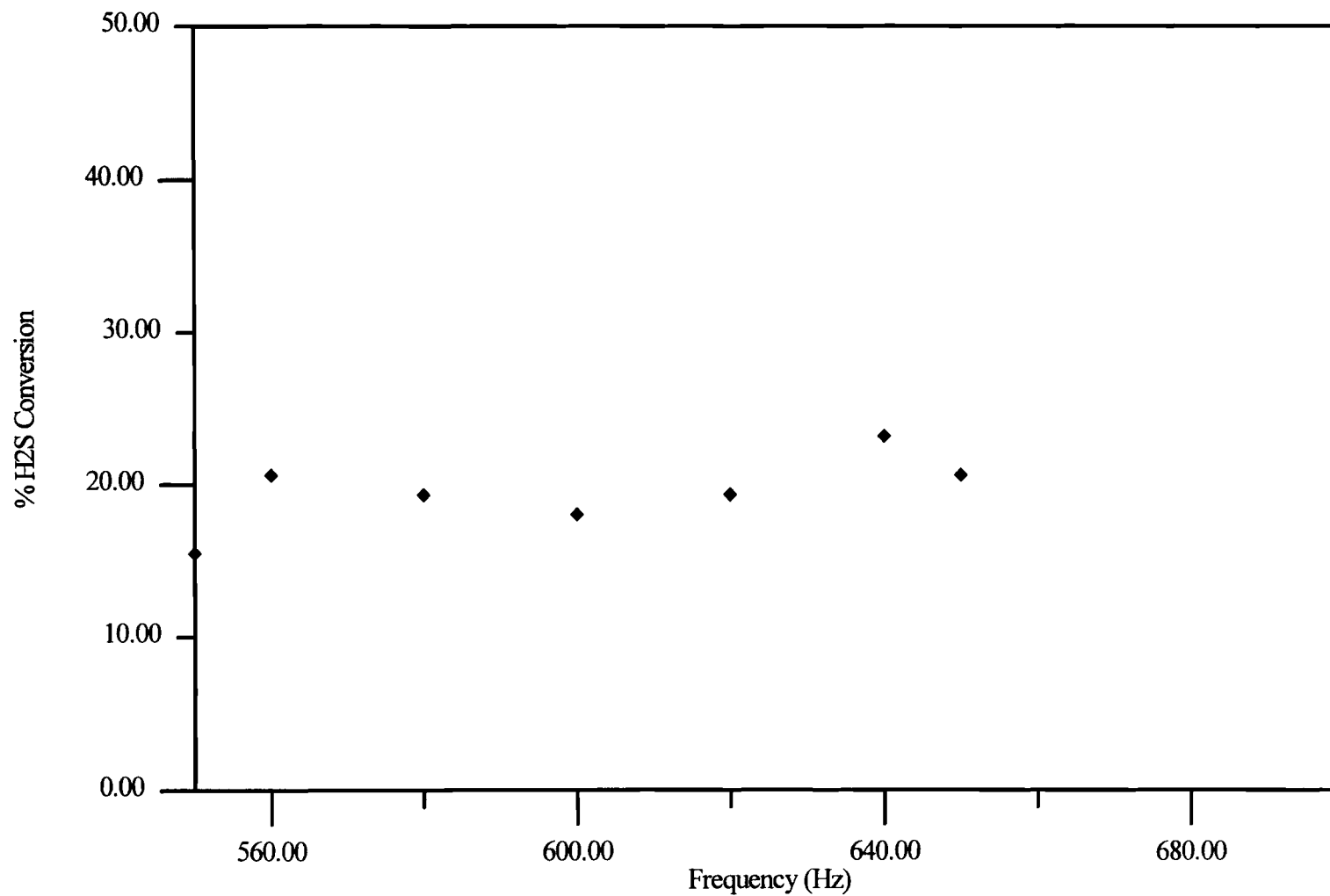


Figure 5.8. dependence of H<sub>2</sub>S conversion on frequency at a primary voltage of 70 V in the presence of CO<sub>2</sub> at a H<sub>2</sub>S/CO<sub>2</sub> molar ratio of 90/10 using reactor configuration B.

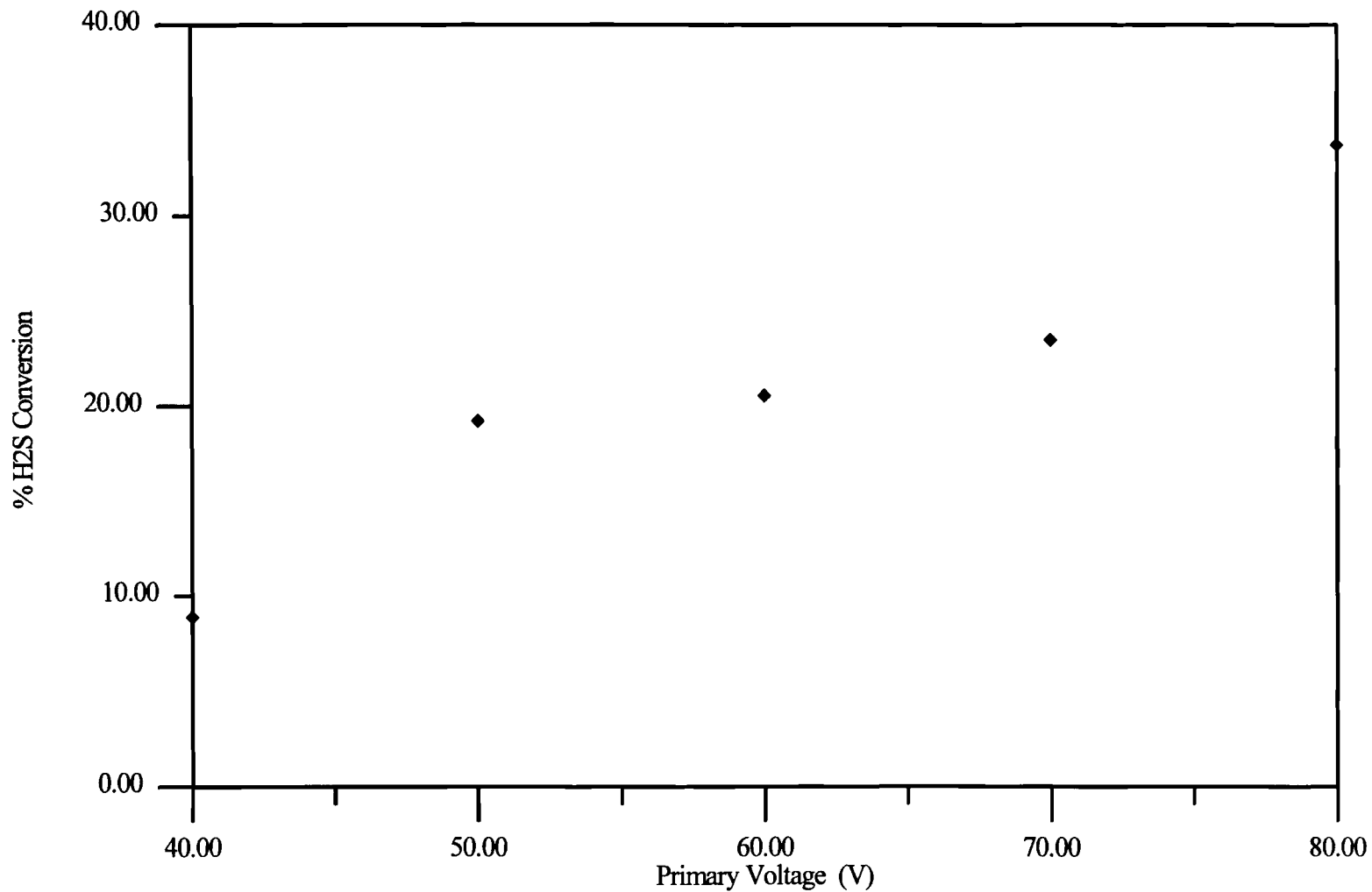


Figure 5.9. Effect of primary voltage on H<sub>2</sub>S conversion at a flow rate of 50.7 cc/min and a frequency of 600 Hz using reactor configuration B.

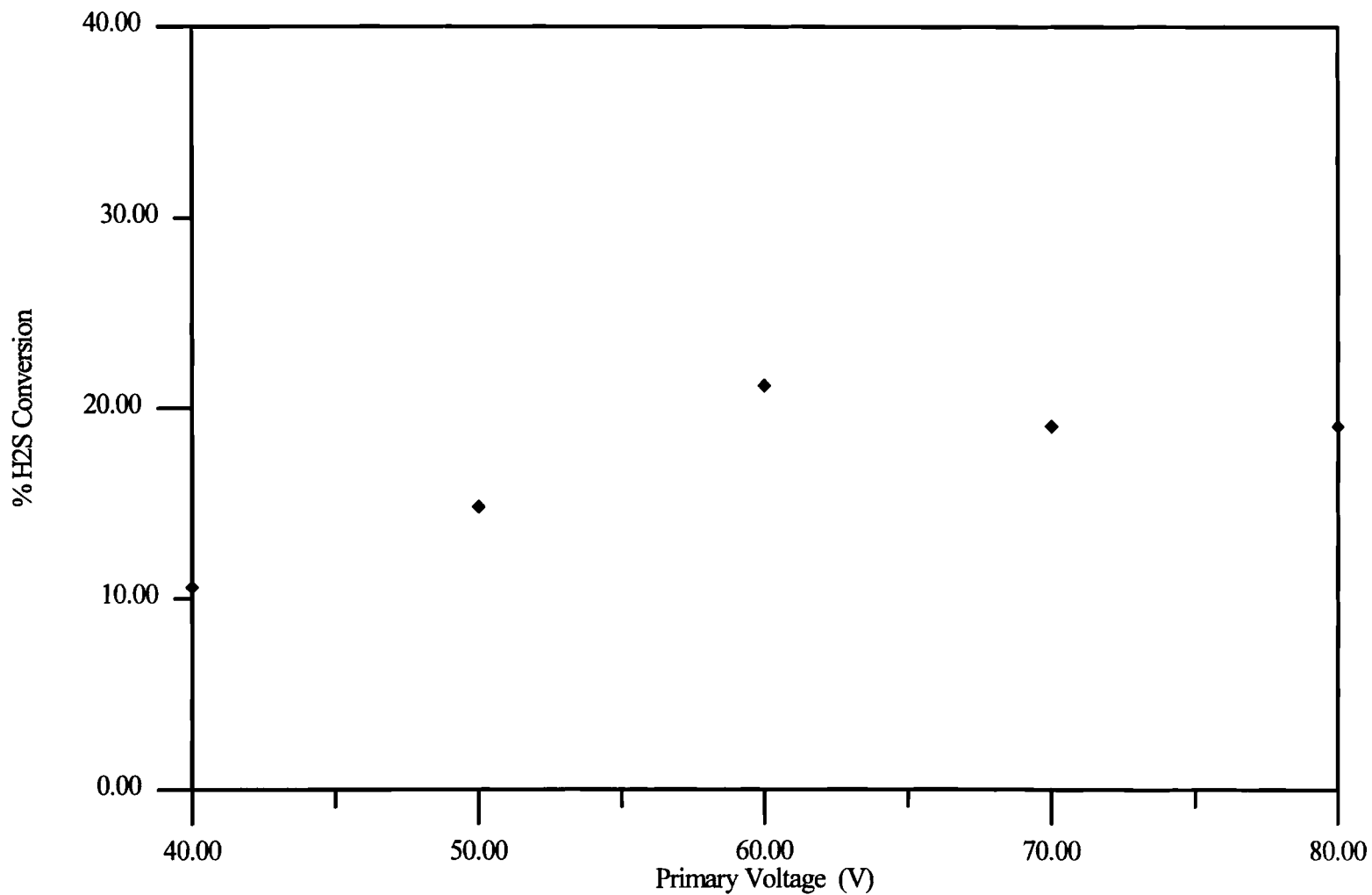


Figure 5.10. Effect of primary voltage on H<sub>2</sub>S conversion at a frequency of 600 Hz in the presence of CO<sub>2</sub> at a H<sub>2</sub>S/CO<sub>2</sub> molar ratio of 10/90 using reactor configuration B.

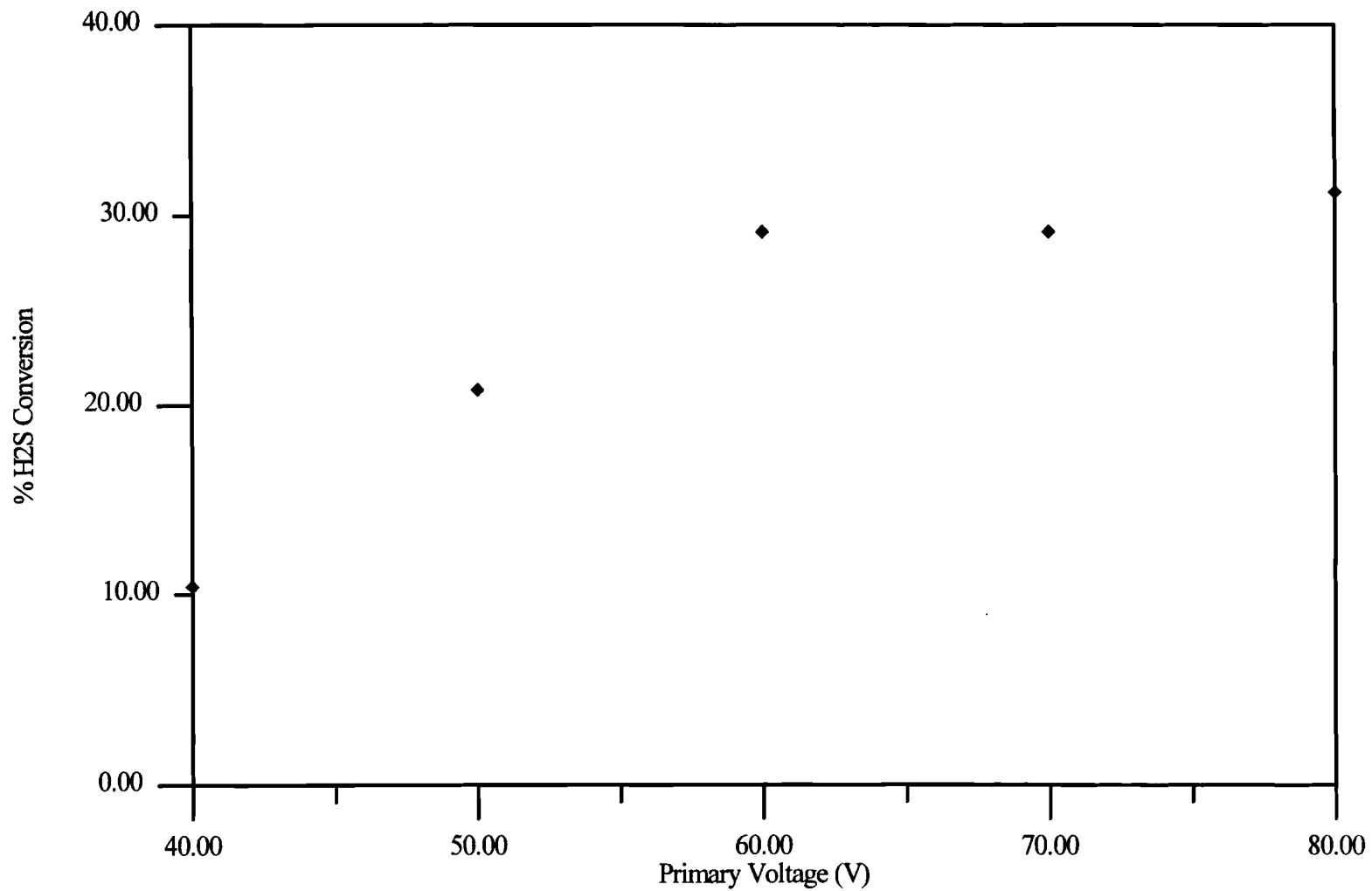


Figure 5.11. Effect of primary voltage on H<sub>2</sub>S conversion at a frequency of 600 Hz in the presence of CO<sub>2</sub> at a H<sub>2</sub>S/CO<sub>2</sub> molar ratio of 50/50 using reactor configuration B.

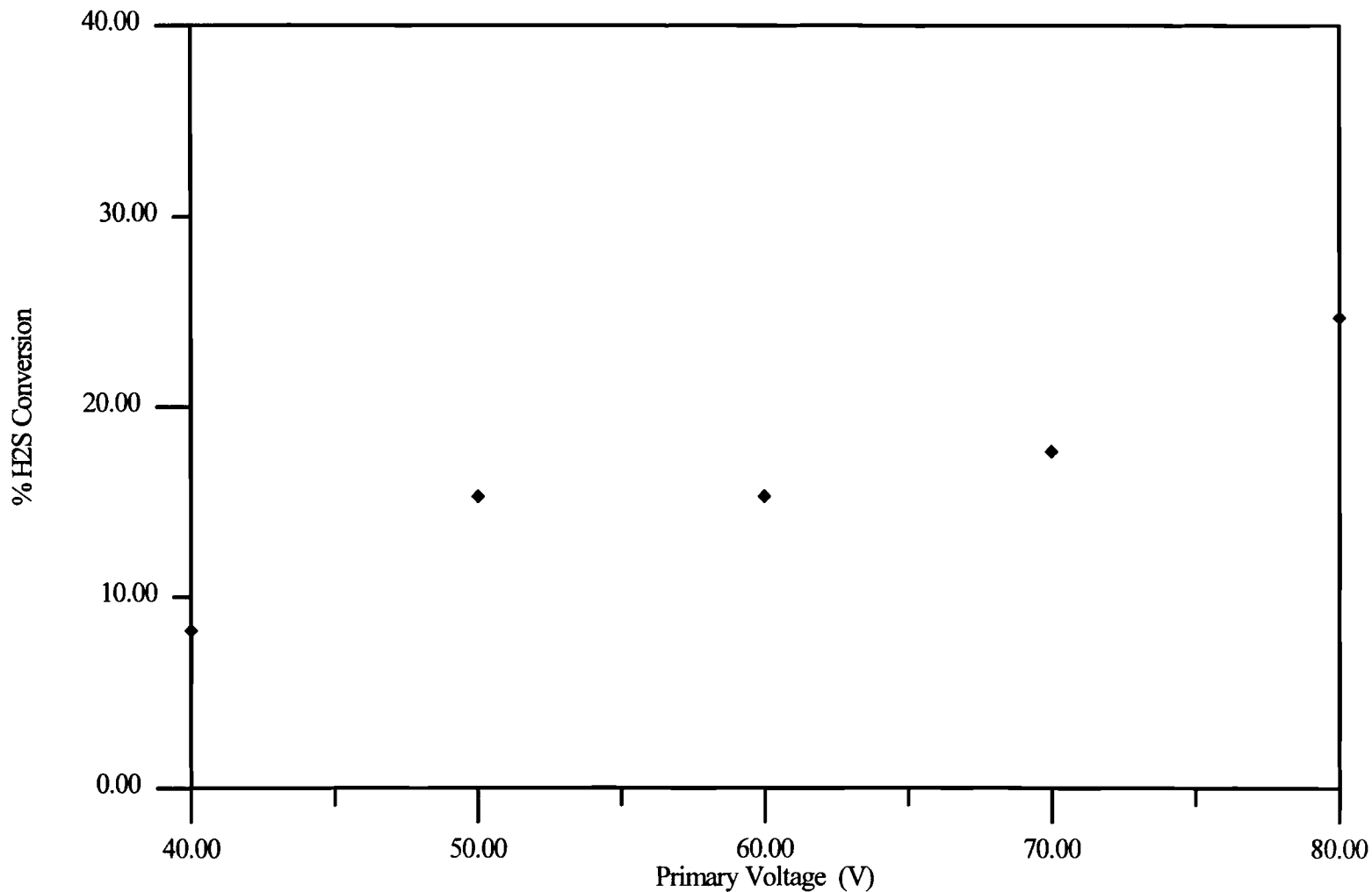


Figure 5.12. Effect of primary voltage on H<sub>2</sub>S conversion at a frequency of 600 Hz in the presence of CO<sub>2</sub> at a H<sub>2</sub>S/CO<sub>2</sub> molar ratio of 90/10 using reactor configuration B.

voltages were not tried due to arcing problems and damage to the transformer. The same trend was observed by several other authors working on alternating current plasmas as well as microwave plasmas.

#### Effect of increasing humidity on H<sub>2</sub>S conversion

Humidity was increased by bubbling H<sub>2</sub>S through water. From Figure 5.13 we can see that the conversions followed the same trend as that of dry gas. It can also be observed that the conversion rate increases with an increase in relative humidity (36.5%).

#### Dependence of H<sub>2</sub>S conversion on residence time

Figure 5.14 shows the dependence of H<sub>2</sub>S conversion on residence time for a fixed primary voltage and fixed frequency using reactor configuration B. The residence time was changed by varying the flow rate or by reducing the effective plasma volume, keeping the flow rate constant. Though the plasma reactions are assumed instantaneous it seems that more time is required in the reaction zone for the larger molecules to break. It can be seen from the figure that as the residence time increases the conversion increases. By changing the effective length of plasma zone and keeping the flow rate constant the degree of conversion changes significantly.

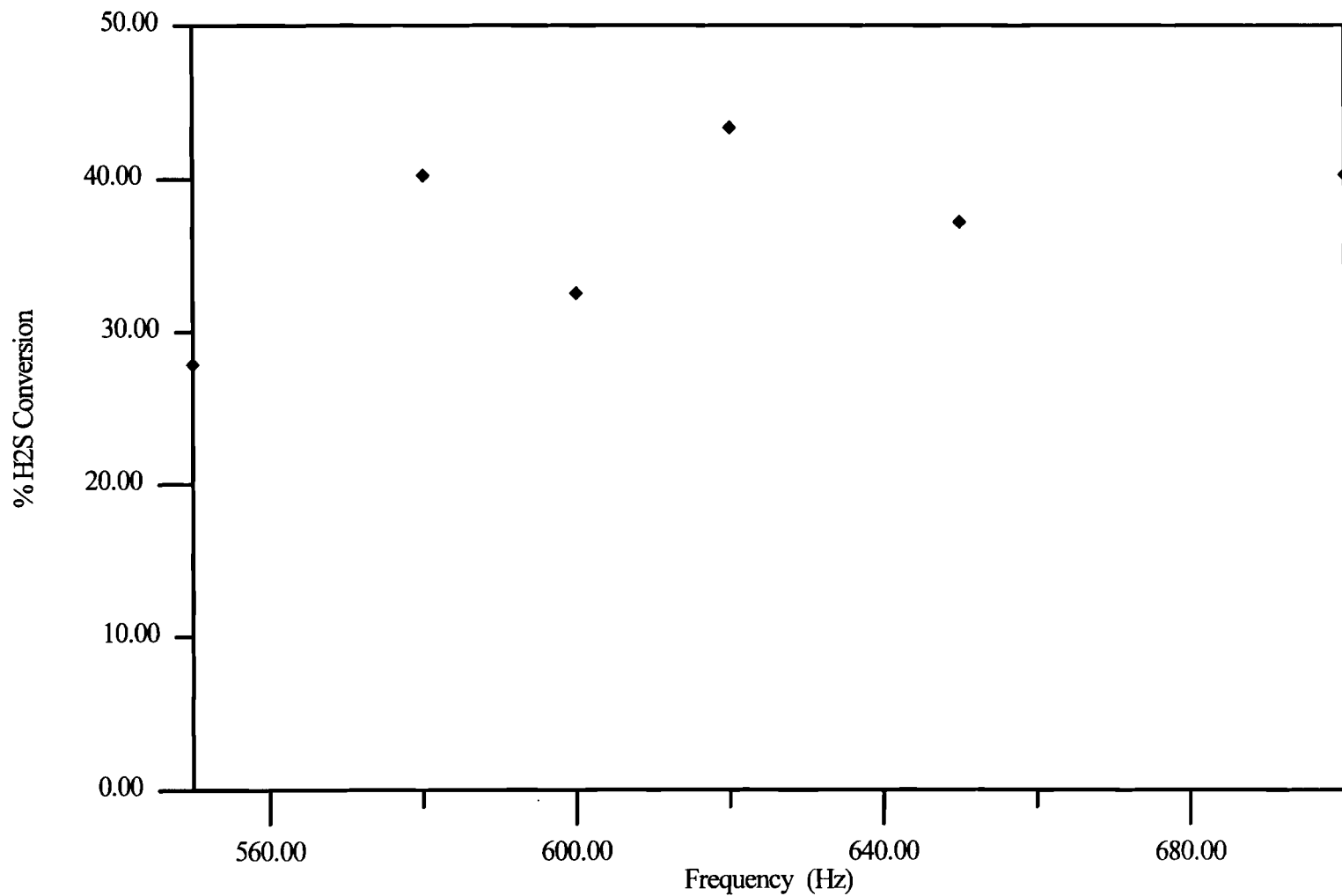


Figure 5.13. Effect of increasing humidity (36.5%) on H<sub>2</sub>S conversion at a primary voltage of 80 V and a flow rate of 48 cc/min using reactor configuration B.



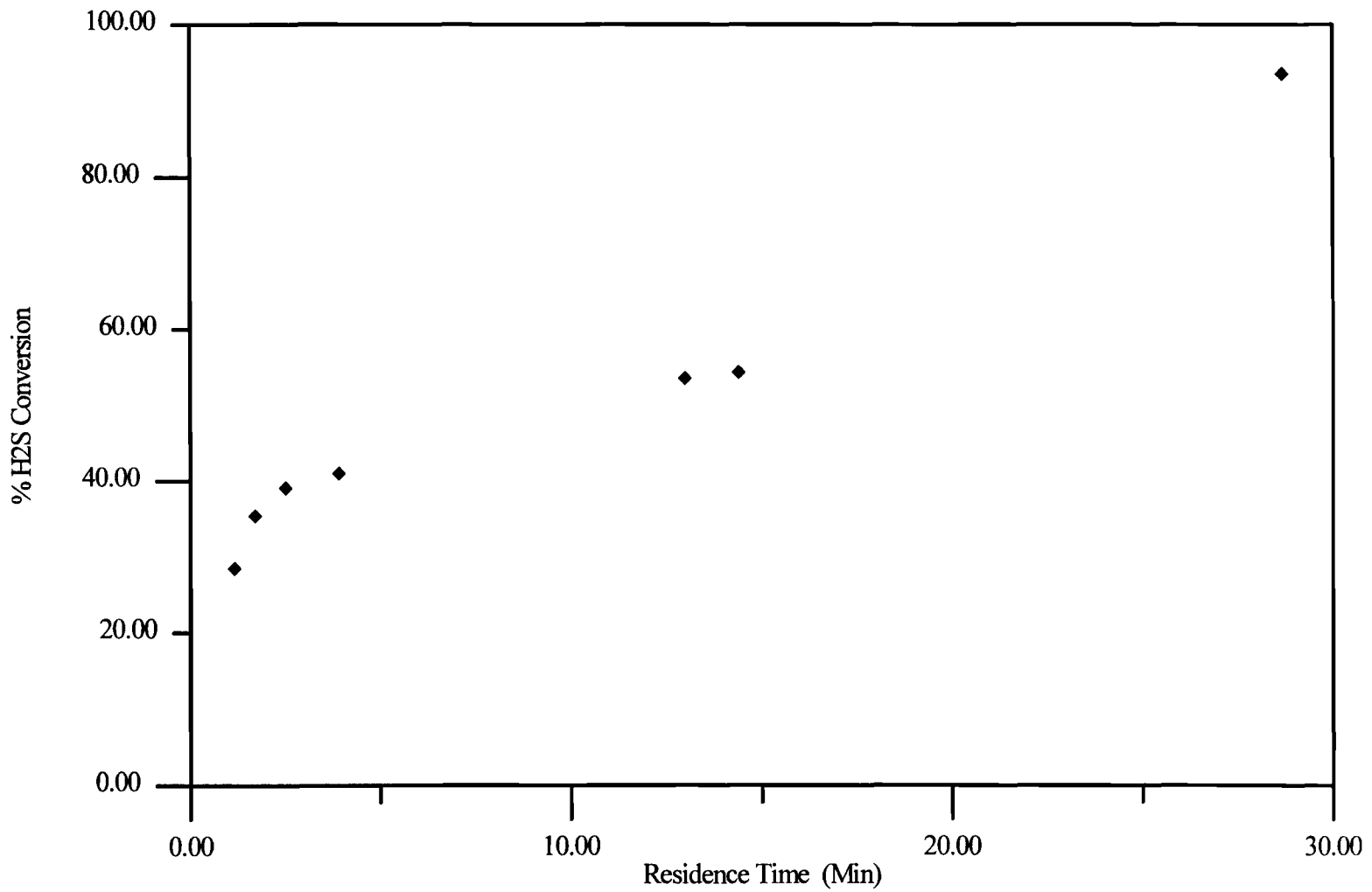


Figure 5.14. Effect of residence time on H2S conversion at a primary voltage of 80 V and at a frequency of 600 Hz using reactor configuration B.

### Dependence of H<sub>2</sub>S conversion on Duration of Experiment

Figure 5.15 shows that conversion of H<sub>2</sub>S increases initially and then remains constant. After a period of time the increase in conversion is balanced by the recombination of the sulfur formed.

### Dependence of H<sub>2</sub>S conversion on the presence of Carbon Dioxide

Figure 5.16 shows the conversion of H<sub>2</sub>S in the presence of carbon dioxide at different compositions. It can be seen from the graph that for a fixed flow rate as the mole fraction of H<sub>2</sub>S increases the conversion decreases. The conversion of H<sub>2</sub>S to hydrogen and sulfur is weakly effected by the presence of carbon dioxide.

### Reproducibility

Table 5.1 presents reproducibility data used to determine the experimental error. Data are presented for duplicate or triplicate data runs.

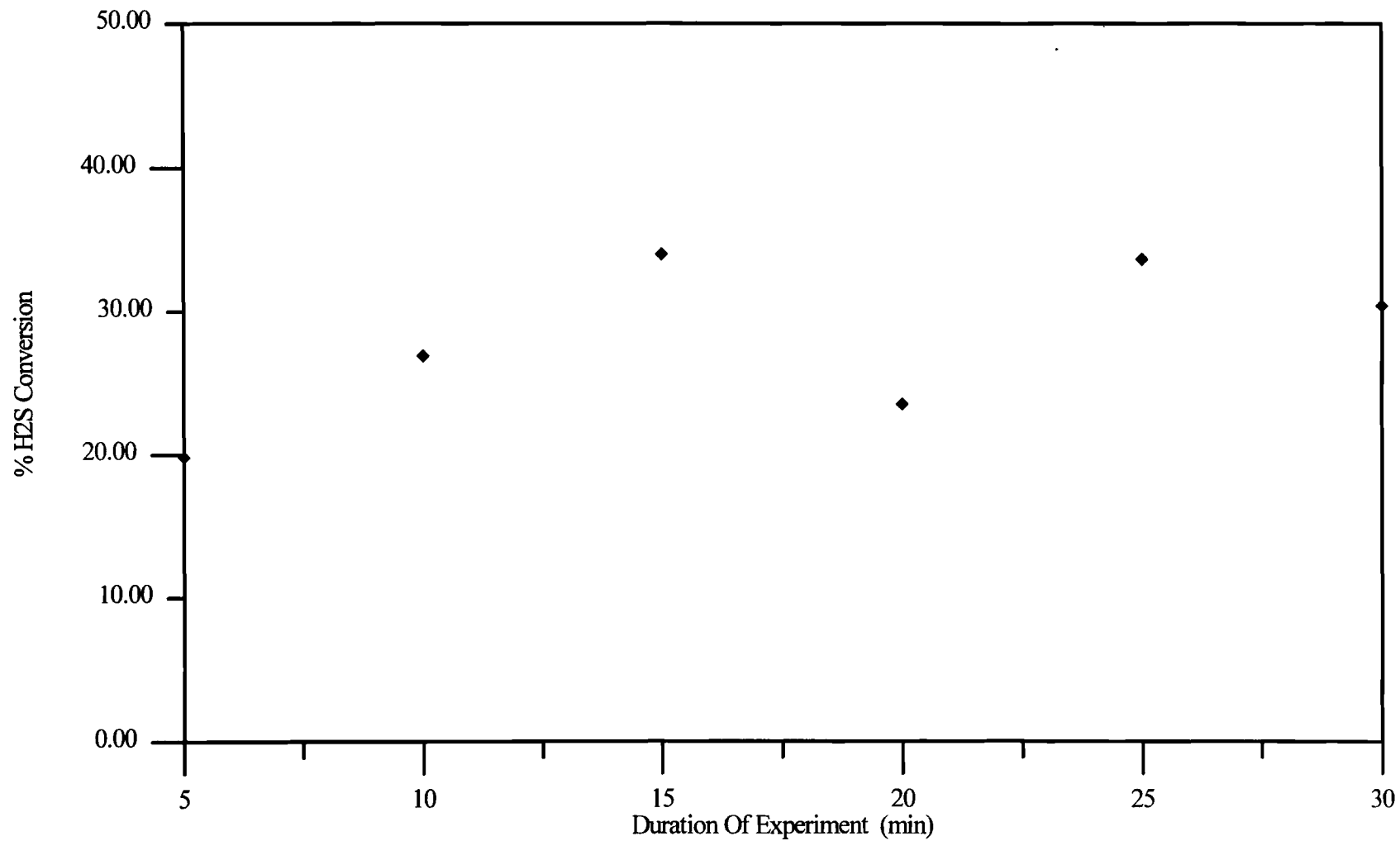


Figure 5.15. Dependence of H<sub>2</sub>S Conversion on duration of experiment at a primary voltage of 80 V and a flow rate of 50.7 cc/min using reactor configuration B.

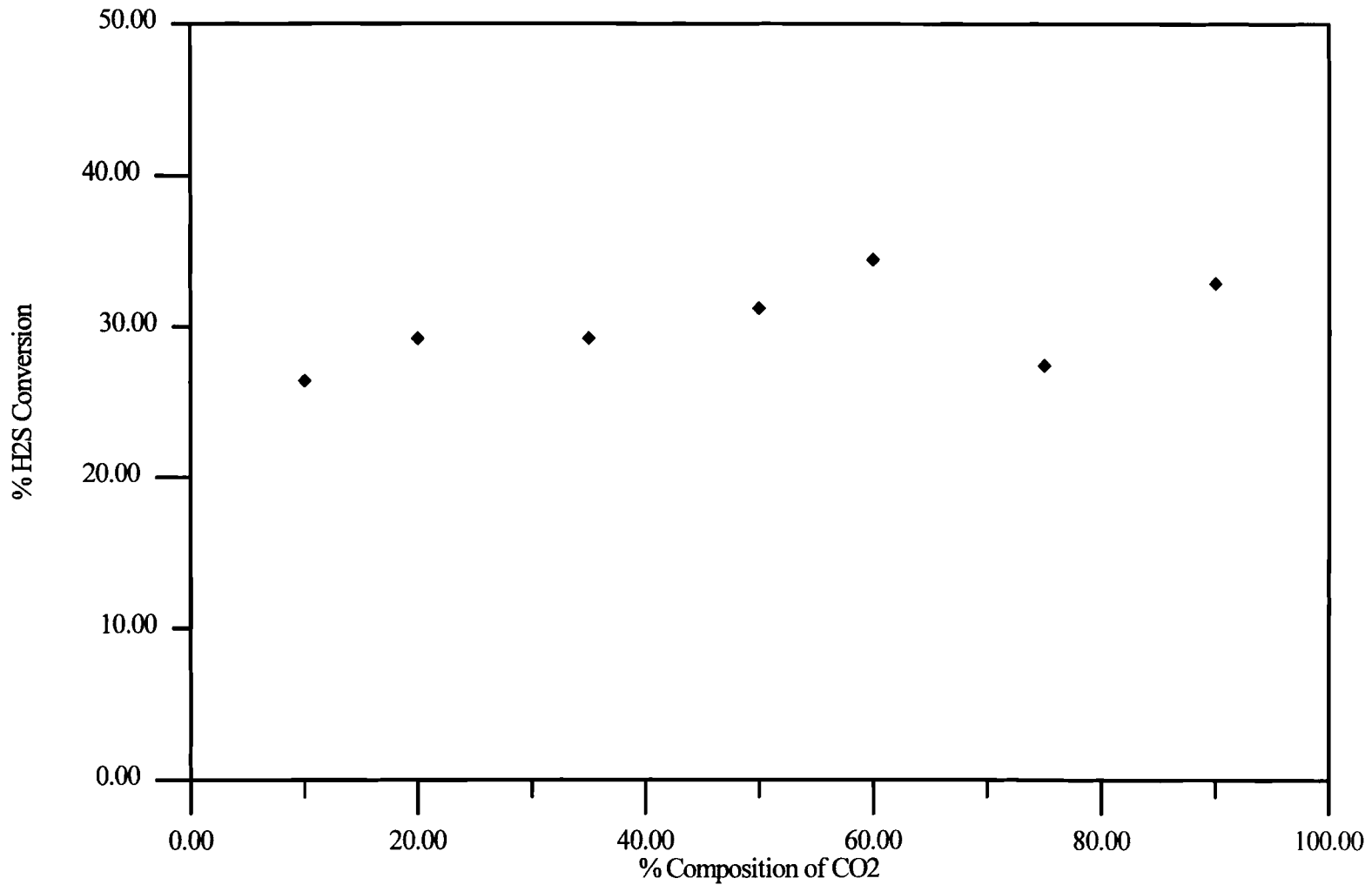


Figure 5.16. Effect of Carbon Dioxide composition on % H<sub>2</sub>S conversion at a primary voltage of 80 V, at a Frequency of 600 Hz and at a flow rate of 70 cc/min using reactor B configuration.

TABLE 5.1  
REPRODUCIBILITY DATA

Sr. No.	Reactor config.	Frequency Hz	Prim.Volt V	Flow rate cc/min	Duration of run min	% H <sub>2</sub> S conversion	Maximum % error
1	B	560	80	50.7	10	30.88	
2	B	560	80	50.7	10	28.60	
3	B	560	80	50.7	10	31.46	1.23
4	B	600	80	50.7	10	29.48	
5	B	600	80	50.7	10	30.01	
6	B	600	80	50.7	10	31.46	0.837
7	B	660	80	50.7	10	25.72	
8	B	660	80	50.7	10	24.05	
9	B	660	80	50.7	10	28.31	1.75
10	C	600	80	50.7	60	93.55	
11	C	600	80	50.7	60	88.15	
12	C	600	80	50.7	60	90.46	2.21

The above range of error seems to be realistic and a relative error of  $\pm 10\%$  seems to be realistic for the equipment and the various analysis methods used in these experiments. The drastic changes in weather conditions and the electrical behavior of the electrical equipment also plays an important role.

## CHAPTER VI

### THERMODYNAMIC CONSIDERATIONS

#### Introduction

Whenever a chemical reaction is being carried out, whether on paper, in the pilot plant or full-scale operation, it is often useful to know the distribution of products that is expected at equilibrium for a given set of conditions. Such information can be used to deduce the maximum product yield at equilibrium or to optimize the conditions necessary for its production.

The principles applied to solution of problems involving chemical equilibrium has been stated by Oliver et. al [20] as that composition which satisfies the mass balance and total pressure specifications and also satisfies all the many simultaneous equilibria involved. The advent of high speed digital computers and their suitability to the use of iterative procedures promoted the development of a number of techniques which now enjoy wide spread applications.

HSC Chemistry for Windows, a program using the free energy minimization technique developed by Outokumpu Research Oy, Finland was used to calculate the

equilibrium distribution for decomposition of hydrogen sulfide. The free energy minimization technique is based on the simple and basic thermodynamic concept, that equilibrium is the state of system in which the total free energy of the system is at a minimum.

The objectives of these calculations are to estimate the equilibrium distribution of products for the decomposition of hydrogen sulfide at various temperatures and at atmospheric pressure and the effect of the presence of carbon dioxide on the decomposition products of hydrogen sulfide.

### Inference

Using the HSC program for Windows, equilibrium product distributions were calculated at atmospheric pressure and at different temperatures. Figure 6.1 shows the equilibrium product distributions calculated on the basis of a simple model including only hydrogen sulfide, hydrogen and sulfur. Figure 6.2 shows those obtained from a complex model including not only hydrogen sulfide, hydrogen and sulfur but also other  $S_x$  ( $x = 1..8$ ) polymers. It can be seen that the complex model predicts higher hydrogen yields than the simple model below 2500 K and that as the temperature increases the relative magnitude of the decrease, increases.

Figures 6.3, 6.4 and 6.5 are similar plots with  $CO_2$  added to the mixture at various initial mole ratios. From figures 6.3, 6.4 and 6.5 it can be seen that as the amount of the hydrogen sulfide decreases in the mixture, the temperature at which the complete

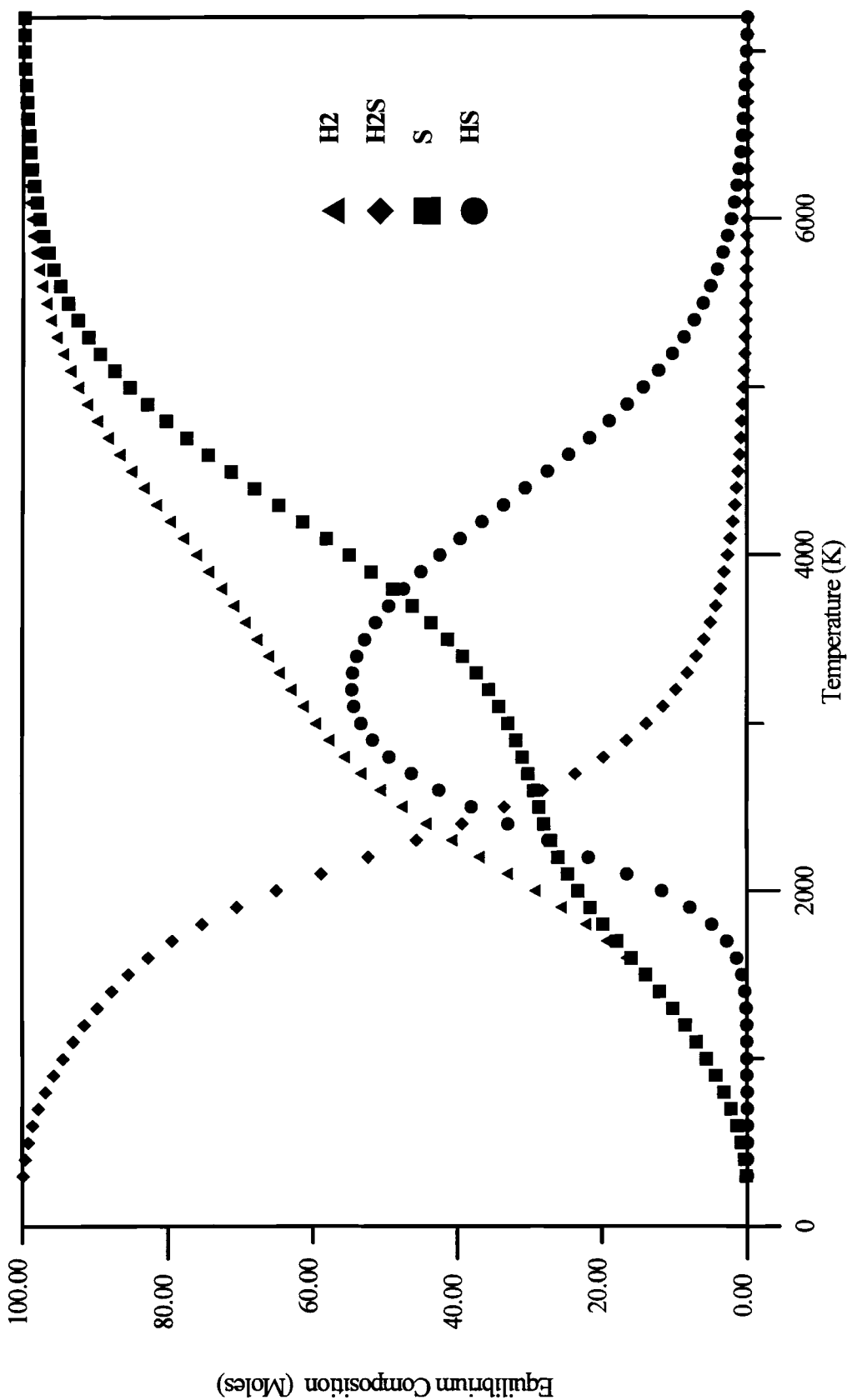


Figure 6.1. Product Distribution for H<sub>2</sub>S Decomposition Process at atmospheric Pressure and Various Temperatures.



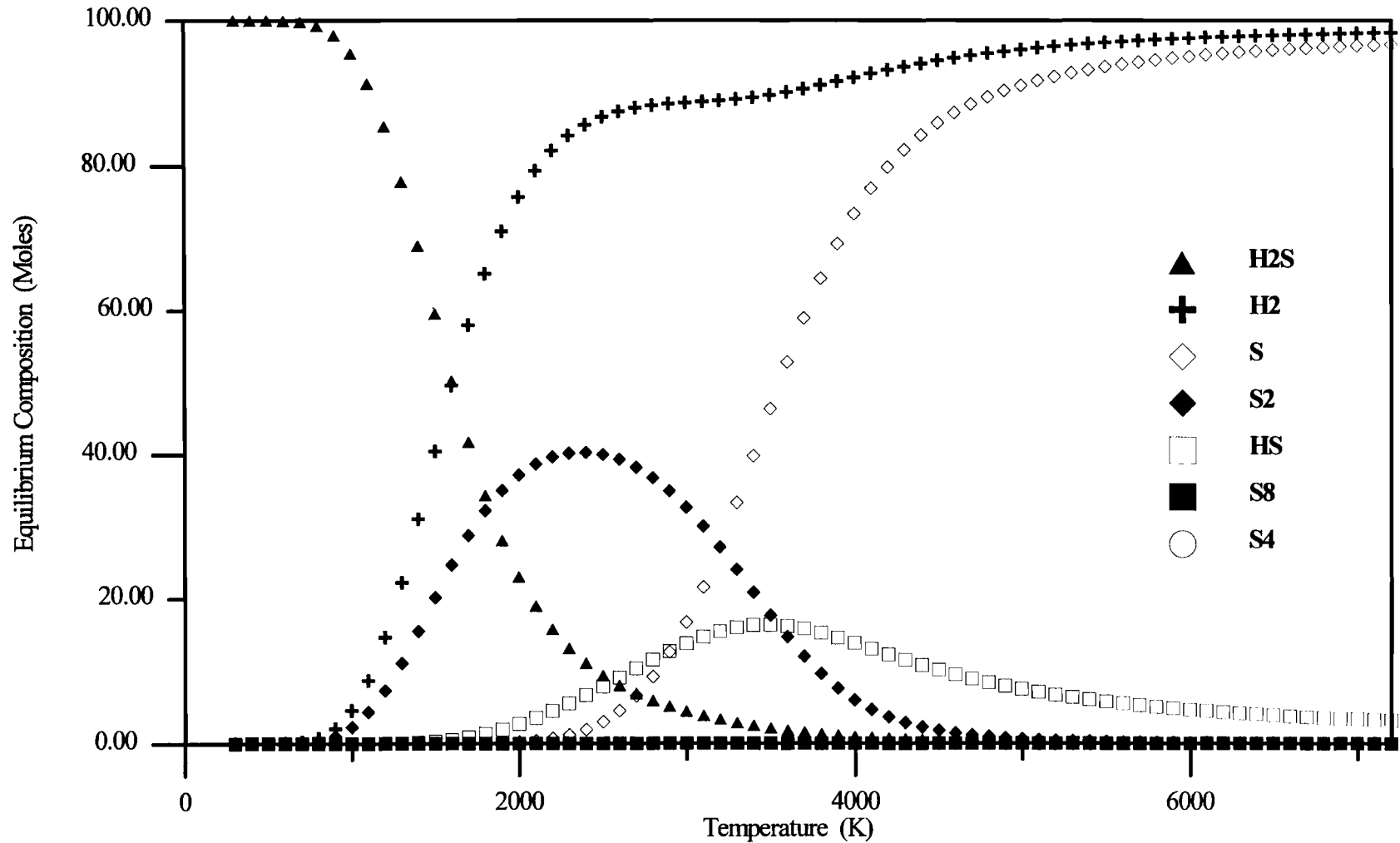


Figure 6.2. Product Distribution for H<sub>2</sub>S Decomposition Process at Atmospheric Pressure and Various temperatures including Sulfur Polymers.

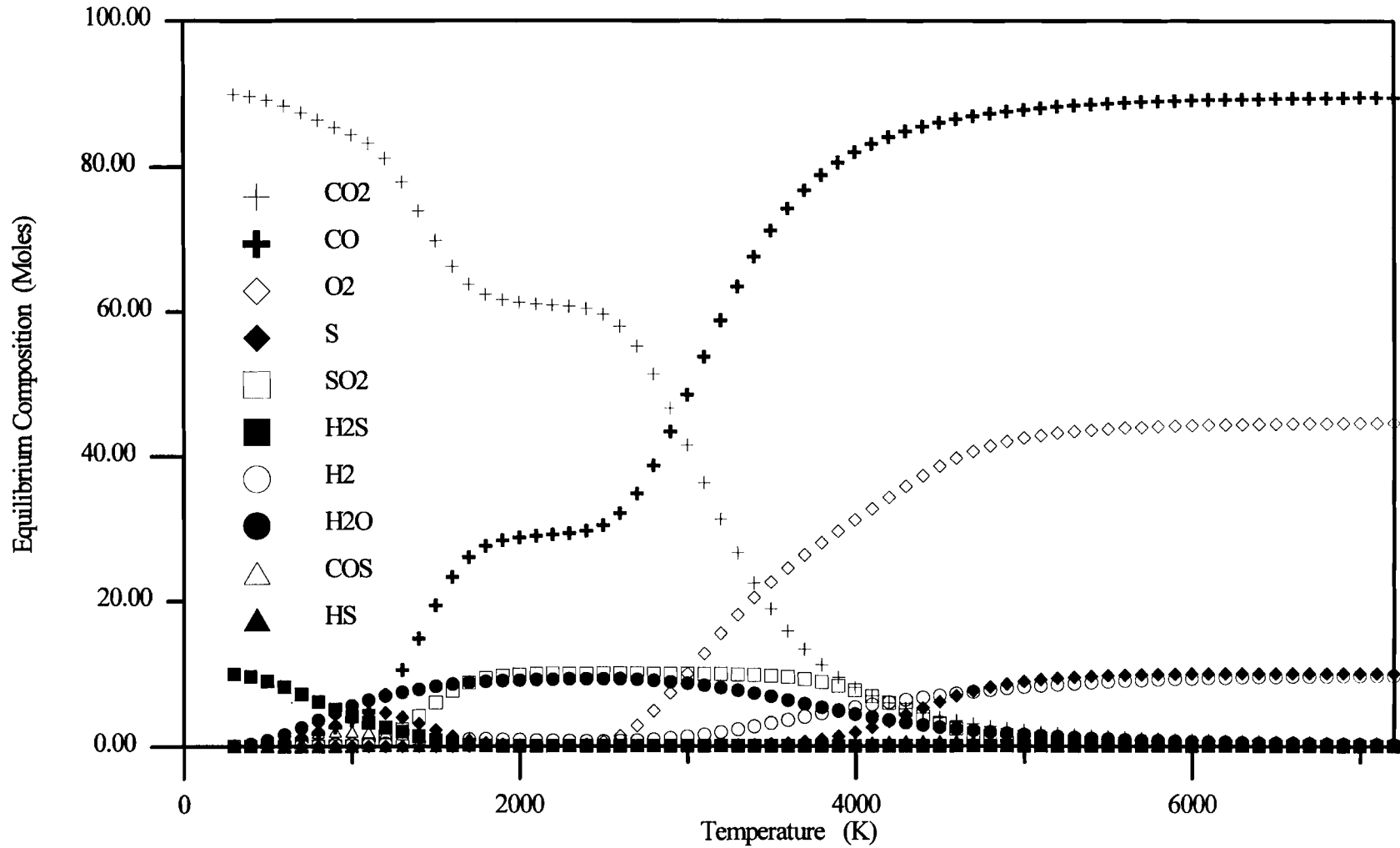


Figure 6.3. Product distribution for H<sub>2</sub>S decomposition process at atmospheric pressure and various temperatures in presence of carbon dioxide at a H<sub>2</sub>S/CO<sub>2</sub> molar ratio of 10/90.

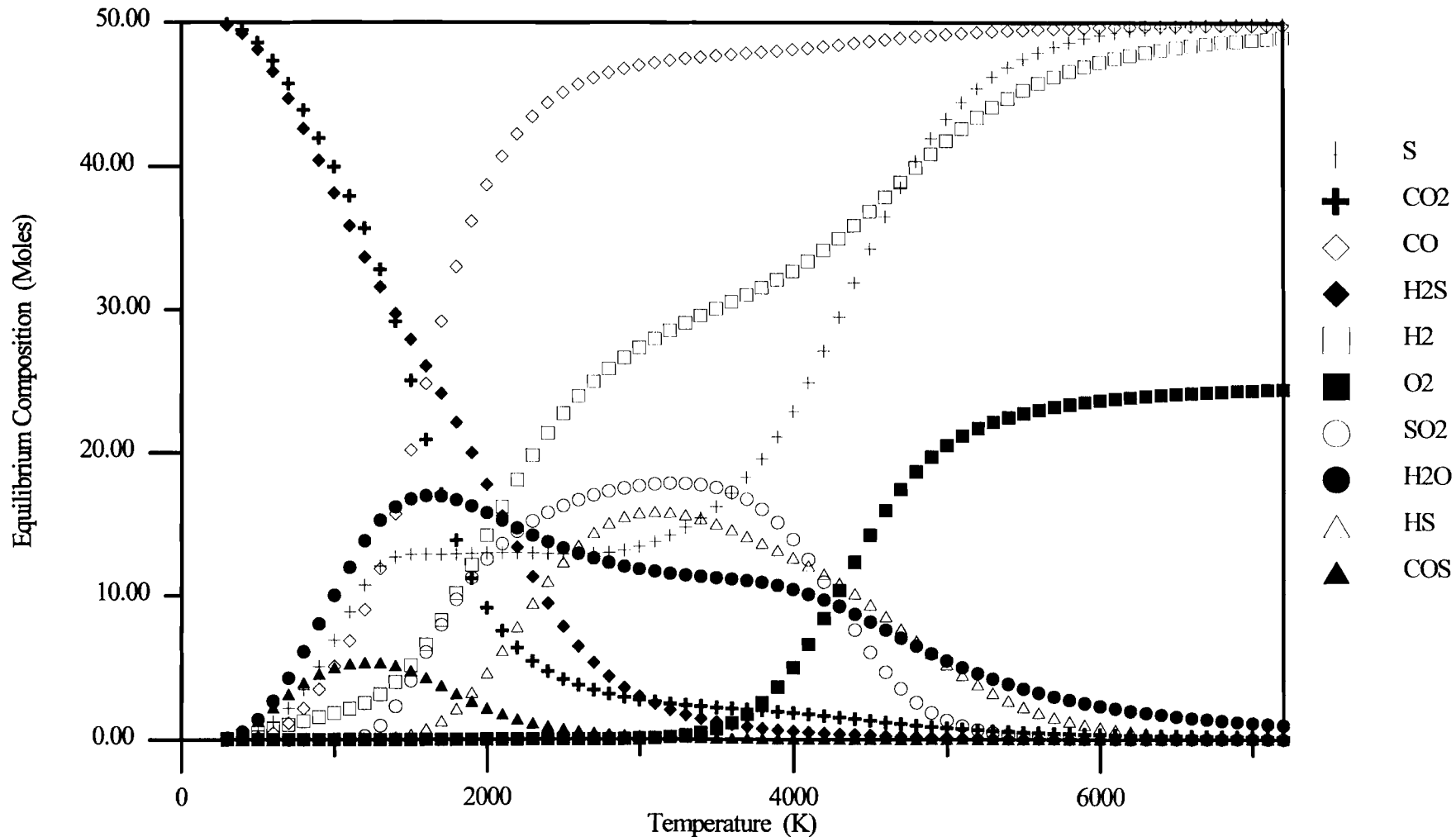


Figure 6.4. Product distribution for H<sub>2</sub>S decomposition process at atmospheric pressure and various temperatures in presence of Carbon Dioxide at a H<sub>2</sub>S/CO<sub>2</sub> molar ratio of 50/50.

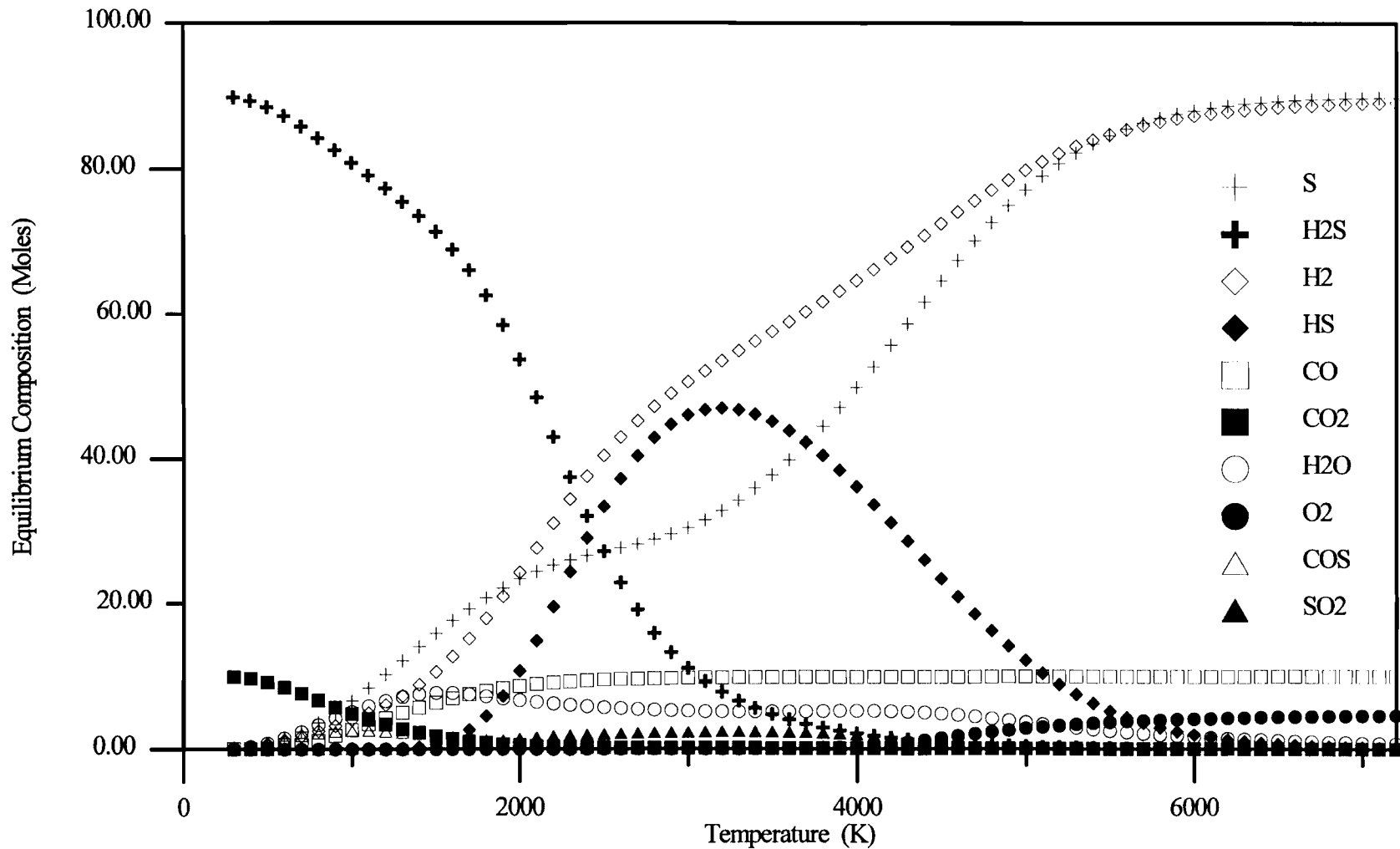


Figure 6.5. Product distribution for H<sub>2</sub>S decomposition process at atmospheric pressure and various temperatures in presence of Carbon Dioxide at a H<sub>2</sub>S/CO<sub>2</sub> molar ratio of 90/10.

decomposition of hydrogen sulfide occurs decreases. This explains the experimental observation that destruction efficiency increases, with a decrease in the hydrogen sulfide composition. Since the temperature in the plasmas is approximately constant a decrease in hydrogen sulfide composition increases the destruction efficiency.

From the equilibrium calculations using the HSC program for Windows we can see that a maximum conversion of 93.5%, which was observed experimentally is possible approximately at 5300 K. This not only gives an idea of what the effective temperature of the plasma is, but also points out another major aspect of the plasma technology that thermal energy is substituted by the electrical energy.

## **CHAPTER VII**

### **CONCLUSIONS AND RECOMMENDATIONS**

This chapter briefly reviews the pertinent findings of the experiments used to study the feasibility of destruction of hydrogen sulfide in alternating current plasma reactors with and without the presence of impurities. It also gives a brief review of electrical characteristics of the plasma reactors and further recommendations to continue this work.

#### **Conclusions**

The following conclusions can be drawn from the experimental results:

1. For a particular gas under consideration there exists an optimum frequency at which the secondary voltage and the power input to the reactor are maximum. This optimum frequency is dependent upon the primary voltage, reactor size, electrode material, gas composition and nature of the transformer.

2. As the primary voltage is increased the maximum secondary voltage increases and the optimum frequency decreases. The power input and the maximum secondary voltage increase with an increase in the size of the reactor.
3. Electrode material and their configuration makes a major difference in the value of the optimum frequency. Copper can be used as an electrode material because it is cheaper and does not have corrosion problems at high voltages and temperatures. Copper mesh as inner and outer electrode seems to work well and gives maximum secondary voltage for a range of frequencies, which can not be achieved in any other configuration.
4. Electrical transformers used to boost the secondary voltage seem to play a major role in the electrical behavior of the system in total.
5. As the primary voltage is increased the destruction of hydrogen sulfide to hydrogen and sulfur increases. For a fixed primary voltage the conversion starts only when a certain frequency is reached. The conversion then slightly increases and remains approximately constant for a range of frequencies. Then the conversion decreases.
6. Hydrogen sulfide conversion strongly increases with an increase in residence time . The same trend was observed by several authors. At a fixed flow rate the frequency at which the conversion starts decreases with increase in primary voltage. Hydrogen sulfide destruction increases initially with an increase in the duration of experiment and then remains constant because of recombination of sulfur formed over a period of time.

7. It was observed that most of the sulfur condensed near the reactor exit. There was also a lot of sulfur condensed in the tubing connecting the reactor to the cold trap. This was of particular significance when the room temperatures were low. Since the reactor walls are warm most of the sulfur gets condensed in the tube connecting reactor outlet and cold trap
8. Increasing the relative humidity of the hydrogen sulfide gas increases the destruction efficiency.
9. For a fixed flow rate the destruction of hydrogen sulfide increases with an increase in the mole fraction of carbon dioxide. As the mole fraction of the carbon dioxide increased, the amount of water vapor condensing on the outer edges of the reactor increased.
10. Finally, it can be concluded that the destruction of hydrogen sulfide is possible in the presence of Carbon Dioxide.

## RECOMMENDATIONS

1. The equipment used for the experiments needs refinement. Ways to stop current losses and energy losses have to be further studied because they effect the feasibility of the process on an industrial scale. The reactor electrodes and the cables need to be insulated so that there is no local arcing which results in a lower effective plasma volume.



2. Equipment is needed to analyze the reaction products on line. This would allow determination of products. This could be of importance to study the kinetics, propose the reaction mechanisms and to estimate the economics and the feasibility of the process.
3. Future experiments should include an even wider range of gas compositions, those more typical of natural gas production. The impact of other impurities and their reactions in the plasma needs to be studied. The effect of these impurities may primarily impact the economics, because they could complicate the purification of product streams by forming other compounds.
4. Reactor design should be further studied to increase the residence times and allow collection of sulfur more easily. Since it is observed that the sulfur formed always deposit on the reactor walls, ways to remove sulfur from the walls needs to be studied.
5. Research is required into the kinetics and reaction mechanisms which further would give information required for reactor design and on-line process control of the plasmas. Scale up equations that relate process variables to process parameters and conditions for plasmas also needs to be studied.
6. The process economics and the potential energy savings have to be calculated based upon the latest figures available, since the costs vary rapidly, to develop a commercial process for the destruction of hydrogen sulfide to hydrogen and sulfur.

## BIBLIOGRAPHY

1. A. V. Balebanov, et al., *Doklady Akadonii Nauk SSSR*, **283**, No.3, 657-660 (1985).
2. I. E. Besten, P. W. Selwood, *J. Catalysis*, **1**, 93 (1962).
3. J. L. Blanchet, J. R. Parent, H. C Lavalee, *Can. J. Chem.*, **47**, 160 (1969).
4. A. M. Boonstra, T. Vanruler, *Surface Sci.*, **4**, 141 (1966).
5. A. Czernichowski, P. Jorgensen, H. Lesueur, J. Chapelle, *Colloque de physique*, c5-65-c5-71 (1990).
6. B. Darwent, R. Roberts, *Proc. Roy. Soc. (London)*, **216 a**, 344 (1953).
7. V. R. Desai, Masters Thesis, Oklahoma State University, Stillwater, OK (1992).
8. A. J. Gorski, E. J. Daniels, J. B. L. Harkness, Energy systems division, Argonne National Laboratories., Treatment of hydrogen sulfide waste gas., Annual report for fiscal year 1990 (1990).
9. M. Gratzel, *Chem. Engg. News*, **59**, 40 (1981).
10. J. B. L. Harkness, R. D. Doctor, *ASME*, **41**, 31-35 (1992).
11. V. B. Herman, *Fundamentals of plasma chemistry and technology* (Technomic Publication Company, 1988).
12. D. W. Huyton, T. W. Woodward, *Can. J. Chem.*, **48**, 2300 (1970).
13. A. H. Johannes, (Oklahoma State University), Personal communication.
14. V. Kaloidas, N. Papayannakos, *Chemical Engineering Science*, **44**, 2493-2500 (1989).
15. T. Kappauf, E. A. Fletcher, *Energy*, **14**, 443-449 (1989).
16. M. D. Koenigatuhl, *Chimie & industrie*, **29**, 1057 (1933).

17. A. R. Laengrich, W. L. Cameron, *The oil and gas journal* , 158-162 (1978).
18. Maruzen Oil Company Limited, Japan, July 9 (1965); 14413.
19. S. A. Nester, V. D. Rusanov, A. A. Fridman, *Khim. Vys. Energy*, **22**, 452-461 (1988).
20. R. C. Oliver, S. E. Stephanou, R. W. Baier, *Chemical Engineering*, 121-128 (1962).
21. M. A. Piatt, Masters Thesis, Oklahoma State University, Stillwater, OK (1988).
22. B. V. Potapkin, V. D. Rusanov, M. I. Strelkova, A. A. Fridman, *Khim. Vys. Energy*, **22**, 537-540 (1988).
23. M. E. D. Raymont, *Hydrocarbon processing*, 139-142 (1975).
24. V. D. Rusanov, A. A. Fridman, S. O. Macheret, *Doll. Akad. Nauk SSSR*, **283**, 590-594 (1985).
25. R. Schwarz, W. Kunzer, *Z. Anorg. Allgem. Chem.*, **183**, 287 (1929).
26. T. L. Slager, C. H. Amber, *Can. J. Chem.*, **50**, 3416 (1972).
27. A. Smits, A. H. W. Aten, *Z. Electrochem.*, **16**, 264 (1910).
28. C. L. Thomas, G. Egloff, J. C. Morrel, *Chem. Revs.*, **28**, (1941).
29. W. J. Thomas, U. Ullam, *Jour. Catalysis*, **15**, 342 (1969).
30. M. Thorpe, *Chem.Eng.Prog.*, **85**, 43-53 (1989).
31. R. M. P. Torrey, *Diss. Abs. Int. B.*, **30**, 3599 (1970).
32. F. J. Vastola, W. O. Satcy, *Am. Chem. Soc. Div. Fuel Chem.*, **11**, 234 -237 (1967).
33. T. VenYen, Masters Thesis, Oklahoma State University, Stillwater, OK (1990).
34. E. Wourtsel, *Radium*, **11**, 332 (1914).

## **APPENDICES**

## **APPENDIX A**

### **SAMPLE CALCULATION**

## Experimental Data:

Reactor configuration:	C
Gas:	H <sub>2</sub> S
Flow rate:	50.7 cc/min
Temperature:	304.3 K
Humidity:	18.2%
Pressure:	1 atm
Duration of run:	60 min
Amount of sulphur collected	3.647 g

## Assumptions:

1. Ideal gas.
2. Overall stoichiometric reaction is
$$\text{H}_2\text{S} \rightarrow \text{H}_2 + \text{S}$$
$$\text{H}_2\text{S} + 3\text{CO}_2 \rightarrow \text{H}_2\text{O} + 3\text{CO} + \text{O}_2 + \text{S}$$

H<sub>2</sub>S going in = 0.0507 liters/min

$$\begin{aligned}\text{Therefore moles of H}_2\text{S in} &= \frac{1 \text{ atm} \times 0.0507 \text{ liters/min} \times 60 \text{ min}}{0.0821 \text{ atm-liter/K-mol} \times 304.26 \text{ K}} \\ &= 0.122 \text{ moles}\end{aligned}$$

$$\begin{aligned}\text{Moles of sulfur collected} &= 3.647 \text{ g} / (32.02 \text{ g/mole}) \\ &= 0.114 \text{ moles}\end{aligned}$$

$$\begin{aligned}\text{H}_2\text{S going out} &= 0.122 \text{ moles} - 0.114 \text{ moles} \\ &= 0.008 \text{ moles}\end{aligned}$$

$$\begin{aligned}\% \text{ Conversion} &= \frac{\text{Moles of H}_2\text{S in} - \text{Moles of H}_2\text{S out}}{\text{Moles of H}_2\text{S in}} \times 100 \\ &= 93.55\%\end{aligned}$$

**APPENDIX B**

**NON-DESTRUCTIVE TEST DATA**

TABLE B1

EXPERIMENTAL DATA CORRESPONDING  
TO FIGURE 4.1

Reactor A with wrapped outer electrode configuration

Ambient Air

Temperature 84.5F

Humidity 19.12%

PRIM VOLT FREQUENCY	30 SC.VOLT	40 SC.VOLT	50 SC.VOLT	60 SC.VOLT	70 SC.VOLT
60	3.66	4.70	5.96	7.54	8.52
80	3.62	4.86	6.12	7.36	8.60
100	3.54	4.76	6.00	7.24	08.46
120	3.48	4.66	5.88	7.10	8.28
140	3.40	4.56	5.74	6.92	8.12
160	3.32	4.44	5.60	6.74	7.90
180	3.22	4.30	5.46	6.54	7.68
200	3.12	4.18	5.30	6.36	7.48
220	3.06	4.06	5.14	6.16	7.26
240	2.94	3.94	5.00	5.98	7.06
260	2.84	3.82	4.86	5.80	6.86
280	2.76	3.70	4.72	5.64	6.66
300	2.68	3.60	4.60	5.48	6.46
320	2.60	3.50	4.46	5.30	6.28
340	2.52	3.40	4.34	5.16	6.14
360	2.44	3.32	4.24	5.04	5.98
380	2.40	3.24	4.16	4.92	5.86
400	2.34	3.18	4.08	4.82	5.76
420	2.28	3.12	4.02	4.74	5.66
440	2.24	3.08	3.98	4.68	5.60
460	2.22	3.04	3.94	4.64	5.56
480	2.14	3.02	3.94	4.62	5.56
500	2.14	3.04	3.94	4.64	5.54
520	2.14	3.04	3.96	4.66	5.52
540	2.14	3.08	4.00	4.74	5.56
560	2.18	3.10	4.04	4.62	5.36
580	2.26	3.12	4.06	4.56	5.06
600	2.30	3.12	4.02	4.38	4.72
620	2.34	3.08	3.90	4.12	4.42
640	2.36	3.00	3.76	3.92	4.12
660	2.30	2.88	3.58	3.68	3.88
680	2.24	2.74	3.40	3.46	3.58
700	2.14	2.56	3.20	3.28	3.32

SC.VOLT represents secondary voltage in kV.



TABLE B2

EXPERIMENTAL DATA CORRESPONDING  
TO FIGURE 4.2

Reactor B with copper mesh outer electrode configuration

Ambient Air

Temperature 84.5F

Humidity 19.12%

PRIM VOLT FREQUENCY	30 SC. VOLT	40 SC. VOLT	50 SC. VOLT	60 SC. VOLT	70 SC. VOLT
60	3.46	5.00	5.94	7.16	8.5
80	3.54	4.80	6.06	7.30	8.52
100	3.46	4.70	5.94	7.18	8.38
120	3.38	4.60	5.80	7.06	8.20
140	3.28	4.48	5.66	6.82	8.00
160	3.18	4.36	5.50	6.64	7.78
180	3.08	4.20	5.32	6.42	7.56
200	2.98	4.06	5.16	6.30	7.34
220	2.88	3.82	4.98	6.12	7.10
240	2.78	3.74	4.82	5.94	6.90
260	2.68	3.60	4.68	5.66	6.68
280	2.58	3.58	4.52	5.48	6.48
300	2.48	3.56	4.36	5.36	6.28
320	2.40	3.42	4.22	5.24	6.08
340	2.32	3.30	4.10	5.08	5.90
360	2.24	3.24	3.98	4.92	5.74
380	2.18	3.14	3.88	4.84	5.60
400	2.12	3.04	3.78	4.70	5.48
420	2.06	2.96	3.70	4.50	5.50
440	2.02	2.90	3.62	4.42	5.50
460	1.96	2.84	3.58	4.38	5.52
480	1.94	2.78	3.54	4.46	5.46
500	1.92	2.74	3.56	4.46	5.30
520	1.92	2.70	3.58	4.50	5.04
540	1.92	2.70	3.62	4.38	4.76
560	1.94	2.70	3.58	4.20	4.42
580	1.98	2.72	3.54	3.96	4.12
600	2.04	2.76	3.36	3.74	3.80
620	2.10	2.86	3.20	3.52	3.52
640	2.20	2.96	3.02	3.30	3.30
660	2.26	2.86	2.84	3.12	3.08
680	2.30	2.78	2.70	2.76	2.88
700	2.22	2.68	2.60	2.64	2.74

SC.VOLT represents secondary voltage in kV.

TABLE B3

EXPERIMENTAL DATA CORRESPONDING  
TO FIGURE 4.3

Reactor C with copper mesh outer electrode configuration

Ambient Air

Temperature 84.5F

Humidity 19.12%

PRIM VOLT FREQUENCY	30 SC.VOLT	40 SC.VOLT
60	3.44	4.84
80	3.56	4.80
100	3.50	4.74
120	3.46	4.68
140	3.42	4.62
160	3.36	4.56
180	3.30	4.50
200	3.22	4.46
220	3.18	4.42
240	3.16	4.38
260	3.14	4.36
280	3.14	4.36
300	3.16	4.38
320	3.18	4.44
340	3.24	4.52
360	3.32	4.64
380	3.44	4.82
400	3.62	5.08
420	3.86	5.42
440	4.18	5.98
460	4.64	6.74
480	5.32	7.68
500	6.12	8.06
520	6.38	7.84
540	6.04	7.52

SC.VOLT represents secondary voltage in kV.

TABLE B4

EXPERIMENTAL DATA CORRESPONDING  
TO FIGURE 4.4

Reactor B with copper mesh outer electrode configuration

Carbon dioxide

Temperature 63.8F

Flow rate 79 cc/min

PRIM VOLT FREQUENCY	30 SC.VOLT	40 SC.VOLT	50 SC.VOLT	60 SC.VOLT	70 SC.VOLT
200	3.0	3.9	4.94	6.04	7.16
220	2.8	3.74	4.72	5.78	6.88
240	2.68	3.58	4.52	5.58	6.62
260	2.56	3.42	4.34	5.32	6.36
280	2.44	3.26	4.14	5.10	6.10
300	2.28	3.10	3.96	4.98	5.84
320	2.18	2.96	3.78	4.88	5.60
340	2.06	2.84	3.62	4.78	5.38
360	1.98	2.72	3.48	4.60	5.20
380	1.90	2.62	3.36	4.42	5.02
400	1.84	2.52	3.26	4.28	4.88
420	1.78	2.44	3.18	4.16	4.76
440	1.72	2.38	3.12	4.06	4.68
460	1.70	2.36	3.08	3.96	4.66
480	1.68	2.34	3.10	3.90	4.72
500	1.68	2.38	3.16	3.9	4.82
520	1.72	2.46	3.22	4	5.00
540	1.80	2.60	3.38	4.16	5.04
560	1.88	2.80	3.64	4.34	5.00
580	2.18	3.04	3.84	4.44	4.96
600	2.34	3.34	4.02	4.58	4.94
620	2.58	3.58	4.18	4.64	4.92
640	2.82	3.76	4.32	4.70	4.94
660	2.98	3.94	4.4	4.74	5.00
680	3.18	4.06	4.48	4.76	5.06
700	3.36	4.14	4.54	4.78	5.16
720	3.48	4.28	4.6	4.86	5.24
740	3.54	4.36	4.66	4.94	5.40
760	3.50	4.46	4.68	5.02	5.52
780	3.42	4.54	4.76	5.04	5.60
800	3.30	4.42	4.88	5.06	5.64

SC.VOLT represents secondary voltage in kV.

TABLE B5

EXPERIMENTAL DATA CORRESPONDING  
TO FIGURE 4.5

Reactor B with copper mesh outer electrode configuration

Hydrogen Sulfide

Temperature 59.6F

Flow Rate 27 cc/min

PRIM VOLT FREQUENCY	30 SC.VOLT	40 SC.VOLT	50 SC.VOLT	60 SC.VOLT	70 SC.VOLT
200	2.9	3.8	4.84	5.78	6.78
220	2.8	3.62	4.61	5.54	6.5
240	2.68	3.46	4.38	5.3	6.2
260	2.58	3.30	4.18	5.06	5.92
280	2.46	3.16	3.98	4.82	5.66
300	2.36	3.00	3.8	4.62	5.40
320	2.22	2.86	3.64	4.42	5.16
340	2.12	2.74	3.5	4.24	4.96
360	2.04	2.64	3.38	4.10	4.78
380	2.00	2.56	3.26	3.98	4.68
400	1.98	2.48	3.18	3.92	4.64
420	1.96	2.44	3.16	3.88	4.66
440	1.92	2.44	3.2	3.88	4.82
460	1.9	2.48	3.24	3.98	5.02
480	1.92	2.54	3.38	4.16	5.16
500	2.00	2.68	3.58	4.44	5.22
520	2.16	2.9	3.8	4.72	5.12
540	2.34	3.16	3.92	5.08	5.08
560	2.56	3.5	4.08	5.40	5.00
580	2.82	3.76	4.28	5.70	5.00
600	3.10	4.1	4.72	5.86	5.12
620	3.38	4.34	5.04	6.00	5.26
640	3.62	4.56	5.24	6.12	5.42
660	3.76	4.84	5.4	6.26	5.62
680	3.82	5.1	5.48	6.40	5.78
700	3.88	5.32	5.58	6.44	5.94
720	3.94	5.46	5.66	6.50	6.16
740	3.9	5.62	5.7	6.56	6.34
760	3.92	5.7	5.74	6.62	6.5
780	3.72	5.72	5.78	6.7	6.66
800	3.6	5.54	5.9	6.74	6.78

SC.VOLT represents secondary voltage in kV.

TABLE B6

EXPERIMENTAL DATA CORRESPONDING  
TO FIGURE 4.6

Reactor B with copper mesh outer electrode configuration  
 Carbon Dioxide and Water  
 Relative humidity 32.8%  
 Temperature 78 F  
 Flow Rate 79 cc/min

PRIM VOLT FREQUENCY	50 SC.VOLT	60 SC.VOLT	70 SC.VOLT
200	5.40	6.50	7.62
220	5.20	6.24	7.24
240	5.04	6.02	7.04
260	4.88	5.80	6.80
280	4.74	5.58	6.64
300	4.52	5.40	6.46
320	4.38	5.20	6.34
340	4.34	5.12	6.22
360	4.22	5.06	6.04
380	4.10	4.94	5.74
400	3.98	4.88	5.46
420	3.90	4.78	5.32
440	3.76	4.60	5.32
460	3.70	4.40	5.30
480	3.68	4.28	5.22
500	3.68	4.24	5.02
520	3.60	4.26	4.80
540	3.50	4.14	4.56
560	3.52	3.94	4.28
580	3.36	3.78	4.10
600	3.24	3.56	3.82
620	3.18	3.40	
640	3.00	3.22	
660	2.86	3.06	
680	2.80	2.88	
700	2.66	2.70	

SC.VOLT represents secondary voltage in kV.

TABLE B7

EXPERIMENTAL DATA CORRESPONDING  
TO FIGURE 4.7

Reactor B with copper mesh outer electrode configuration  
 Hydrogen Sulfide and Water  
 Relative humidity 34.2%  
 Temperature 78 F  
 Flow Rate 27 cc/min

PRIM VOLT	50	60	70
FREQUENCY	SC.VOLT	SC.VOLT	SC.VOLT
200	5.44	6.42	7.50
220	5.26	6.20	7.24
240	5.08	5.96	6.98
260	4.92	5.76	6.74
280	4.78	5.56	6.50
300	4.62	5.38	6.30
320	4.50	5.20	6.08
340	4.38	5.04	5.90
360	4.26	4.90	5.74
380	4.12	4.76	5.58
400	4.06	4.64	5.50
420	3.90	4.56	5.42
440	3.82	4.48	5.42
460	3.76	4.42	5.50
480	3.72	4.38	5.40
500	3.68	4.44	5.18
520	3.68	4.46	4.94
540	3.68	4.32	4.70
560	3.74	4.14	4.42
580	3.68	3.94	4.12
600	3.54	3.70	3.84
620	3.42	3.50	
640	3.24	3.32	
660	3.02	3.04	
680	2.86	2.86	
700	2.72	2.00	

SC.VOLT represents secondary voltage in kV.

TABLE B8

EXPERIMENTAL DATA CORRESPONDING  
TO FIGURE 4.8

Reactor B with copper mesh outer electrode configuration  
Carbon dioxide with and without Water  
Flow rate 79 cc/min  
Primary voltage 70 V

FREQUENCY	Dry gas	Increased Humidity (32.8% RH)
	SC. VOLT	SC. VOLT
200	7.16	7.62
220	6.88	7.24
240	6.62	7.04
260	6.36	6.80
280	6.10	6.64
300	5.84	6.46
320	5.60	6.34
340	5.38	6.22
360	5.20	6.04
380	5.02	5.74
400	4.88	5.46
420	4.76	5.32
440	4.68	5.32
460	4.66	5.30
480	4.72	5.22
500	4.82	5.02
520	5.00	4.80
540	5.04	4.56
560	5.00	4.28
580	4.96	4.10
600	4.94	3.82
620	4.92	
640	4.94	
660	5.00	
680	5.06	
700	5.16	
720	5.24	
740	5.40	
760	5.52	
780	5.60	
800	5.64	

SC.VOLT represents secondary voltage in kV.

TABLE B9

EXPERIMENTAL DATA CORRESPONDING  
TO FIGURE 4.9

Reactor B with copper mesh outer electrode configuration  
Hydrogen Sulfide with and without Water  
Flow rate 79 cc/min  
Primary Voltage 70 V

FREQUENCY	Dry gas	Increased Humidity (34.2% RH)
	SC.VOLT	SC. VOLT
200	6.78	7.50
220	6.5	7.24
240	6.2	6.98
260	5.92	6.74
280	5.66	6.50
300	5.40	6.30
320	5.16	6.08
340	4.96	5.90
360	4.78	5.74
380	4.68	5.58
400	4.64	5.50
420	4.66	5.42
440	4.82	5.42
460	5.02	5.50
480	5.16	5.40
500	5.22	5.18
520	5.12	4.94
540	5.08	4.70
560	5.00	4.42
580	5.00	4.12
600	5.12	3.84
620	5.26	
640	5.42	
660	5.62	
680	5.78	
700	5.94	
720	6.16	
740	6.34	
760	6.5	
780	6.66	
800	6.78	

SC.VOLT represents secondary voltage in kV.



TABLE B10

EXPERIMENTAL DATA CORRESPONDING  
TO FIGURE 4.10

Reactor A  
Ambient Air  
Temperature 84.5F  
Primary Voltage 60 V

FREQUENCY	Wire inside and outside SEC. VOL	wire inside wrap outside SEC. VOL	Wrap inside wire outside SEC. VOL	wrap inside wrap outside SEC. VOL
200	6.06	5.56	6.36	7.32
220	5.84	5.26	6.16	7.16
240	5.64	4.98	5.98	6.98
260	5.42	4.72	5.8	6.78
280	5.22	4.48	5.64	6.54
300	5.04	4.24	5.48	6.32
320	4.86	4.02	5.3	6.06
340	4.68	3.82	5.16	5.82
360	4.50	3.64	5.04	5.58
380	4.36	3.5	4.92	5.34
400	4.22	3.4	4.82	5.10
420	4.08	3.32	4.74	4.88
440	3.96	3.34	4.68	4.68
460	3.86	3.36	4.64	4.48
480	3.96	3.46	4.62	4.3
500	3.7	3.62	4.64	4.24
520	3.66	3.82	4.66	4.16
540	3.62	4.0	4.74	4.1
560	3.62	4.2	4.62	4.06
580	3.68	4.48	4.56	3.98
600	3.74	4.81	4.38	3.92
620	3.8	5.18	4.12	3.84
640	3.88	5.46	3.92	3.78
660	3.92	5.64	3.68	3.76
680	3.9	5.84	3.46	3.78
700	3.78	6.02	3.28	3.76
720	3.6	6.18		3.76
740	3.4	6.3		3.76
760	3.2	6.36		3.76
780	3.04	6.42		3.8
800	2.90	6.48		3.88

SC.VOLT represents secondary voltage in kV.

TABLE B11

EXPERIMENTAL DATA CORRESPONDING  
TO FIGURE 4.11

Reactor B with copper mesh outer electrode configuration

Carbon dioxide

Temperature 78 F

Primary Voltage 60 V

FLOW RATE FREQUENCY	79cc/min SC.VOLT	118.5cc/min SC.VOLT	158 cc/min SC.VOLT
200	6.56	6.52	6.52
220	6.34	6.30	6.32
240	6.02	6.08	6.12
260	5.80	5.84	5.90
280	5.68	5.70	5.72
300	5.54	5.54	5.50
320	5.40	5.30	5.32
340	5.22	5.18	5.18
360	5.00	5.06	4.90
380	4.88	4.92	4.86
400	4.74	4.70	4.68
420	4.60	4.62	4.58
440	4.52	4.46	4.44
460	4.36	4.36	4.32
480	4.48	4.44	4.48
500	4.32	4.36	4.38
520	4.28	4.32	4.26
540	4.16	4.06	4.12
560	3.92	3.78	3.80
580	3.72	3.60	3.66
600	3.44	3.42	3.50

SC.VOLT represents secondary voltage in kV.

TABLE B12

EXPERIMENTAL DATA CORRESPONDING  
TO FIGURE 4.12

Reactor B with copper mesh outer electrode configuration

Hydrogen Sulfide

Temperature 78 F

Primary Voltage 60 V

FLOW RATE FREQUENCY	27cc/min SC.VOLT	58cc/min SC.VOLT	76 cc/min SC.VOLT
200	5.82	5.86	5.86
220	5.60	5.66	5.62
240	5.32	5.40	5.36
260	5.12	5.22	5.14
280	4.88	5.00	4.92
300	4.72	4.84	4.76
320	4.46	4.52	4.48
340	4.32	4.24	4.38
360	4.16	4.12	4.12
380	4.02	3.96	3.94
400	3.96	3.88	3.94
420	3.90	3.86	3.98
440	3.84	3.86	4.08
460	3.84	3.98	4.16
480	3.96	4.04	4.28
500	4.12	4.16	4.44
520	4.34	4.38	4.58
540	4.68	4.70	4.72
560	4.98	4.98	5.02
580	5.26	5.28	5.26
600	5.62	5.60	5.72

SC.VOLT represents secondary voltage in kV.

TABLE B13

EXPERIMENTAL DATA CORRESPONDING  
TO FIGURE 4.13

Reactor B with copper mesh outer electrode configuration

Carbon Dioxide

Temperature 59.6 F

Flow rate 79 cc/min

PRIM.VOLT FREQUENCY	50 POWER	60 POWER	PRIM. VOLT FREQUENCY	50 POWER	60 POWER
60	70	76	560	68	69
70	69	74	570	68	71
80	69	74	580	68	71
90	69	71	590	68	72
100	69	69	600	69	74
120	68	69	610	69	74
140	68	68	620	69	74
160	68	68	630	71	74
180	68	68	640	72	74
200	68	67	650	72	74
220	68	67	660	73	76
240	68	67	670	73	77
260	68	67	680	73	77
280	68	67	690	74	77
300	68	67	700	73	77
320	68	67	710	73	77
340	68	67	720	73	77
360	68	67	730	73	77
380	68	67	740	73	77
400	68	67	750	73	77
420	68	67	760	73	77
440	68	67	780	73	77
450	68	67	800	73	77
460	68	67	820	73	77
470	68	67	840	73	77
480	68	67	860	73	77
490	68	67	880	73	77
500	68	69	900	73	77
510	68	69	920	71	77
520	68	69	940	71	77
530	68	69	960	71	75
540	68	69	980	71	75
550	68	69	1000	70	68

TABLE B14

EXPERIMENTAL DATA CORRESPONDING  
TO FIGURE 4.14

Reactor B with copper mesh outer electrode configuration

Hydrogen Sulfide

Temperature 59.6F

Flow rate 25 cc/min

PRIM.VOLT FREQUENCY	50 POWER	60 POWER	70 POWER	PRIM. VOLT FREQUENCY	50 POWER	60 POWER	70 POWER
60	70	78	85	560	69	68	80
70	69	76	80	570	69	68	81
80	69	75	78	580	69	69	81
90	69	74	73	590	69	72	82
100	69	71	70	600	70	74	82
120	69	70	70	610	70	75	82
140	69	70	70	620	70	75	82
160	69	69	70	630	70	75	82
180	69	69	70	640	70	75	82
200	69	67	70	650	71	75	82
220	69	67	70	660	71	76	82
240	69	67	70	670	72	77	82
260	69	67	70	680	72	77	81
280	69	67	70	690	72	77	81
300	69	67	70	700	73	77	81
320	69	67	70	710	73	77	81
340	69	67	70	720	73	77	81
360	69	67	70	730	73	77	81
380	69	67	70	740	73	77	81
400	69	67	70	750	73	77	81
420	69	67	70	760	73	77	81
440	69	67	70	780	73	77	80
450	69	67	70	800	73	77	79
460	69	67	70	820	73	77	79
470	69	67	70	840	73	77	79
480	69	67	70	860	73	77	79
490	69	67	70	880	72	76	78
500	69	67	70	900	72	75	78
510	69	67	71	920	72	75	78
520	69	67	74	940	72	75	78
530	69	67	76	960	72	75	77
540	69	67	77	980	72	74	75
550	69	67	80	1000	70	70	73

TABLE B15

EXPERIMENTAL DATA CORRESPONDING  
TO FIGURE 4.15

Reactor C with copper mesh outer electrode configuration  
Ambient A  
Primary voltage 40V

FREQUENCY	TRANS 1 SC.VOLT	TRANS 2 SC.VOLT
220	1.56	4.42
240	1.63	4.38
260	1.70	4.36
280	1.77	4.36
300	1.89	4.38
320	2.02	4.44
340	2.18	4.52
360	2.37	4.64
380	2.61	4.82
400	3.00	5.08
420	3.68	5.42
440	4.79	5.98
460	6.64	6.74
480	8.28	7.68
500	8.46	8.06
520	8.52	7.84
540	8.33	7.52

SC.VOLT represents secondary voltage in kV.

TABLE B16

EXPERIMENTAL DATA CORRESPONDING  
TO FIGURE 4.16

Reactor C with copper mesh outer electrode configuration

Ambient Air

Primary voltage 40 V

FREQUENCY	TRANS 1 POWER	TRANS 2 POWER
200	80	83
220	80	83
240	80	83
260	80	83
280	80	83
300	80	83
320	80	83
340	80	83
360	80	85
380	80	88
400	80	94
420	80	96
440	92	102
460	113	102
480	125	103
500	128	103
520	128	103
540	127	103
560	126	101
580	117	101
600	109	98

## **APPENDIX C**

### **DESTRUCTIVE TEST DATA**



TABLE C1

## DESTRUCTIVE TEST DATA CORRESPONDING TO FIGURE 5.1

---

Primary voltage : 80V

Reactor configuration B

Gas : H<sub>2</sub>S

Flow rate : 50.7 cc/min

Duration of each run : 10 min

---

Serial Number	Frequency Hz	Sec. Vol. kV	Temp. K	Amount of sulfur gm	percentage conversion
1	550	10.72	278.15	0.13	18.25
2	560	10.92	278.15	0.22	30.88
3	580	10.56	278.15	0.22	30.88
4	600	10.08	278.15	0.21	29.48
5	620	9.78	278.15	0.25	35.10
6	640	9.32	278.15	0.19	26.68
7	660	8.38	283.15	0.18	25.72
8	700	8.74	283.15	0.14	20.00

---

TABLE C2

## DESTRUCTIVE TEST DATA CORRESPONDING TO FIGURE 5.2

---

Primary voltage : 70V

Reactor configuration B

Gas : H<sub>2</sub>S

Flow rate : 50.7 cc/min

Duration of each run : 10 min

---

Serial Number	Frequency Hz	Sec. Vol. kV	Temp. K	Amount of sulfur gm	percentage conversion
1	550	8.32	292.03	0.16	23.58
2	560	8.54	292.03	0.19	28.00
3	580	9.20	292.03	0.15	22.11
4	600	9.04	292.03	0.15	22.11
5	620	9.16	292.03	0.16	23.58
6	640	9.02	292.03	0.18	26.58
7	660	8.84	292.03	0.15	22.11
8	700	8.52	292.03	0.17	25.11

---

TABLE C3

## DESTRUCTIVE TEST DATA CORRESPONDING TO FIGURE 5.3

---

Primary voltage : 80V

Reactor configuration B

Gas : Mixture of Hydrogen Sulfide and Carbon Dioxide

Flow rate : 35 cc/min H<sub>2</sub>S + 316 cc/min CO<sub>2</sub>

Duration of each run : 10 min

---

Serial Number	Frequency Hz	Sec. Vol. kV	Temp. K	Amount of sulfur gm	percentage conversion
1	550	4.84	285.32	0.04	8.36
2	560	4.72	285.32	0.05	10.45
3	580	4.46	285.32	0.09	18.81
4	600	4.04	285.48	0.09	18.82
5	620	3.96	285.48	0.09	18.82
6	640	4.02	285.48	0.06	12.55
7	650	4.24	285.48	0.09	18.82
8	700	4.98	285.48	0.10	20.91

---

TABLE C4

## DESTRUCTIVE TEST DATA CORRESPONDING TO FIGURE 5.4

---

Primary voltage : 70V

Reactor configuration B

Gas : Mixture of Hydrogen Sulfide and Carbon Dioxide

Flow rate : 35 cc/min H<sub>2</sub>S + 316 cc/min CO<sub>2</sub>

Duration of each run : 10 min

---

Serial Number	Frequency Hz	Sec. Vol. kV	Temp. K	Amount of sulfur gm	percentage conversion
1	550	4.78	289.37	0.11	23.3
2	560	4.66	289.37	0.07	14.83
3	580	4.42	288.76	0.09	19.03
4	600	4.16	288.76	0.10	21.15
5	620	4.22	288.76	0.09	19.03
6	640	4.36	290.87	0.08	17.05
7	650	4.42	290.87	0.09	19.17
8	700	4.94	290.87	0.09	19.17

---

TABLE C5

## DESTRUCTIVE TEST DATA CORRESPONDING TO FIGURE 5.5

---

Primary voltage : 80V

Reactor configuration B

Gas : Mixture of Hydrogen Sulfide and Carbon Dioxide

Flow rate : 35 cc/min H<sub>2</sub>S + 35 cc/min CO<sub>2</sub>

Duration of each run : 10 min

---

Serial Number	Frequency Hz	Sec. Vol. kV	Temp. K	Amount of sulfur gm	percentage conversion
1	550	4.04	283.15	0.08	16.59
2	560	3.92	283.15	0.12	24.89
3	580	3.74	283.15	0.16	33.18
4	600	3.50	284.05	0.15	31.21
5	620	3.28	284.05	0.15	31.21
6	640	3.14	284.05	0.16	33.19
7	650	3.02	284.15	0.16	33.19
8	700	2.54	284.15	0.13	27.07

---

TABLE C6

## DESTRUCTIVE TEST DATA CORRESPONDING TO FIGURE 5.6

---

Primary voltage : 70V

Reactor configuration B

Gas : Mixture of Hydrogen Sulfide and Carbon dioxide

Flow rate : 35 cc/min H<sub>2</sub>S + 35 cc/min CO<sub>2</sub>

Duration of each run : 10 min

---

Serial Number	Frequency Hz	Sec. Vol. kV	Temp. K	Amount of sulfur gm	percentage conversion
1	550	4.02	284.05	0.13	27.05
2	560	3.84	284.05	0.10	20.80
3	580	3.68	284.05	0.14	29.13
4	600	3.42	284.05	0.14	29.13
5	620	3.34	284.25	0.12	24.99
6	640	3.26	284.25	0.14	29.15
7	650	3.10	284.25	0.15	31.23
8	700	2.62	284.25	0.11	22.90

---

TABLE C7

## DESTRUCTIVE TEST DATA CORRESPONDING TO FIGURE 5.7

---

Primary voltage : 80V

Reactor configuration B

Gas : Mixture of Carbon Dioxide and Hydrogen Sulfide

Flow rate : 62 cc/min of Hydrogen Sulfide + 10 cc/min of Carbon Dioxide

Duration of each run : 10 min

---

Serial Number	Frequency Hz	Sec. Vol. kV	Temp. K	Amount of sulfur gm	percentage conversion
1	550	4.12	293.15	0.15	18.79
2	560	3.96	293.15	0.20	25.05
3	580	3.72	293.15	0.24	30.06
4	600	3.40	294.26	0.21	26.40
5	620	3.18	294.26	0.23	28.92
6	640	3.34	294.47	0.21	26.42
7	650	3.48	294.47	0.22	27.68
8	700	4.02	294.47	0.18	22.65

---

TABLE C8

## DESTRUCTIVE TEST DATA CORRESPONDING TO FIGURE 5.8

---

Primary voltage : 70V

Reactor configuration B

Gas : Mixture of Carbon Dioxide and Hydrogen Sulfide

Flow rate : 62 cc/min of Hydrogen Sulfide + 10 cc/min of Carbon Dioxide

Duration of each run : 10 min

---

Serial Number	Frequency Hz	Sec. Vol. kV	Temp. K	Amount of sulfur gm	percentage conversion
1	550	5.02	301.48	0.12	15.46
2	560	4.94	301.48	0.16	20.61
3	580	4.78	301.20	0.15	19.30
4	600	4.64	301.20	0.14	18.02
5	620	4.72	301.20	0.15	19.30
6	640	4.84	301.09	0.18	23.16
7	650	4.98	301.04	0.16	20.58
8	700	5.22	301.04	0.14	18.01

---



TABLE C9

DESTRUCTIVE TEST DATA CORRESPONDING TO FIGURE 5.9

---

Reactor configuration B

Gas : Pure Hydrogen Sulfide

Flow rate : 50.7cc/min

Duration of each run : 10 min

Frequency : 600 Hz

---

Serial Number	Primary Volt. kV	Sec. Vol. kV	Temp. K	Amount of sulfur gm	percentage conversion
1	40	4.34	292.04	0.06	8.86
2	50	4.38	292.04	0.13	19.20
3	60	4.50	289.93	0.14	20.52
4	70	4.54	289.93	0.16	23.46
5	80	4.66	289.98	0.23	33.73

---

TABLE C10

## DESTRUCTIVE TEST DATA CORRESPONDING TO FIGURE 5.10

---

Reactor configuration B

Gas : Mixture of Hydrogen Sulfide and Carbon Dioxide

Flow rate : 35 cc/min of Hydrogen Sulfide + 316.8 cc/min of Carbon Dioxide

Duration of each run : 10 min

Frequency : 600 Hz

---

Serial Number	Primary Volt. kV	Sec. Vol. kV	Temp. K	Amount of sulfur gm	percentage conversion
1	40	2.96	288.76	0.05	10.58
2	50	3.02	288.98	0.07	14.81
3	60	3.26	288.98	0.10	21.17
4	70	3.32	289.09	0.09	19.06
5	80	3.48	289.09	0.09	19.06

---

TABLE C11

## DESTRUCTIVE TEST DATA CORRESPONDING TO FIGURE 5.11

---

Reactor configuration B

Gas : Mixture of Hydrogen Sulfide and Carbon Dioxide

Flow rate : 35 cc/min of Hydrogen Sulfide + 35.55 cc/min of Carbon Dioxide

Duration of each run : 10 min

Frequency : 600 Hz

---

Serial Number	Primary Volt. kV	Sec. Vol. kV	Temp. K	Amount of sulfur gm	percentage conversion
1	40	3.34	284.05	0.05	10.40
2	50	3.38	284.05	0.10	20.80
3	60	3.44	284.05	0.14	29.13
4	70	3.42	284.05	0.14	29.13
5	80	3.50	284.05	0.15	31.21

---

TABLE C12

## DESTRUCTIVE TEST DATA CORRESPONDING TO FIGURE 5.12

---

Reactor configuration B

Gas : Mixture of Hydrogen Sulfide and Carbon Dioxide

Flow rate : 62 cc/min of Hydrogen Sulfide + 10 cc/min of Carbon Dioxide

Duration of each run : 10 min

Frequency : 600 Hz

---

Serial Number	Primary Volt. kV	Sec. Vol. kV	Temp. K	Amount of sulfur gm	percentage conversion
1	40	3.52	284.26	0.07	8.23
2	50	3.58	284.32	0.13	15.28
3	60	3.66	284.32	0.13	15.28
4	70	3.74	284.43	0.15	17.64
5	80	3.82	284.43	0.21	24.70

---

TABLE C13

## DESTRUCTIVE TEST DATA CORRESPONDING TO FIGURE 5.13

---

Primary voltage : 80V

Reactor configuration B

Gas : Hydrogen Sulfide gas Bubbled through the Water (36.5% Relative humidity)

Flow rate : 48 cc/min of Hydrogen Sulfide

Duration of each run : 10 min

---

Serial Number	Frequency Hz	Sec. Vol. kV	Temp. K	Amount of sulfur gm	percentage conversion
1	550	5.16	289.81	0.18	27.86
2	580	4.98	289.81	0.26	40.25
3	600	5.04	289.92	0.21	32.52
4	620	5.16	289.92	0.28	43.36
5	650	5.28	289.92	0.24	37.17
6	700	5.54	289.98	0.26	40.27

---

TABLE C14

DESTRUCTIVE TEST DATA CORRESPONDING TO FIGURE 5.14

---

 Primary voltage : 80V

Gas : Hydrogen Sulfide

Frequency : 600 Hz

---

Serial Number	Reactor Config.	Run Time min	Flow rate cc/min	Vol. cc	Res. Time min	Temp K	Sulfur Collected gm	% H <sub>2</sub> S Conv.
1	B	10	22	87.5	3.9	293.15	.120	40.99
2	B	10	35	87.5	2.5	293.15	.182	39.08
3	B	10	51	87.5	1.7	293.26	.240	35.38
4	B	10	75	87.5	1.16	293.37	.284	28.48
5	C	60	50.7	1456.5	28.7	304.26	3.647	93.55
6	C	10	112	1456.5	13.0	304.42	.768	53.52
7	C	10	50.7	728.22	14.4	304.48	.352	54.29

---

TABLE C15

DESTRUCTIVE TEST DATA CORRESPONDING TO FIGURE 5.15

---

Primary voltage : 80V

Reactor configuration B

Gas: Pure H<sub>2</sub>S

Flow rate : 50.7 cc/min

Frequency 580 Hz

---

Serial Number	Time min	Temp. K	Amount of sulfur gm	percentage conversion
1	5	280.37	0.07	19.81
2	10	280.37	0.19	26.88
3	15	280.37	0.36	33.96
4	20	282.04	0.33	23.49
5	25	282.04	0.59	33.60
6	30	282.04	0.64	30.36

---

TABLE C16

DESTRUCTIVE TEST DATA CORRESPONDING TO FIGURE 5.16

---

Primary voltage : 80V

Gas : Mixture of Hydrogen Sulfide and Carbon Dioxide

Duration of each run : 10 min

Frequency : 600 Hz

Reactor Configuration B

Flow rate : 70 cc/min

---

Serial Number	% Molar Composition of CO <sub>2</sub>	Sec.Volt kV	Temp K	Sulfur Collected gm	% Conv.
1	10/90	3.4	294.26	.21	26.40
2	20/80	3.76	299.26	.20	29.23
3	35/75	3.84	299.26	.16	29.23
4	50/50	3.5	284.05	.15	31.21
5	60/40	3.96	299.26	.11	34.45
6	75/25	3.98	299.26	.05	27.40
7	90/10	4.02	299.26	.03	32.88

---



## VITA

SREENIVASULA REDDY MAGUNTA

Candidate for the Degree of

Master of Science

Thesis: STUDIES ON DESTRUCTION OF HYDROGEN SULFIDE MIXED WITH CARBON DIOXIDE IN AN ALTERNATING CURRENT PLASMA ARC REACTOR.

Major Field: Chemical Engineering

Biographical:

Personal Data: Born in India, January 30, 1971.

Education: Received Bachelor of engineering degree in Chemical Engineering from Shivaji University at Kolhapur, Maharashtra in May, 1991; Completed requirements for the master of science degree at Oklahoma State University in May, 1995.

Professional Experience: Teaching Assistant, Department of Chemical Engineering, Oklahoma State University, August, 1992 to December, 1993.

Process Engineer: Paramount Distilleries, Jeedimetla, Hyderabad, India, September, 1991 to May, 1992.